



**NAVAL
POSTGRADUATE
SCHOOL**

MONTEREY, CALIFORNIA

THESIS

**COMPUTATIONAL INVESTIGATION OF
FLAPPING-WING PROPULSION
FOR A MICRO AIR VEHICLE**

by

Seng Chuan Lim

December 2006

Thesis Advisor:

Kevin D. Jones

Second Reader:

Christopher Brophy

Approved for public release; distribution is unlimited

THIS PAGE INTENTIONALLY LEFT BLANK

REPORT DOCUMENTATION PAGE			<i>Form Approved OMB No. 0704-0188</i>
Public reporting burden for this collection of information is estimated to average 1 hour per response, including the time for reviewing instruction, searching existing data sources, gathering and maintaining the data needed, and completing and reviewing the collection of information. Send comments regarding this burden estimate or any other aspect of this collection of information, including suggestions for reducing this burden, to Washington headquarters Services, Directorate for Information Operations and Reports, 1215 Jefferson Davis Highway, Suite 1204, Arlington, VA 22202-4302, and to the Office of Management and Budget, Paperwork Reduction Project (0704-0188) Washington DC 20503.			
1. AGENCY USE ONLY (Leave blank)	2. REPORT DATE December 2006	3. REPORT TYPE AND DATES COVERED Master's Thesis	
4. TITLE AND SUBTITLE : Computational Investigation of Flapping-Wing Propulsion for a Micro-Air Vehicle		5. FUNDING NUMBERS	
6. AUTHOR(S) Seng Chuan Lim		8. PERFORMING ORGANIZATION REPORT NUMBER	
7. PERFORMING ORGANIZATION NAME(S) AND ADDRESS(ES) Naval Postgraduate School Monterey, CA 93943-5000		10. SPONSORING/MONITORING AGENCY REPORT NUMBER	
9. SPONSORING /MONITORING AGENCY NAME(S) AND ADDRESS(ES) N/A		11. SUPPLEMENTARY NOTES The views expressed in this thesis are those of the author and do not reflect the official policy or position of the Department of Defense or the U.S. Government.	
12a. DISTRIBUTION / AVAILABILITY STATEMENT Approved for public release; distribution is unlimited		12b. DISTRIBUTION CODE	
13. ABSTRACT (maximum 200 words) The low Reynolds number aerodynamics of the flapping wing Micro-Air Vehicle (MAV) developed at NPS by Max Platzer and Kevin Jones was studied numerically. The dynamic mesh simulation model of the full multi-wing configuration, which consists of a fixed wing and a pair of aft position, opposed pitch/ plunge flapping wings was developed using an advanced CFD code that is available commercially. The unsteady Navier-Stokes flow fields, wake structures and forces variations were determined and compared with reference to past experimental observations. The results were encouraging and provided impetus for future computational optimization studies on the NPS flapping wing MAV.			
14. SUBJECT TERMS Micro Air Vehicle, Flapping-Wing Propulsion, Unsteady Aerodynamics, Computational Fluid Dynamics, Numerical Analysis			15. NUMBER OF PAGES 109
			16. PRICE CODE
17. SECURITY CLASSIFICATION OF REPORT Unclassified	18. SECURITY CLASSIFICATION OF THIS PAGE Unclassified	19. SECURITY CLASSIFICATION OF ABSTRACT Unclassified	20. LIMITATION OF ABSTRACT UL

THIS PAGE INTENTIONALLY LEFT BLANK

Approved for public release; distribution is unlimited

**COMPUTATIONAL INVESTIGATION OF
FLAPPING-WING PROPULSION
FOR A MICRO AIR VEHICLE**

Seng Chuan Lim
DSO National Laboratories, Singapore
B. Engineering, (Mechanical Engineering), National University of Singapore, 1994

Submitted in partial fulfillment of the
requirements for the degree of

MASTER OF SCIENCE IN MECHANICAL ENGINEERING

from the

**NAVAL POSTGRADUATE SCHOOL
December 2006**

Author: Seng Chuan Lim

Approved by: Professor Kevin Jones
Thesis Advisor

Professor Christopher Brophy
Second Reader

Professor Anthony Healey
Chairman, Department of Mechanical and Astronautical
Engineering

THIS PAGE INTENTIONALLY LEFT BLANK

ABSTRACT

The low Reynolds number aerodynamics of the flapping wing Micro-Air Vehicle (MAV) developed at NPS by Max Platzer and Kevin Jones was studied numerically. The dynamic mesh simulation model of the full multi-wing configuration, which consists of a fixed wing and a pair of aft position, opposed pitch/ plunge flapping wings was developed using an advanced CFD code that is available commercially. The unsteady flow fields, wake structures and forces were determined by solving the incompressible Navier-Stokes equations, and the results were compared to past experimental observations. The results were encouraging and provided impetus for future computational optimization studies on the NPS flapping wing MAV.

THIS PAGE INTENTIONALLY LEFT BLANK

TABLE OF CONTENTS

I.	INTRODUCTION.....	1
	A. OVERVIEW	1
	B. BACKGROUND OF FLAPPING WING PROPULSION	1
	C. OBJECTIVES	4
II.	GENERAL KINEMATICS.....	5
	A. THE NPS FLAPPING WING FLYING MODEL.....	5
	B. OPERATIONAL CHARACTERISTICS.....	6
	C. EQUATIONS OF MOTION OF FLAPPING WING	7
	1. Test Configuration	7
	2. Test Variables.....	8
	3. Equation of Motion.....	8
III.	NUMERICAL SIMULATIONS	9
	A. CFD-ACE+	9
	B. MOVING GRID/GRID DEFORMATION	9
	C. SPRAY INJECTION FOR UNSTEADY FLOW VISUALIZATION.....	9
	D. SIMULATION PROCESS USING CFD ACE+	10
	E. GRID GENERATION.....	10
	F. BOUNDARY CONDITIONS.....	13
	1. Boundary Conditions for the Flow Problem	13
	2. Boundary Conditions for Moving/Grid Deformation	14
	<i>a. Case of Pitch/Plunge 90° Out of Phase at Flapping</i>	
	<i>Frequency, f=25Hz</i>	<i>14</i>
	<i>b. Case of Pitch/Plunge Motion in Phase, Flapping</i>	
	<i>Frequency, f=25Hz</i>	<i>15</i>
	<i>c. Moving Boundary Conditions For Fluid-Fluid Wake</i>	
	<i>Interfaces.....</i>	<i>15</i>
	3. User Input for Spray Problem.....	15
	G. SOLUTION PARAMETERS	16
IV.	VERIFICATION OF THE DYNAMIC SIMULATION MODELS	19
	A. VERIFICATION OF THE DYNAMIC MESHING MODEL	19
	B. VERIFICATION OF THE MOVING /GRID DEFORMATION	
	SOLUTION	21
V.	RESULTS	23
	A. SOLUTION RESIDUAL PLOT	23
	B. SIMULATION TEST CASE: NON-FLAPPING	24
	1. Lift and Drag History of Non-Flapping Case.....	28
	2. Flow Visualization for Non-Flapping Case.....	30
	C. SIMULATION TEST CASE: ZERO INLET VELOCITY	31
	1. Lift and Drag History of Flapping Case with $U_{\infty}=0$.....	31
	2. Flow Visualization for Flapping Case with $U_{\infty}=0$	32

D.	FULL SIMULATION RESULTS	33
1.	Full Flapping Wing Configuration: $U_{\infty}=3\text{m/s}$, $\alpha=10^{\circ}$, $f=25\text{Hz}$, $H=15\text{mm}$, $\Phi=10^{\circ}$, Pitch/Plunge Out of Phase.....	33
2.	Full Flapping Wing Configuration: $U_{\infty}=3\text{m/s}$, $\alpha=10^{\circ}$, $f=25\text{Hz}$, $H=15\text{mm}$, $\Phi=15^{\circ}$, Pitch/Plunge Out of Phase.....	36
3.	Full Flapping Wing Configuration: $U_{\infty}=3\text{m/s}$, $\alpha=10^{\circ}$, $f=25\text{Hz}$, $H=15\text{mm}$, $\Phi=20^{\circ}$, Pitch/Plunge Out of Phase.....	39
3.	Full Flapping Wing Configuration: $U_{\infty}=3\text{m/s}$, $\alpha=10^{\circ}$, $f=25\text{Hz}$, $H=15\text{mm}$, $\Phi=10^{\circ}$, Pitch/Plunge In-Phase ($\psi=0^{\circ}$)	42
VI.	DISCUSSION	45
A.	COMPARISON OF FORCE HISTORIES: CASE OF IN-PHASE VS OUT-OF-PHASE PITCH/PLUNGE MOTION.....	45
B.	PITCH AMPLITUDE EFFECTS ON FORCES HISTORY: CASE OF OUT-OF-PHASE PITCH/PLUNGE MOTION	46
C.	EFFECTS OF PITCH/PLUNGE HEAVING MOTION: FROM PERSPECTIVE OF FLOW VISUALIZATION RESULTS	53
VII.	CONCLUSIONS	57
VIII.	RECOMMENDATIONS.....	59
	APPENDIX A. SIMULATION DATA	61
A.	$U_{\infty}=0$, $f=25\text{HZ}$, $\Phi=10^{\circ}$, PITCH/PLUNGE OUT OF PHASE	61
B.	$U_{\infty}=3\text{M/S}$, $\alpha=10^{\circ}$, $f=0\text{HZ}$, WING SEPARATION: 82.5MM.....	66
C.	$U_{\infty}=3\text{M/S}$, $f=25\text{HZ}$, $\Phi=10^{\circ}$, PITCH/PLUNGE IN-PHASE	68
D.	$U_{\infty}=3\text{M/S}$, $f=25\text{HZ}$, $\Phi=10^{\circ}$, PITCH/PLUNGE OUT OF PHASE	72
E.	$U_{\infty}=3\text{M/S}$, $f=25\text{HZ}$, $\Phi=15^{\circ}$, PITCH/PLUNGE OUT OF PHASE	76
F.	$U_{\infty}=3\text{M/S}$, $f=25\text{HZ}$, $\Phi=20^{\circ}$, PITCH/PLUNGE OUT OF PHASE	80
	APPENDIX B. MEAN LIFT & DRAG VARIATION FOR CASE OF OUT-OF- PHASE PITCH/PLUNGE MOTION.....	85
	LIST OF REFERENCES	87
	INITIAL DISTRIBUTION LIST	89

LIST OF FIGURES

Figure 1.	(a) (Left) and (b) (Right) Flow Re-attachment Phenomenon Due to Flapping Wing Motion (Picture on the Right) and (c) The NPS Flapping Wing MAV - Flying Prototype (Developed by Professors Max Platzer and Kevin Jones.) (From: [2])	3
Figure 2.	(a) NPS Flapping Wing MAV- Wing Tunnel Variant (From: [2]) and (b) Schematic of the MAV Model (From: [3]).....	5
Figure 3.	Rigid Body Kinematics of the Opposed Flapping Wing with Pitch Leading the Plunge Motion by 90°	7
Figure 4.	Multi-Block Grid Generation around Wing Bodies.....	11
Figure 5.	Structured Meshing Around The Fixed Wing	12
Figure 6.	Entire Computational Domain - 1810 x 1800mm.....	12
Figure 7.	Simulation Model – Schematic Showing Various Boundary Conditions (Not Shown to Scale).....	13
Figure 8.	Pitch/Plunge Phase Relationship: Bottom Curves Show the Plunge Vs Pitch Motion as a Function of Time Step.	14
Figure 9.	Location of Spray Injector for Unsteady Flow Visualization (Image Captured from CFD ACE GUI Environment).....	16
Figure 10.	Plots showing the Rigid Body Kinematic Solution of the Moving/Grid Deformation Run. ($H=15\text{mm}$, $\Phi=10^\circ$, $f=25\text{Hz}$, Pitch Leads Plunge by $\pi/2$)...20	20
Figure 11.	Solution of Vorticity Distribution at Various Meshing Sequences. (Moving/Grid Deformation Setup: $H=15\text{mm}$, $\Phi=10^\circ$, $f=25\text{Hz}$, Pitch Leads Plunge by $\pi/2$).....	21
Figure 12.	Residual Plot: Case of Pitch/Pitch in Phase, $U_\infty = 3\text{m/s}$, $\alpha=10^\circ$, $f=25\text{Hz}$, 1000th Time Step.....	23
Figure 13.	Residual Plot: Case of Pitch/Plunge 90° Out of Phase, $U_\infty = 3\text{m/s}$, $\alpha=10^\circ$, $f=25\text{Hz}$, 1000th Time Step.....	24
Figure 14.	Vorticity Distribution (Transient Vorticity Field at 1000 th step, $U_\infty = 3\text{m/s}$, $\alpha=10^\circ$, $f=0\text{ Hz}$,)	25
Figure 15.	Vorticity Distribution (Transient Vorticity Field at 1000 th step, $U_\infty = 3\text{m/s}$, $\alpha=10^\circ$, $f=0\text{Hz}$)	25
Figure 16.	Velocity Magnitude Field (Transient Flow Field at 1000 th step, $U_\infty = 3\text{m/s}$, $\alpha=10^\circ$, $f=0\text{Hz}$)	26
Figure 17.	Velocity Field at the Leading and Trailing Edge of the Fixed Wing (Transient Flow Field at 1000 th step. $U_\infty = 3\text{m/s}$, $\alpha=10^\circ$, $f=0\text{Hz}$)	26
Figure 18.	Pressure Field of the Multi-Wing Configuration (Transient Flow Field at 1000 th step, $U_\infty = 3\text{m/s}$, $\alpha=10^\circ$, $f=0\text{Hz}$).....	27
Figure 19.	Pressure Distribution of the Fixed and Flapping Wing Surfaces (Transient Solution at 1000 th step, $U_\infty = 3\text{m/s}$, $\alpha=10^\circ$, $f=0\text{Hz}$).....	27
Figure 20.	Simulation Model of Non-Flapping Case.....	28
Figure 21.	Lift per Unit Length ($U_\infty = 3\text{m/s}$, $\alpha=10^\circ$, $f=0\text{Hz}$).....	29
Figure 22.	Drag per Unit Length ($U_\infty = 3\text{m/s}$,)	29

Figure 23.	Flow Visualization Simulations - Shows Streaklines at 1000 th Time Step ($U_{\infty} = 3\text{m/s}$, $\alpha=10^{\circ}$, $f=0\text{Hz}$).....	30
Figure 24.	Experimental Flow Visualization - Showing Flow Separation Immediately After Leading Edge for the case of $U_{\infty} = 2\text{m/s}$, $\alpha=15^{\circ}$, $f=0\text{Hz}$. (From: [2]).....	30
Figure 25.	Lift History with $U_{\infty}=0$, $f=25\text{Hz}$, $\Phi=10^{\circ}$, $H=15\text{mm}$, Pitch/Plunge 90° Out of Phase.....	31
Figure 26.	Drag History with $U_{\infty}=0$, $f=25\text{Hz}$, $\Phi=10^{\circ}$, $H=15\text{mm}$, Pitch/Plunge 90° Out of Phase.....	32
Figure 27.	Flow Visualization for the Case of $U_{\infty}=0$, $f=25\text{Hz}$, $\Phi=10^{\circ}$, $H=15\text{mm}$, Pitch/Plunge 90° Out of Phase.....	33
Figure 28.	Lift History: $U_{\infty}= 3\text{m/s}$, $\alpha=10^{\circ}$, $f=25\text{Hz}$, $H=15\text{MM}$, $\Phi=10^{\circ}$, Out of Phase.	34
Figure 29.	Drag History: $U_{\infty}= 3\text{m/s}$, $\alpha=10^{\circ}$, $f=25\text{Hz}$, $H=15\text{MM}$, $\Phi=10^{\circ}$, Out of Phase. ...	34
Figure 30.	Velocity Field with Streaklines from Time Step 1000 - 1018: ($U_{\infty}= 3\text{m/s}$, $\alpha=10^{\circ}$, $f=25\text{Hz}$, $H=15\text{MM}$, $\Phi=10^{\circ}$, Out of Phase.).....	35
Figure 31.	Lift History: $U_{\infty}= 3\text{m/s}$, $\alpha=10^{\circ}$, $f=25\text{Hz}$, $H=15\text{MM}$, $\Phi=15^{\circ}$, Out of Phase.	36
Figure 32.	Drag History: $U_{\infty}= 3\text{m/s}$, $\alpha=10^{\circ}$, $f=25\text{Hz}$, $H=15\text{MM}$, $\Phi=15^{\circ}$, Out of Phase. ...	37
Figure 33.	Velocity Field with Streaklines from Time Step 1000 - 1018: ($U_{\infty}= 3\text{m/s}$, $\alpha=10^{\circ}$, $f=25\text{Hz}$, $H=15\text{MM}$, $\Phi=15^{\circ}$, Out of Phase.).....	38
Figure 34.	Lift History: $U_{\infty}= 3\text{m/s}$, $\alpha=10^{\circ}$, $f=25\text{Hz}$, $H=15\text{MM}$, $\Phi=20^{\circ}$, Out of Phase.	39
Figure 35.	Drag History: $U_{\infty}= 3\text{m/s}$, $\alpha=10^{\circ}$, $f=25\text{Hz}$, $H=15\text{MM}$, $\Phi=20^{\circ}$, Out of Phase. ...	40
Figure 36.	Velocity Field with Streaklines from Time Step 1000 - 1018: ($U_{\infty}= 3\text{m/s}$, $\alpha=10^{\circ}$, $f=25\text{Hz}$, $H=15\text{MM}$, $\Phi=20^{\circ}$, Out of Phase.).....	41
Figure 37.	Lift History: $U_{\infty}= 3\text{m/s}$, $\alpha=10^{\circ}$, $f=25\text{Hz}$, $H=15\text{MM}$, $\Phi=10^{\circ}$, In- Phase.....	42
Figure 38.	Drag History: $U_{\infty}= 3\text{m/s}$, $\alpha=10^{\circ}$, $f=25\text{Hz}$, $H=15\text{MM}$, $\Phi=10^{\circ}$, In- Phase.....	43
Figure 39.	Velocity Field with Streaklines from Time Step 1000 - 1018: ($U_{\infty}= 3\text{m/s}$, $\alpha=10^{\circ}$, $f=25\text{Hz}$, $H=15\text{MM}$, $\Phi=10^{\circ}$, In-Phase.)	44
Figure 40.	Time History of Drag: Comparison between Pitch/Plunge In-Phase and Out-of-Phase ($U_{\infty}= 3\text{m/s}$, $\alpha=10^{\circ}$, $f=25\text{Hz}$, $H=15\text{mm}$, $\Phi=10^{\circ}$) with Reference to the Non-Flapping Case	45
Figure 41.	Time History of Lift: Comparison between Pitch/Plunge In-Phase and Out-of-Phase ($U_{\infty}= 3\text{m/s}$, $\alpha=10^{\circ}$, $f=25\text{Hz}$, $H=15\text{mm}$, $\Phi=10^{\circ}$) with Reference to the Non-Flapping Case	46
Figure 42.	Effects of Pitch Amplitude on Lift of Fixed Wing (Case of Pitch/Plunge Out-of-Phase. $U_{\infty}= 3\text{m/s}$, $\alpha=10^{\circ}$, $f=25\text{Hz}$, $H=15\text{mm}$, $\Phi=10^{\circ}$, 15° , 20°).....	48
Figure 43.	Effects of Pitch Amplitude on Lift of Top Wing (Case of Pitch/Plunge Out-of-Phase. $U_{\infty}= 3\text{m/s}$, $\alpha=10^{\circ}$, $f=25\text{Hz}$, $H=15\text{mm}$, $\Phi=10^{\circ}$, 15° , 20°).....	48
Figure 44.	Effects of Pitch Amplitude on Lift of Bottom Wing (Case of Pitch/Plunge Out-of-Phase. ($U_{\infty}= 3\text{m/s}$, $\alpha=10^{\circ}$, $f=25\text{Hz}$, $H=15\text{mm}$, $\Phi=10^{\circ}$, 15° , 20°)	49
Figure 45.	Effects of Pitch Amplitude on Overall Lift (Case of Pitch/Plunge Out-of-Phase. ($U_{\infty}= 3\text{m/s}$, $\alpha=10^{\circ}$, $f=25\text{Hz}$, $H=15\text{mm}$, $\Phi=10^{\circ}$, 15° , 20°)	49
Figure 46.	Effects of Pitch Amplitude on Drag of Fixed Wing (Case of Pitch/Plunge Out-of-Phase. ($U_{\infty}= 3\text{m/s}$, $\alpha=10^{\circ}$, $f=25\text{Hz}$, $H=15\text{mm}$, $\Phi=10^{\circ}$, 15° , 20°)	50
Figure 47.	Effects of Pitch Amplitude on Drag of Top Wing (Case of Pitch/Plunge Out-of-Phase. ($U_{\infty}= 3\text{m/s}$, $\alpha=10^{\circ}$, $f=25\text{Hz}$, $H=15\text{mm}$, $\Phi=10^{\circ}$, 15° , 20°)	50

Figure 48.	Effects of Pitch Amplitude on Drag of Bottom Wing (Case of Pitch/Plunge Out-of-Phase. ($U_{\infty}= 3\text{m/s}$, $\alpha=10^{\circ}$, $f=25\text{Hz}$, $H=15\text{mm}$, $\Phi=10^{\circ}$, 15° , 20°).....	51
Figure 49.	Effects of Pitch Amplitude on Overall Drag (Case of Pitch/Plunge Out-of-Phase. ($U_{\infty}= 3\text{m/s}$, $\alpha=10^{\circ}$, $f=25\text{Hz}$, $H=15\text{mm}$, $\Phi=10^{\circ}$, 15° , 20°)	51
Figure 50.	Mean Lift Vs Pitch Amplitude (Case of Pitch/Plunge Out-of-Phase. ($U_{\infty}= 3\text{m/s}$, $\alpha=10^{\circ}$, $f=25\text{Hz}$, $H=15\text{mm}$, $\Phi=10^{\circ}$, 15° , 20°).....	52
Figure 51.	Mean Drag Vs Pitch Amplitude (Case of Pitch/Plunge Out-of-Phase. ($U_{\infty}= 3\text{m/s}$, $\alpha=10^{\circ}$, $f=25\text{Hz}$, $H=15\text{mm}$, $\Phi=10^{\circ}$, 15° , 20°).....	52
Figure 52.	Flow Visualization Simulation Results at 1000 th Time Step: ($U_{\infty}= 3\text{m/s}$, $\alpha=10^{\circ}$, $f=0\text{ Hz}$, $H=15\text{mm}$, $\Phi=10^{\circ}$, 15° , 20°).....	54
Figure 53.	Flow Visualization Simulation Results at 1000 th Time Step: ($U_{\infty}= 3\text{m/s}$, $\alpha=10^{\circ}$, $f=25\text{Hz}$, $H=15\text{mm}$, $\Phi=10^{\circ}$ Pitch/Plunge Out-of-Phase).....	54

THIS PAGE INTENTIONALLY LEFT BLANK

LIST OF TABLES

Table 1. Mean Lift Variation for Case of Out-of-Phase Pitch/Plunge Motion85
Table 2. Mean Drag Variation for Case of Out-of-Phase Pitch/Plunge Motion85

THIS PAGE INTENTIONALLY LEFT BLANK

LIST OF ABBREVIATIONS, ACRONYMS, AND SYMBOLS

AOA	:	angle of attack
BC	:	boundary conditions
CFD	:	computational fluid dynamics
MAV	:	micro-air vehicle
NPS	:	Naval Postgraduate School
H	:	plunge amplitude
Φ	:	pitch amplitude
Ψ	:	pitch/plunge phase difference
f	:	frequency in Hertz (Hz)
α	:	angle of attack in degrees
α_i	:	induced angle of attack
α_{eff}	:	effective angle of attack
U	:	velocity
U_∞	:	free stream velocity
c	:	fixed wing chord length
c'	:	flapping wing chord length
ρ	:	density of working fluid
μ	:	viscosity
k	:	reduced frequency ($\frac{2\pi fc'}{U_\infty}$)
h	:	non-dimensional plunge amplitude ($\frac{H}{c'}$)

v	:	non-dimensional velocity ($\frac{U}{U_\infty}$)
\mathbf{v}	:	velocity vector
t	:	time
Re	:	Reynolds Number
m_d	:	mass of droplets
x,y,z	:	Cartesian position components
u,v,w	:	Cartesian velocity components
C_d	:	drag coefficient
A_d	:	droplet frontal area
V_d	:	droplet volume
P_{ref}	:	reference pressure

ACKNOWLEDGMENTS

The author is immensely thankful to Professor Kevin Jones for granting this interesting thesis opportunity and providing brilliant advice and enthusiastic guidance throughout the course of this research work. Under his supervision, the author acquired vast knowledge from scratch to fulfill the required research milestones.

In addition, the author would also like to extend his sincere gratitude to Professor Christopher Brophy for his kind advice and encouragement out of his busy schedule. Incidentally, Professor Brophy is also the author's instructor in the Advanced Propulsion course modules. He had also offered the use of high speed computing facilities in the NPS Rocket Propulsion Laboratory in order to speed up solution generation process.

Special gratitude is also due to Mr Kartik Shah, senior applications engineer from ESI CFD Inc. for his patient and expert advice in the use of the CFD ACE+ software.

THIS PAGE INTENTIONALLY LEFT BLANK

I. INTRODUCTION

A. OVERVIEW

In this thesis an attempt is made to numerically analyze, the flow field and forces produced by the flapping wing micro-air vehicle (MAV) that is currently under development at the Naval Postgraduate School (NPS). It serves as a starting point for the next phase of CFD research on the area of low Reynolds number, unsteady computational aerodynamics of flapping-wing propulsion at NPS. The Navier-Stokes computational domain in this case involves the entire three-wing configuration with the pair of large amplitude, opposed flapping wings, positioned aft of the large fixed wing. The flapping kinematics selected for the study are based on the combination of opposed pitch and plunge motion which is known to yield higher propulsive efficiency. The results of the study provide a foundation for future work which in turn might potentially provide a better understanding of the complex flow interactive behavior of the multi-wing flapping MAV which is both difficult and time consuming to obtain from experimental measurements.

B. BACKGROUND OF FLAPPING WING PROPULSION

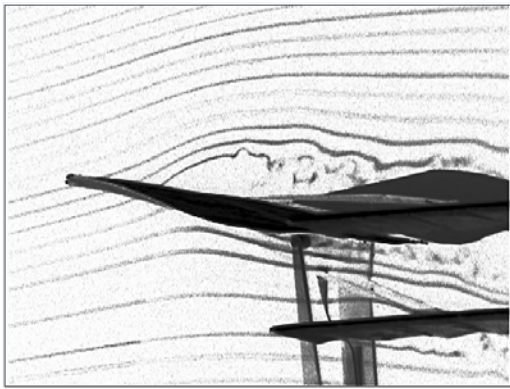
The earliest scientific theories concerning flapping wing flight pertain to purely plunging airfoils. Knoller and Betz provided the first theoretical explanation of thrust generation in independent papers published in 1909 and 1912, respectively. In 1935, von Kármán and Burgers offered the first explanation of drag or thrust production based on the observed location and orientation of the wake vortices for drag-indicative and thrust-indicative wakes, respectively. After which, a number of researchers studied the problem of flapping flight by modeling the flow field induced near the flapping wings caused by the system of trailing and shed vorticity in the wake. Wilmott [1] developed an unsteady lifting-line theory using the method of matched asymptotic expansions for the general motion of a wing with high aspect ratio. Philips et al. [5] modeled flapping wings using an unsteady lifting-line theory in which the shed or transverse vorticity in the wake was lumped at the start of each stroke. Ahmadi and Widnall [6] developed an unsteady lifting line theory using matched asymptotic expansions, with the inverse of the aspect ratio being the small parameter. Lan [7] developed an un-steady quasi-vortex-lattice method,

which he then applied to predict the flapping efficiency of various planforms and flapping motions. All of these theories, however, are restricted to low-frequency flapping in which the reduced frequency is $\ll 1$ and applies to higher Reynolds Number regime. In recent years, Max Platzer and Kevin Jones [3] have studied unsteady flapping wing aerodynamics with much higher reduced frequencies. Several flow solvers using both potential flow and Euler/Navier Stokes were used to simulate the 2D flow field of single flapping and biplane wings and wing combinations.

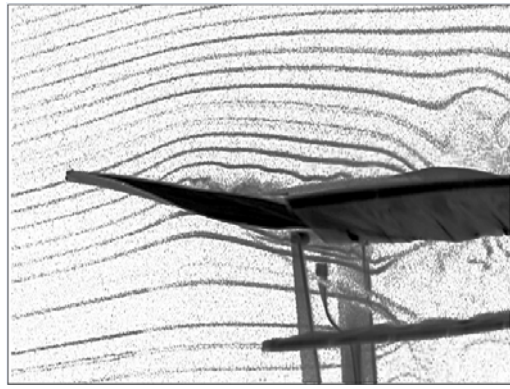
In the area of experimental flow visualization, they have worked to understand the complex flow field of the flapping wing MAV in full configuration. Figures 1a and 1b show their wind tunnel test results where lift generation caused by the flapping wing was explained by evidence of a flow re-attachment phenomenon.

In addition, the development of the NPS flapping wing MAV flying prototype (Figure 1c) signifies significant milestones in flapping wing propulsion research.

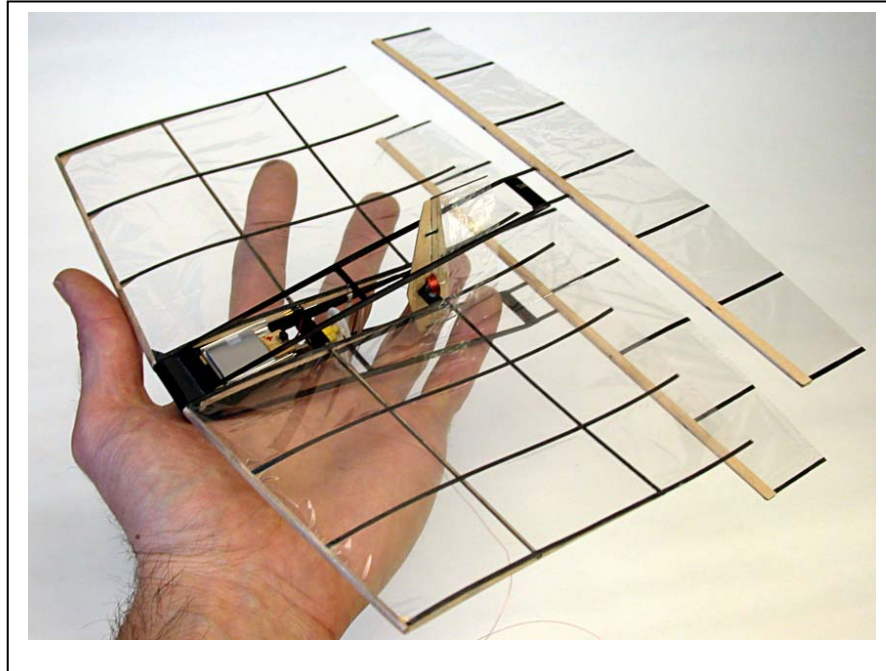
However, in the area of computational research pertaining to flapping wing aerodynamics, many unknowns remain.



(a)



(b)



(c)

Figure 1. (a) (Left) and (b) (Right) Flow Re-attachment Phenomenon Due to Flapping Wing Motion (Picture on the Right) and (c) The NPS Flapping Wing MAV - Flying Prototype (Developed by Professors Max Platzer and Kevin Jones.) (From: [2])

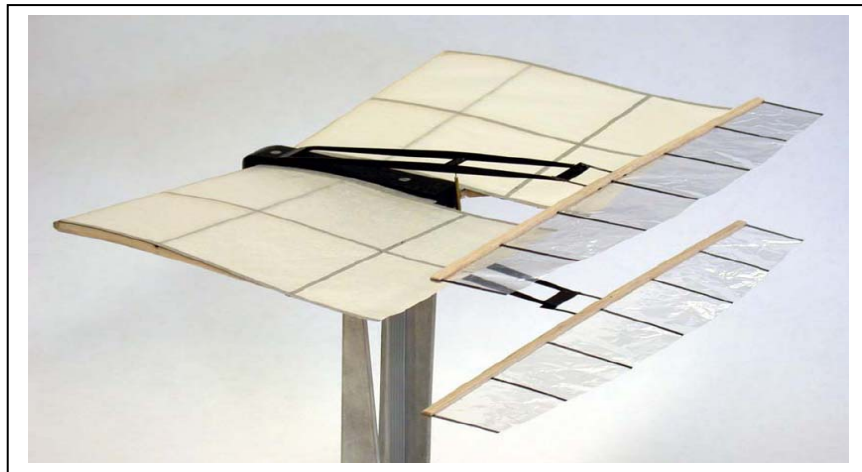
C. OBJECTIVES

The present work seeks to explore numerically, using a commercially available CFD code, the complex interactive flow behavior and resulting forces in the full fixed and flapping wing configuration currently adopted by the NPS flapping wing MAV flying model. Previous 2D numerical studies were focused mainly on single plunging/pitching or the opposed plunging/pitching flapping combination. This study shall provide a foundation for future Navier-Stokes CFD simulation studies involving the geometric complexity of the multi-wing configuration.

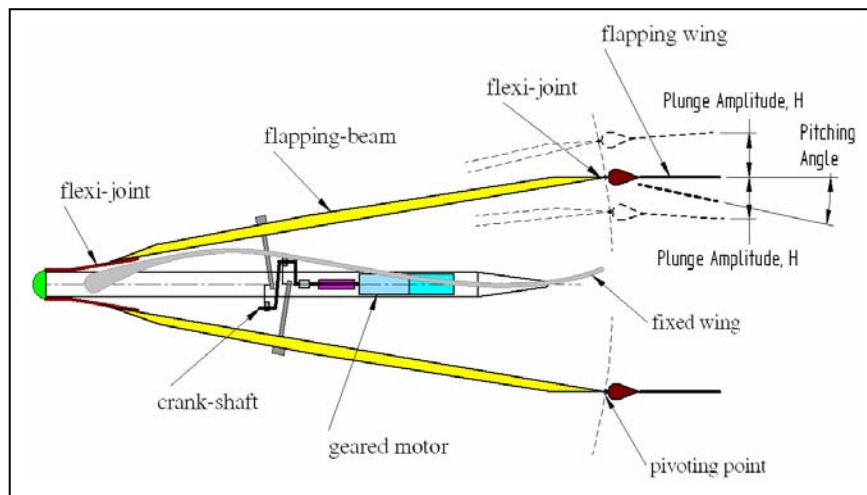
II. GENERAL KINEMATICS

A. THE NPS FLAPPING WING FLYING MODEL

The simulation work in this study is based on the wind tunnel variant of the NPS flapping wing MAV as shown in Figure 2a. Figure 2b illustrates the schematic of the MAV model. It consists of a fixed wing of span, 250mm and chord length, c , of 150mm. The pair of aft positioned opposed pitch/plunge flapping wings have the same span and have a chord length, c' , of 40mm each.



(a)



(b)

Figure 2. (a) NPS Flapping Wing MAV- Wing Tunnel Variant (From: [2]) and (b) Schematic of the MAV Model (From: [3])

B. OPERATIONAL CHARACTERISTICS

The nominal forward flight speed is 3m/s with an angle of attack, α , of roughly 10 degrees. The operating flapping frequency, f , ranges from about 25 to 30 Hz. However in this study, in order to reduce the number of variables, the frequency is fixed at 25Hz.

The Reynolds Number for the main wing is given by:

$$\text{Re}_c = \frac{U_\infty \cdot c \cdot \rho}{\mu} = \frac{3(m/s) \times 0.15(m) \times 1.23(kg/m^3)}{1.78 \times 10^{-5}(kg/m-s)} = 31,000$$

While the Reynolds Number for the flapping wing, Re_c is 8,300.

At such low Reynolds Numbers, some CFD codes have convergence problem. Typical turbulence codes used at high speeds are of no use, and we must assume that the flow is laminar.

The Reduced Frequency of the flapping motion is given by:

$$k = \frac{2\pi f c'}{U_\infty} = 2.1$$

where c' is the flapping wing chord length of 40mm.

The non-dimensional plunge amplitude is given by

$$h = \frac{H}{c'}$$

where H is the plunge amplitude as illustrated in Figure 2. For $H = 15\text{mm}$, the non-dimensional plunge amplitude is 0.375.

The peak non-dimensional plunge velocity is given by:

$$v = h \cdot k = 0.375 \times 2.1 = 0.79$$

The maximum induced angle of attack due to the plunge velocity, α_i can be calculated to be:

$$\alpha_i = \tan^{-1}(h \cdot k) = 38.2^\circ$$

The maximum effective angle of attack, α_{eff} based on the following nominal operating parameters is therefore calculated to be 28.2°.

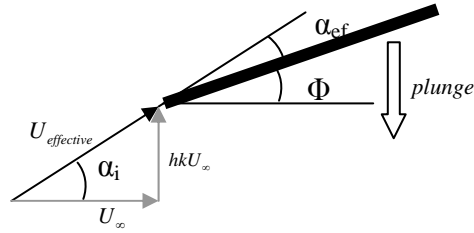
$$H = 15\text{mm}$$

$$f = 25\text{Hz}$$

$$U_\infty = 3\text{m/s}$$

$$\Phi = 10^\circ$$

$$\alpha_{eff} = \alpha_i - \Phi = 38.2^\circ - 10^\circ = 28.2^\circ$$



C. EQUATIONS OF MOTION OF FLAPPING WING

1. Test Configuration

An attempt is made in this CFD study to model and simulate the complete multi-wing combination of the MAV. The rigid body kinematics of the opposed flapping wing adopted for the simulation consists of 2 degrees of freedom constrained motion with simultaneous harmonic (sinusoidal) pitching and plunging motion. Figure 3 shows one possible combined motion. In this case, the pitch leads the plunge motion by 90° .

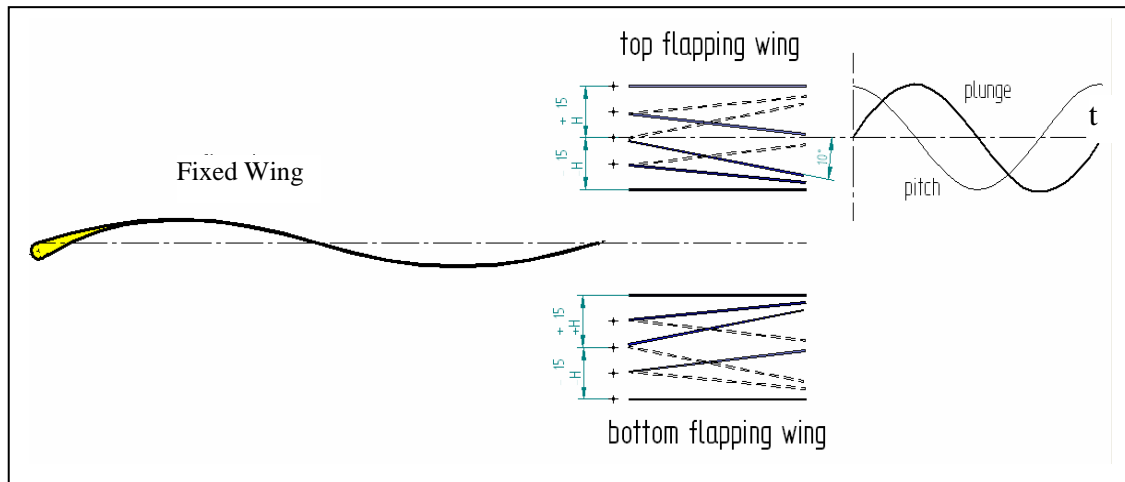


Figure 3. Rigid Body Kinematics of the Opposed Flapping Wing with Pitch Leading the Plunge Motion by 90°

In the case of pitch in phase with plunge motion, the pair of opposed flapping wing will be at the horizontal orientation at the neutral pitching position. The sinusoidal plunging amplitude, H in this study is fixed at H=15mm. The pivoting point for the sinusoidal pitching motion is modeled at 0.125c' or 5mm ahead of the flapping wing leading edge (see Figure 2b).

2. Test Variables

Three different pitching amplitudes were looked at, namely:

$$\Phi=10^\circ, 15^\circ, 20^\circ,$$

and having the corresponding plunging motion configured for 90° phase difference with the pitching motion. This is due to the fact that this particular heaving motion has been found historically to produce near optimum thrust (negative drag) in flapping propulsion.

3. Equation of Motion

The equations of motion used as the dynamic boundary conditions for the plunging and pitching simulation for the top and bottom flapping wings are respectively:

Case of Pitch Leads Plunge by 90°

Top Wing:

$$\text{Plunging motion: } H(1 + \sin(2\pi ft - \psi))$$

$$\text{Pitching motion: } -\Phi \sin(2\pi ft)$$

Bottom Wing:

$$\text{Plunging motion: } -H(1 + \sin(2\pi ft - \psi))$$

$$\text{Pitching motion: } \Phi \sin(2\pi ft)$$

Figure 3 shows the phase relationship between the pitching and plunging motion with respect to time t. In this case, the phase, ψ is $\pi/2$.

For the case of in-phase pitch/plunge motion, the equation of motion was modeled in a similar fashion as presented in section C.2, but the ψ terms in the sine functions are set to zero.

III. NUMERICAL SIMULATIONS

A. CFD-ACE+

CFD-ACE+, is a commercially available CFD and multi-physics software that is utilized for the simulation task. The incompressible Navier-Stokes flow solver within CFD ACE+ is capable of very low Reynolds number processing. Initial evaluation using a NACA 0012 airfoil at $Re=5000$ and 10000 shows good convergence and reliable results. The “Grid Deformation” capability allows large parametric constraint motion required for the flapping wing rigid body kinematics simulations. The “Spray” module within CFD ACE+ permits flow visualization simulation in the unsteady dynamics flow field, similar to smoke wire visualization performed in past wind tunnel experiments[9].

B. MOVING GRID/GRID DEFORMATION

The CFD ACE+ Grid Deformation module is used by the CFD ACE solver to allow for moving/deforming grid problems. The dynamic automatic re-meshing feature supports the standard transfinite interpolation (TFI) scheme to determine the interior node distribution based on the motion of the boundary nodes and is utilized in this study to impose the parametric grid deformation for the time-dependent pitching and plunging motion of the flapping wings.

C. SPRAY INJECTION FOR UNSTEADY FLOW VISUALIZATION

Streaklines in the unsteady flow field can be simulated by physically injecting discrete phase, micro-sized droplets/particles into the free stream. The fluid/particle coupling features should be disabled in this case. The CFD ACE+ spray module can track discrete droplet/particle through the computational domain by solving the Lagrangian equations. The steady state calculations track a particle through its lifetime until it leaves the domain. The local time-step used for integrating the spray equations is estimated based on cell residence time and other applicable criteria. The equation of motion for the droplet can be written as:

$$m_d \frac{du}{dt} = C_D(U - v)|U - v| \frac{A_d}{2} + m_d g + Sm$$

where m_d is the mass of the droplet and $v=ui + vj + wk$ its velocity vector; u , v and w are the Cartesian velocity components; C_d is the drag coefficient; ρ , U and p are the density,

velocity and pressure of the surrounding gas respectively; A_d is the droplet frontal area and V_d is the droplet volume. The gravity vector is represented by g . The equation thus accounts for the acceleration/deceleration of the droplet due to combined effects of drag with gas and body forces such as gravity. The mass source term, S_m is zero in this case. The drag coefficient, C_d for the droplet is a function of the local Reynolds number, which is evaluated as:

$$\text{Re} = \frac{\rho |U - v| d}{\mu}$$

where d is the diameter of the spherical droplet.

D. SIMULATION PROCESS USING CFD ACE+

The basic simulation process using CFD ACE+ is similar to other CFD packages. The geometry and grid generation is done on its pre-processing module- CFD-GEOM; after which the model file is exported to data transfer format (DTF) and the subsequent problem setup is accomplished in the user-friendly CFD-ACE-GUI. Finally, the problem is submitted to CFD-ACE solver for iterative solution generations. CFD VIEW is the post processor for visualization and analysis of results.

E. GRID GENERATION

Modeling of the cambered fixed wing with membrane surface and reflexed at the trailing edge (as shown in Figure 3) requires a mesh that is long in the stream-wise direction, compared to its height. Accurate computation of the boundary layer wake is most easily performed on a C-grid. However, construction of a single-block, C-grid would require a highly skewed grid and an excessive number of grid points in regions far from the airfoil. Furthermore, maintaining grid orthogonality close to the walls using a single-block grid would be difficult. These problems were minimized by using a multi-block grid as shown schematically in Figure 4 where the governing equations are solved in each block separately, and fluid properties at the block boundaries are exchanged at the end of each step.

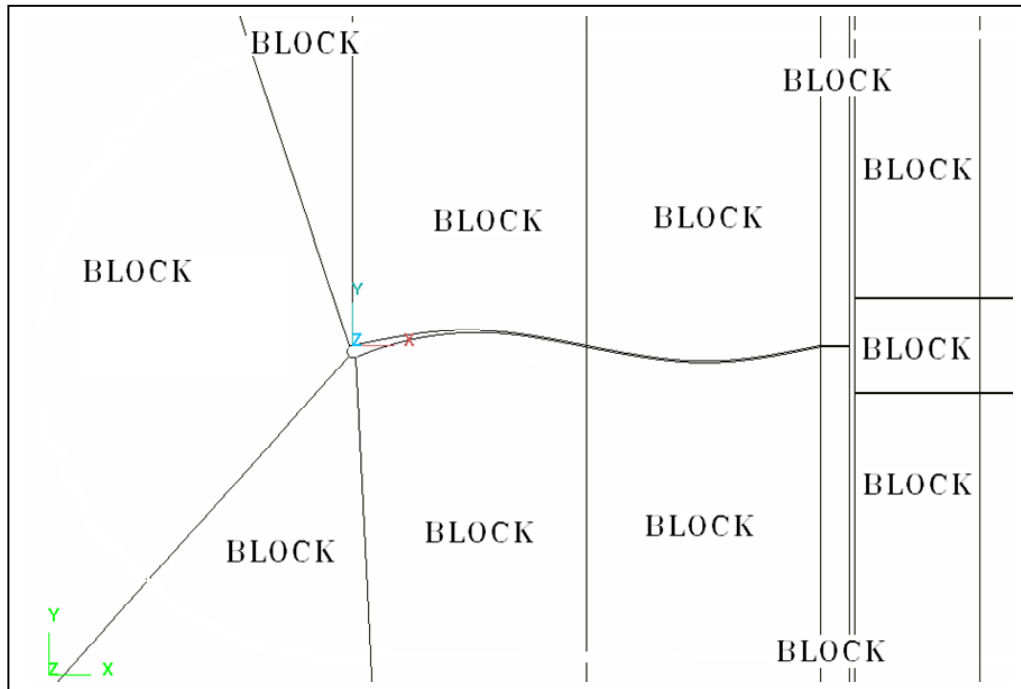


Figure 4. Multi-Block Grid Generation around Wing Bodies

Figure 5 shows the meshing details around the fixed wing. A finer mesh is required near the walls to resolve the boundary layer while the outer grids can be much coarser. In order to reduce the computational effort, the number of cells used was minimized as much as possible. Test cases were performed to determine a suitable outer boundary distance so that the inlet and outlet conditions have negligible effects on the solutions. The grid point distribution is based on hyperbolic tangent and power law. Figure 6 shows the entire computation domain whose total size: 1810mm x 1800mm is gridded with structured meshing. The 2D grid is then extruded 3mm linearly to form solid grid. This thin layer of 3D solid domain will facilitate post processing where wall and interfaces surfaces can be selected directly for study. Following are the model details:

- Total Boundaries : 270
- Total Volumes : 45
- Total Nodes : 98,712
- Total Cells : 46,338
- Total Zones : 45 (45 Structured, 0 Unstructured, 0 Poly)

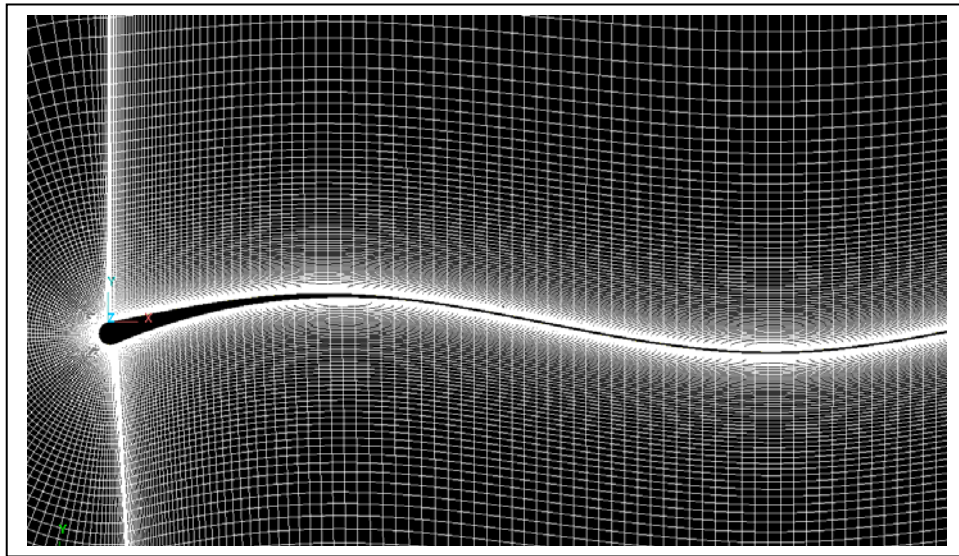


Figure 5. Structured Meshing Around The Fixed Wing

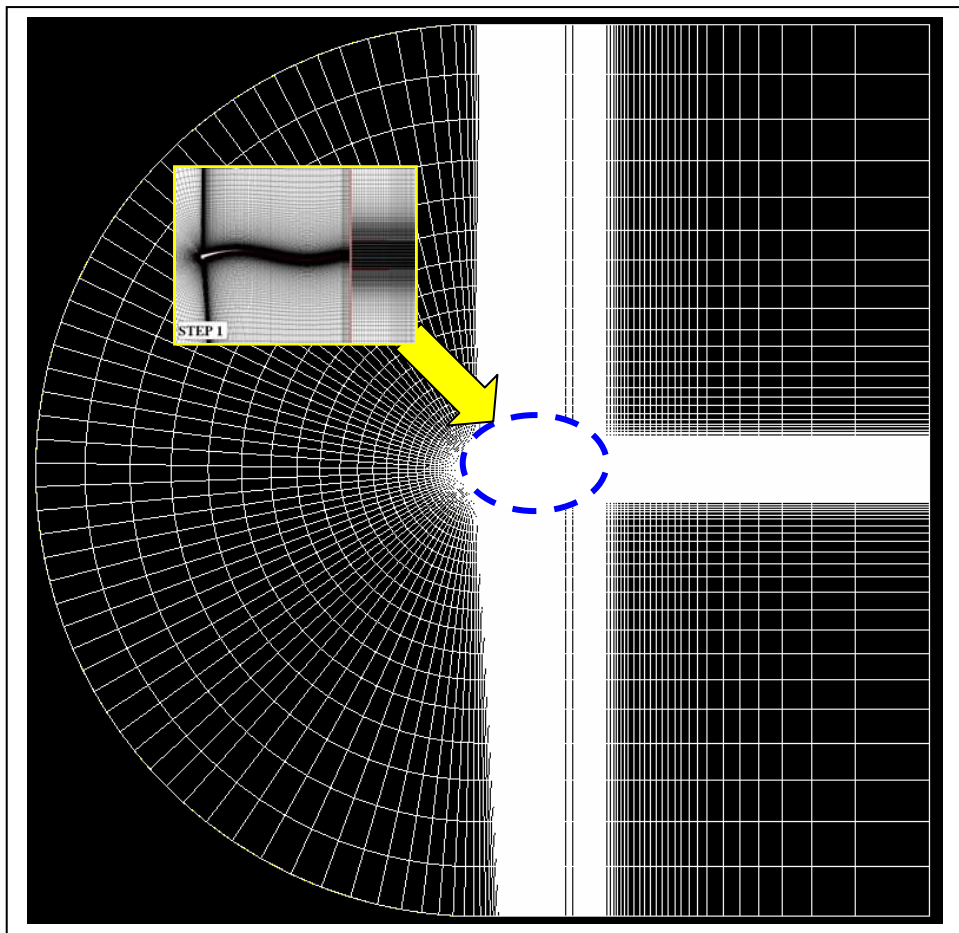


Figure 6. Entire Computational Domain - 1810 x 1800mm

F. BOUNDARY CONDITIONS

This section describes the various key inputs and boundary conditions (BC) used for the simulation. These inputs for the incompressible Navier Stokes flow, grid deformation and the spray problem are different and are elaborated as follows:

1. Boundary Conditions for the Flow Problem

Figure 7 depicts the basic boundary conditions required for the flow problem. The walls are set to no-slip conditions required by the Navier Stokes solution. The out-of-plane and into-the-plane boundaries are set to symmetrical walls. With the flight conditions of 3m/s nominal speed and 10 degrees angle of attack, the inlet boundary (In Flow) thus has velocity components:

$$u = 2.95 \text{ m/s (x axis)}$$

$$v = 0.52 \text{ m/s (y axis)}$$

$$w = 0 \text{ m/s (z axis)}$$

The reference pressure and temperature are set to a constant $P_{\text{ref}} = 100,000 \text{ Pa}$ and 300K respectively. The outlet (Out Flow) boundary has pressure set to the same constant reference pressure. Any back flow temperature is set to 300K . For faster convergence, the initial conditions are set with the same inlet velocity, pressure and temperature.

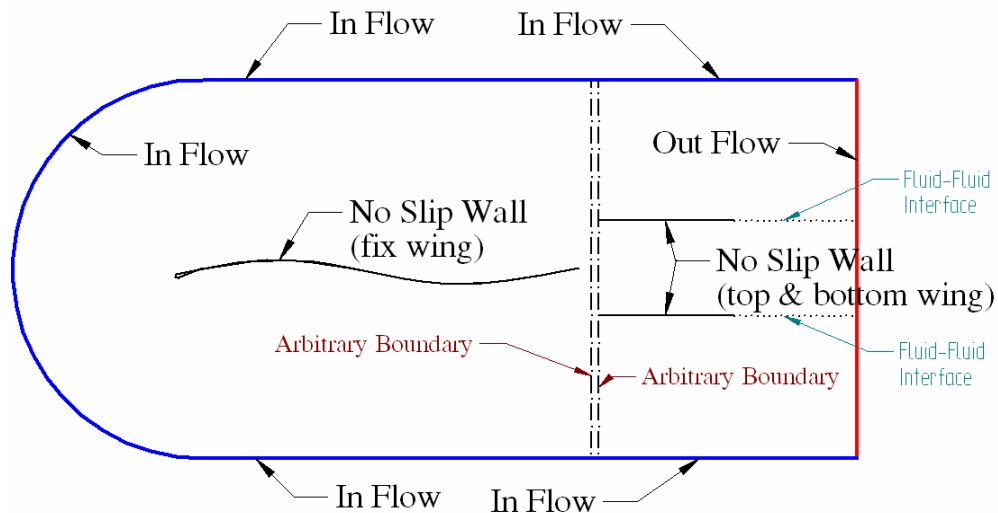


Figure 7. Simulation Model – Schematic Showing Various Boundary Conditions (Not Shown to Scale)

2. Boundary Conditions for Moving/Grid Deformation

The Arbitrary boundary condition is required for the grid deformation solution. A gap of 1.5mm is included between the two arbitrary boundary interfaces as shown in Figure 7. There is no requirement for a node to node matching between these two arbitrary interfaces; however nodal density between the two edges should be as close as possible. The parametric equation of motion required for the walls of the top and bottom flapping wing for two cases of pitch/plunge motion under study are set up using the following simulation parameters:

a. Case of Pitch/Plunge 90° Out of Phase at Flapping Frequency, $f=25\text{Hz}$

In this case, the flapping model has an initial starting position at minimum separation distance of 30mm as illustrated in Figure 3. The plunge amplitude H is fixed at 1.5cm, pitch amplitude $\Phi=10^\circ$, 15° and 20° , respectively. The pivot axis for the pitching motion is defined with coordinates located at a distance of $0.125c$ (or 5mm) ahead of the flapping wing leading edge.

A graphical illustration of the pitch, plunge phase relationship for the case of $\Phi=10^\circ$ is shown in Figure 8 below.

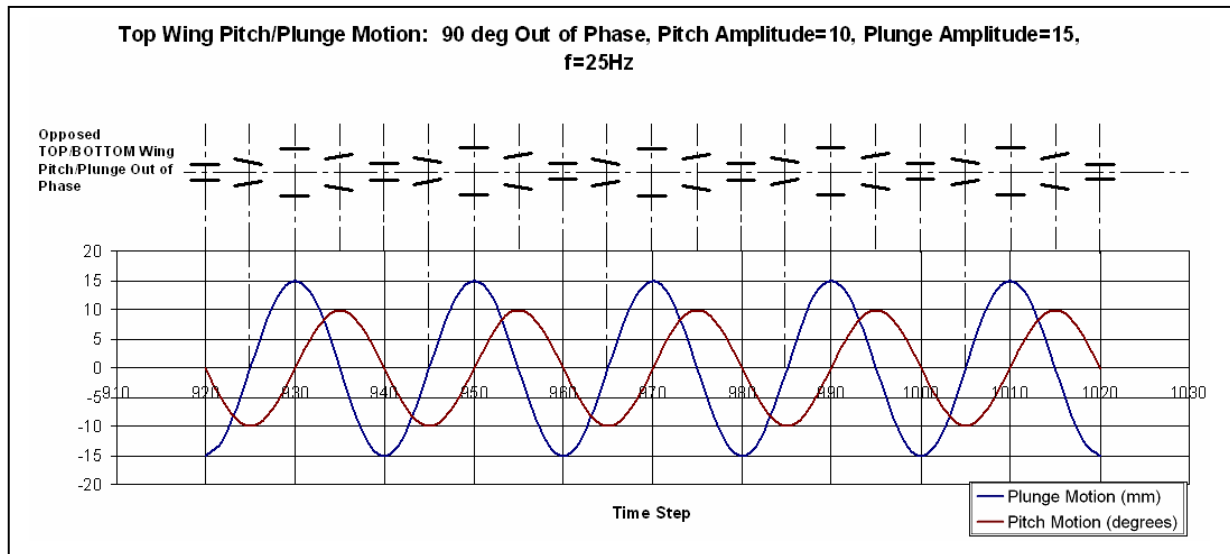


Figure 8. Pitch/Plunge Phase Relationship: Bottom Curves Show the Plunge Vs Pitch Motion as a Function of Time Step.

b. Case of Pitch/Plunge Motion in Phase, Flapping Frequency, $f=25\text{Hz}$

In this test case, the flapping model has an initial starting position at the neutral position. The separation distance between the flapping wings is 82.5mm. The plunge and pitch amplitude are fixed at 1.5cm and 10° respectively.

c. Moving Boundary Conditions For Fluid-Fluid Wake Interfaces

The fluid-fluid wake interfaces directly aft of the flapping wings have a plunging motion constraint that is similar to the corresponding flapping wing so that these fluid volumes will also move together with the wings during the simulations. In this case, the problem with negative volume encounter is minimized. However the pitching motion constraint is not necessary.

3. User Input for Spray Problem

The spray injection coordinates are located 50mm ahead of the fixed wing leading edge and configured in a single column with a separation distance of 1cm between the injectors. Key inputs for the spray problem setup are as follows:

Spray model	: Incompressible, Drag model
Material/size	: Liquid – H ₂ O, 50 μm
Velocity	: zero (release velocity)
Injector type	: Point Injector
Trajectory History	: Enabled
Spray/Fluid Coupling	: Disabled
Coordinate	(see Figure 9, Origin is located at the fixed wing leading edge)

Injector #	Coordinates		
	x	y	z
1	-0.05	0.06	-0.0015
2	-0.05	0.05	-0.0015
3	-0.05	0.04	-0.0015
4	-0.05	0.03	-0.0015
5	-0.05	0.02	-0.0015
6	-0.05	0.01	-0.0015
7	-0.05	0.00	-0.0015
8	-0.05	-0.01	-0.0015
9	-0.05	-0.02	-0.0015
10	-0.05	-0.03	-0.0015
11	-0.05	-0.04	-0.0015
12	-0.05	-0.05	-0.0015

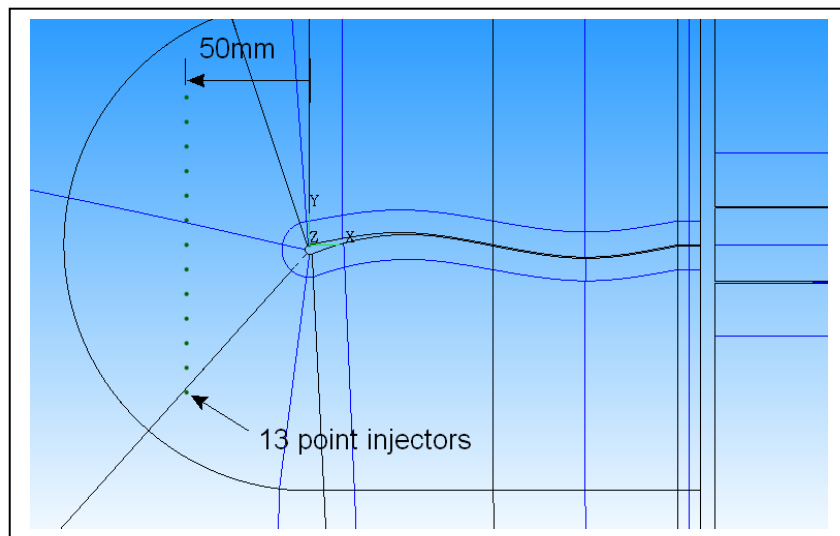


Figure 9. Location of Spray Injector for Unsteady Flow Visualization (Image Captured from CFD ACE GUI Environment)

G. SOLUTION PARAMETERS

The required solution setup has the following key setting:

D1. Transient Conditions

No. of Steps : 1020
 Time Steps : 0.002
 Time Accuracy : Crank Nicolson (2nd Order)
 Blending Factor : 0.6

D2. Solver Control Parameters

Max. Iteration : 50

Convergence Crit : 0.0001

Solver : Velocity – CGS+Pre

P correction – AMG

Output : Print – Force Summary

Graphic – Velocity vector, Velocity magnitude,

Static/Total Pressure, Vorticity

Spray – Velocity magnitude, Trajectory History

Other parameters are set to defaults.

The problem setup is then submitted to solver for solution generation.

THIS PAGE INTENTIONALLY LEFT BLANK

IV. VERIFICATION OF THE DYNAMIC SIMULATION MODELS

The simulation model consists of less than 100,000 nodes. The output file size per time step is about 10.5 MB. Given the solution converges rather rapidly, with the maximum of 50 iterations per time step and running on the laboratory Pentium 4 PC, the full solution generation typically takes less than 2 days to complete. Before the commencement of the full simulation, the moving/grid deformation problem is executed without the flow and spray solution. This is a crucial step in the simulation process. A common error message encountered is caused by “negative volume” due to grid distortion. In this case, the mesh may have to be rectified or the arbitrary gap adjusted. After successful execution of the moving/grid deformation problem, the transient flow and spray injection problems are then executed. The following shows the results of the moving/grid deformation verifications process for a sample test case.

A. VERIFICATION OF THE DYNAMIC MESHING MODEL

The verification of the moving/grid deformation solution involved verifying the geometrical and harmonic relationship between the pitching and plunging motion.

The following plots show the rigid body kinematic solution of the moving/grid deformation run. In this test case, the plunge amplitude H is 15mm, the pitching amplitude is 10° . The pitch and plunge motion is 90° out of phase. The cycle starts with the initial configuration of the flapping wing at the minimum separation distance of 30mm. Each time step is 2ms. For a flapping frequency of 25 Hz, each flapping cycle will therefore consist of 20 steps.

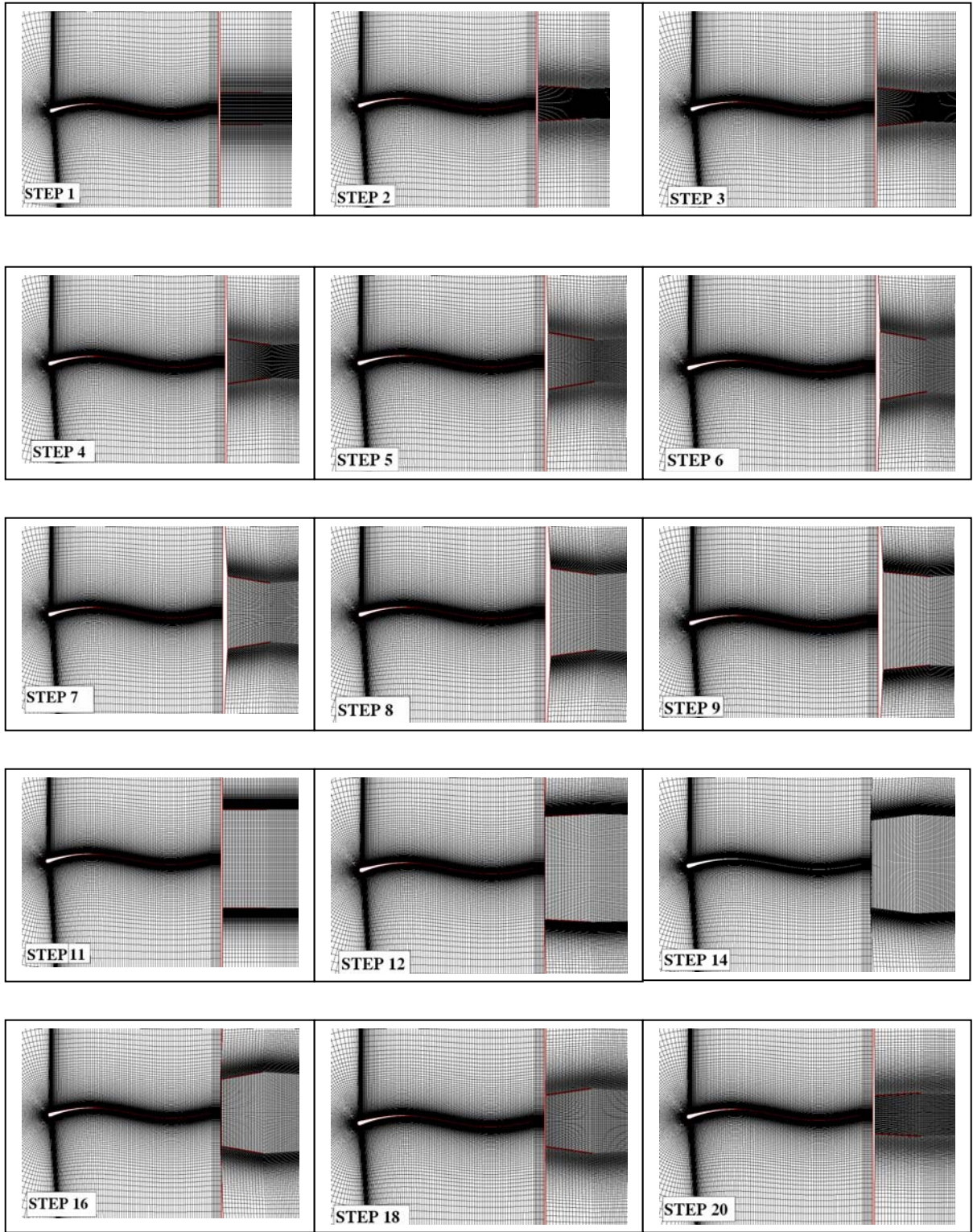


Figure 10. Plots showing the Rigid Body Kinematic Solution of the Moving/Grid Deformation Run. ($H=15\text{mm}$, $\Phi=10^\circ$, $f=25\text{Hz}$, Pitch Leads Plunge by $\pi/2$)

B. VERIFICATION OF THE MOVING /GRID DEFORMATION SOLUTION

This test case simulation was performed in order to verify the dynamic meshing solution. Instead of the flapping wings rigid wall boundaries, they are replaced with fluid-fluid interfaces which are perfectly porous, and the prescribed kinematic motions of the flapping wings were applied to these fluid interfaces instead. Figure 11 shows the various snap shots of the vorticity distribution from time step 480 to 500, at inlet condition of 3m/s, 10° angle of attack. These results concluded that the dynamic meshing solution did not caused significant disturbances to the solution aft of the fixed wing.

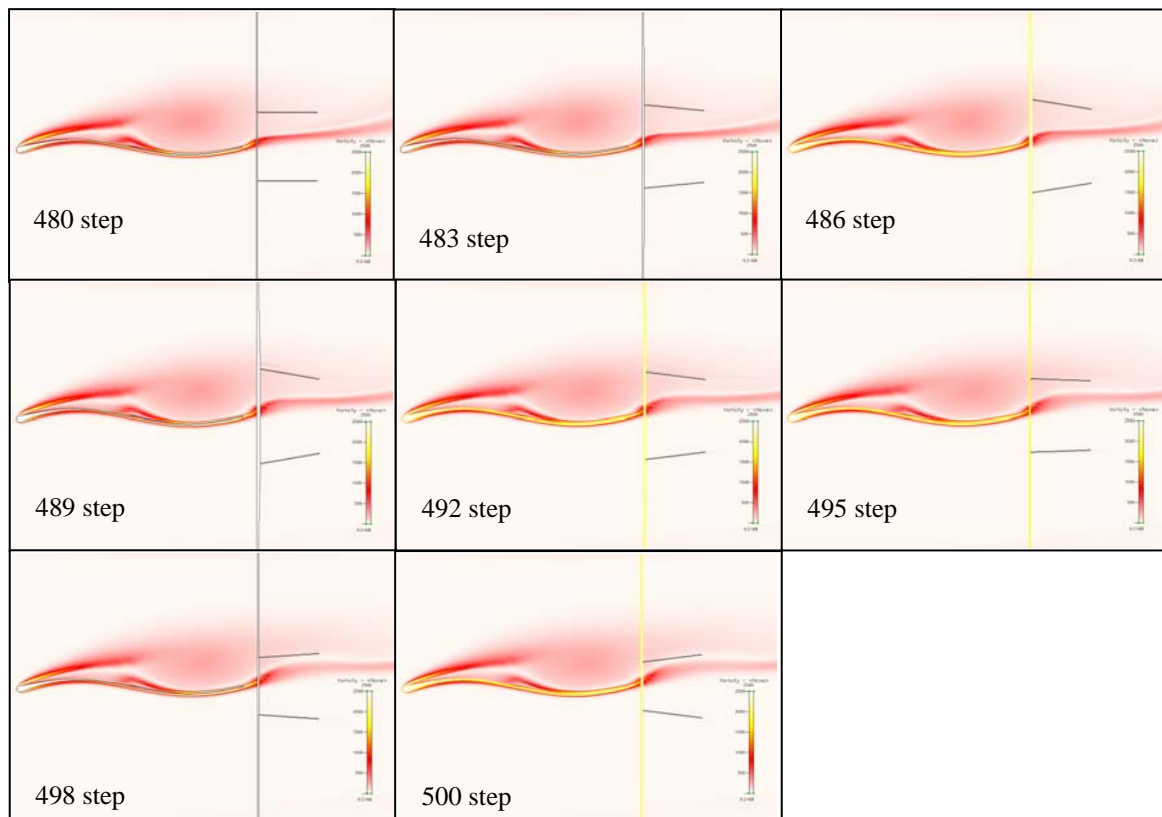


Figure 11. Solution of Vorticity Distribution at Various Meshing Sequences.
(Moving/Grid Deformation Setup: $H=15\text{mm}$, $\Phi=10^\circ$, $f=25\text{Hz}$, Pitch Leads Plunge by $\pi/2$)

THIS PAGE INTENTIONALLY LEFT LANK

V. RESULTS

A. SOLUTION RESIDUAL PLOT

The solutions converge rather rapidly in both cases. Figures 12 and 13 show typical residual plots during the simulation runs. The maximum number of iterations is set to 50 with convergence criteria set to 0.0001. In case of slow convergence for any of the variables, one can decrease the inertial under relaxation (from 0.2 to say 0.02) for that variable. The z velocity, w , is present because the simulation model is a thin 3D model as mentioned earlier, but it is essentially machine zero.

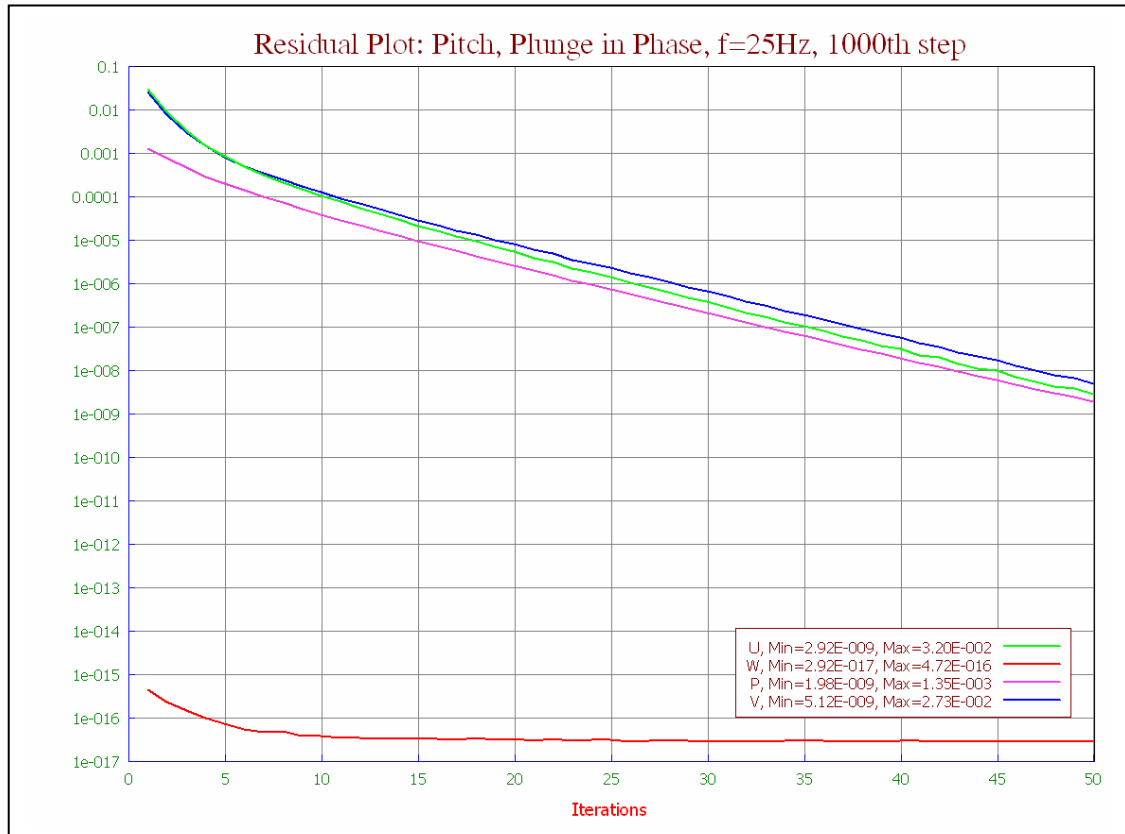


Figure 12. Residual Plot: Case of Pitch/Pitch in Phase, $U_\infty = 3\text{m/s}$, $\alpha=10^\circ$, $f=25\text{Hz}$, 1000th Time Step

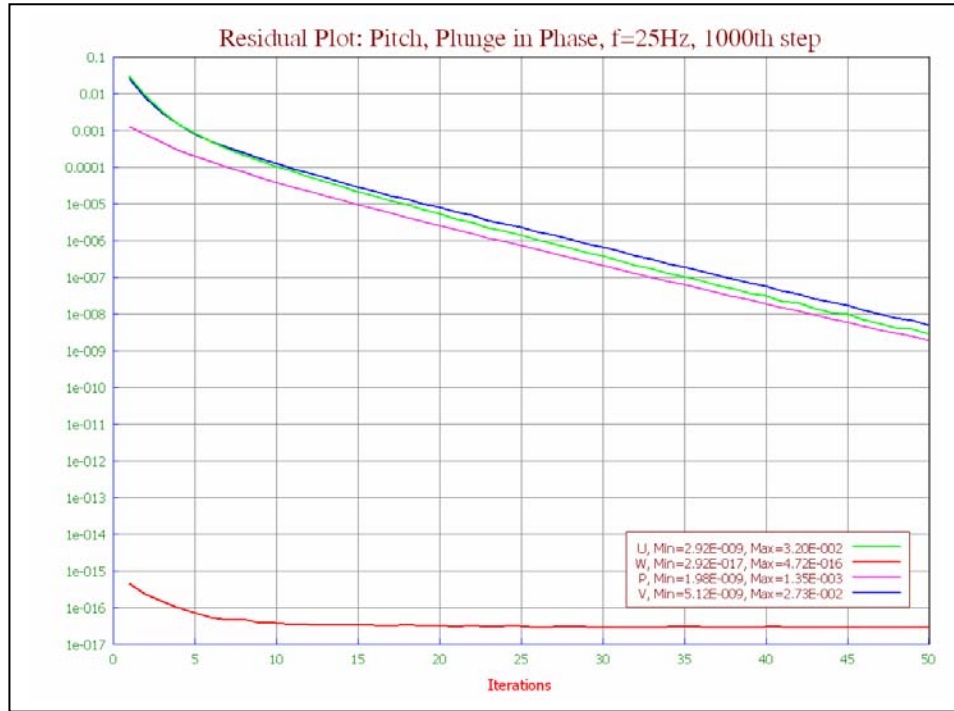


Figure 13. Residual Plot: Case of Pitch/Plunge 90° Out of Phase, $U_\infty = 3\text{m/s}$, $\alpha = 10^\circ$, $f = 25\text{Hz}$, 1000th Time Step

B. SIMULATION TEST CASE: NON-FLAPPING

This simulation result is based on the non-flapping case (ie., $f = 0\text{ Hz}$) where the flapping wings are held at the neutral position with separation distance of 82.5mm . The test case for this transient incompressible Navier-Stokes solution is based on the 3m/s flight at 10° angle of attack. The ‘steady state’ results at the 940^{th} to 1000^{th} time steps were analyzed. Sample plots are shown in Figures 14 and 15. As expected, the regions of high vorticity are concentrated at the leading and trailing edges. It should be noted that these plots only show snap-shot behavior of the active shedding process, the actual flow field is never static; indeed subsequent data analysis revealed that the shedding process is highly periodic, with nearly constant frequency and very small standard deviation (see Appendix B on variation in standard deviations for various simulation cases.)

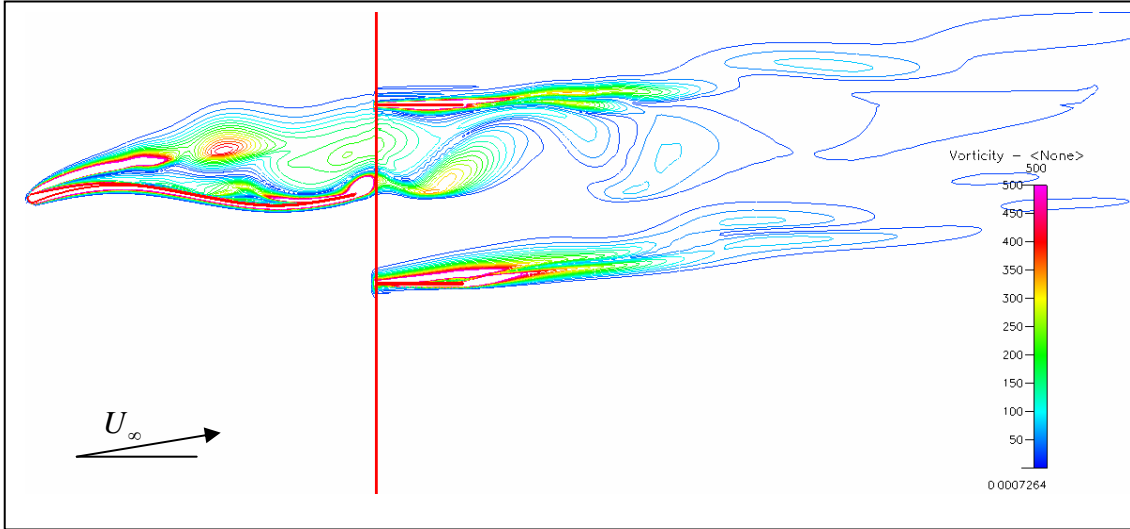


Figure 14. Vorticity Distribution (Transient Vorticity Field at 1000th step, $U_\infty = 3\text{m/s}$, $\alpha = 10^\circ$, $f = 0\text{ Hz}$,)

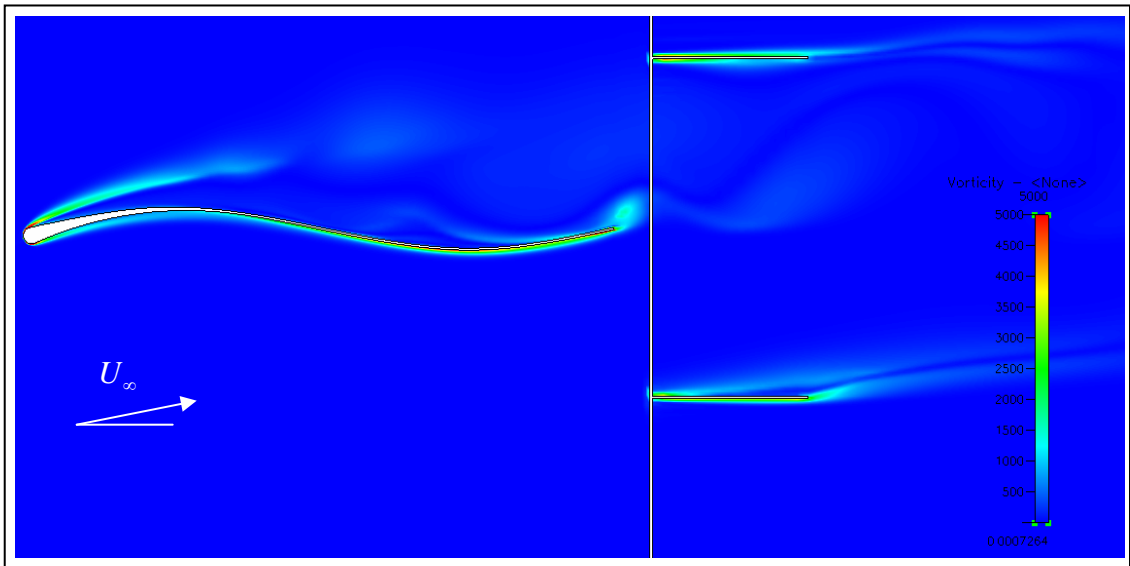


Figure 15. Vorticity Distribution (Transient Vorticity Field at 1000th step, $U_\infty = 3\text{m/s}$, $\alpha = 10^\circ$, $f = 0\text{ Hz}$)

Figure 16 shows the corresponding velocity magnitude distribution. Flow separation occurs immediately aft of the leading edge of the fixed wing. The regions of flow separation and recirculation zones can be deduced through typical velocity vector plots, as shown in Figure 17. Subsequent flow visualization simulation results also confirmed these deductions.

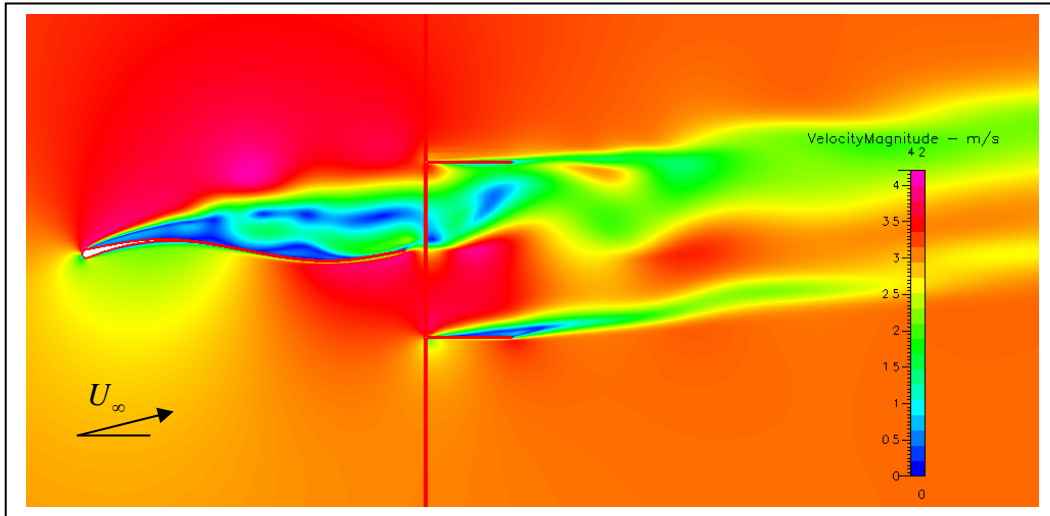


Figure 16. Velocity Magnitude Field (Transient Flow Field at 1000th step, $U_\infty=3\text{m/s}$, $\alpha=10^\circ$, $f=0\text{Hz}$)

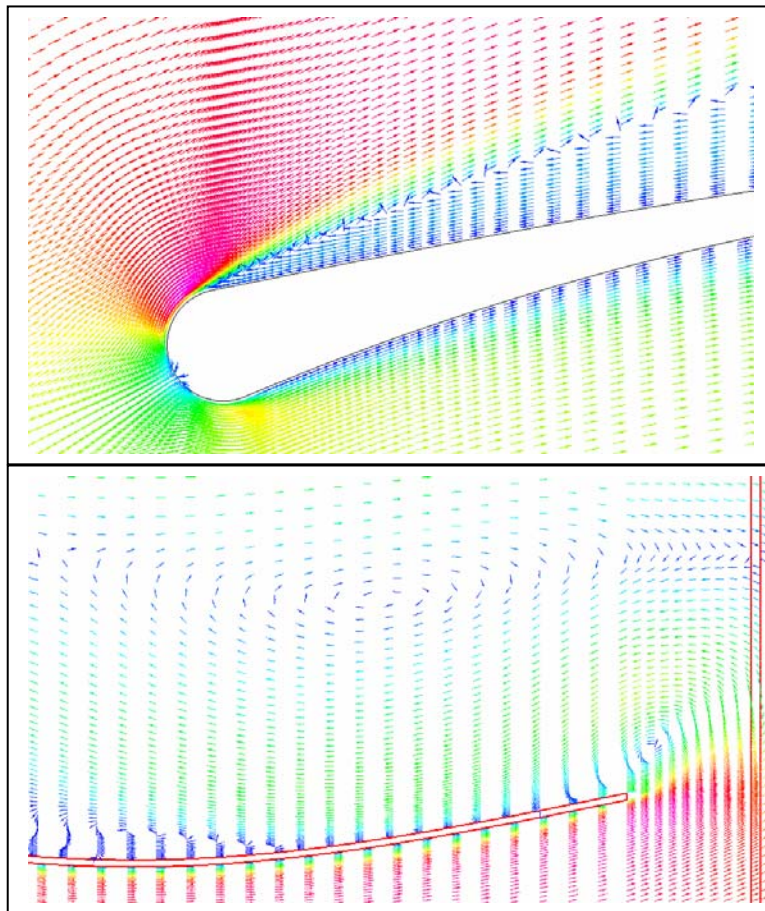


Figure 17. Velocity Field at the Leading and Trailing Edge of the Fixed Wing (Transient Flow Field at 1000th step. $U_\infty=3\text{m/s}$, $\alpha=10^\circ$, $f=0\text{Hz}$)

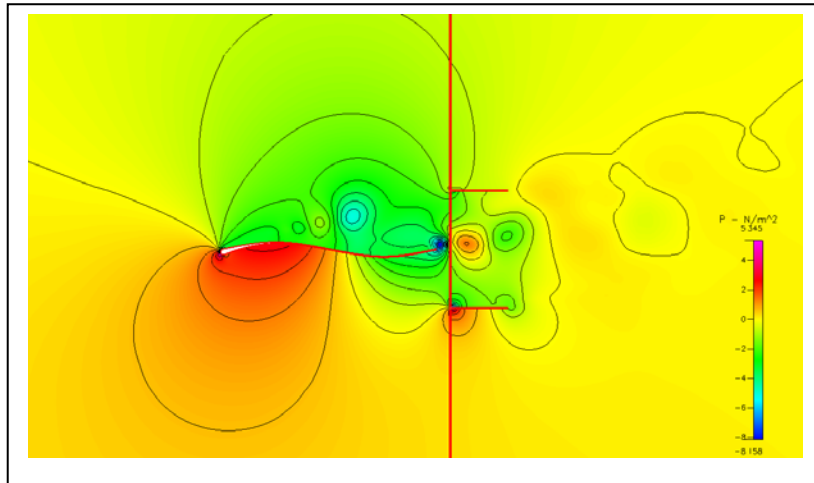


Figure 18. Pressure Field of the Multi-Wing Configuration (Transient Flow Field at 1000th step, $U_\infty=3\text{m/s}$, $\alpha=10^\circ$, $f=0\text{Hz}$)

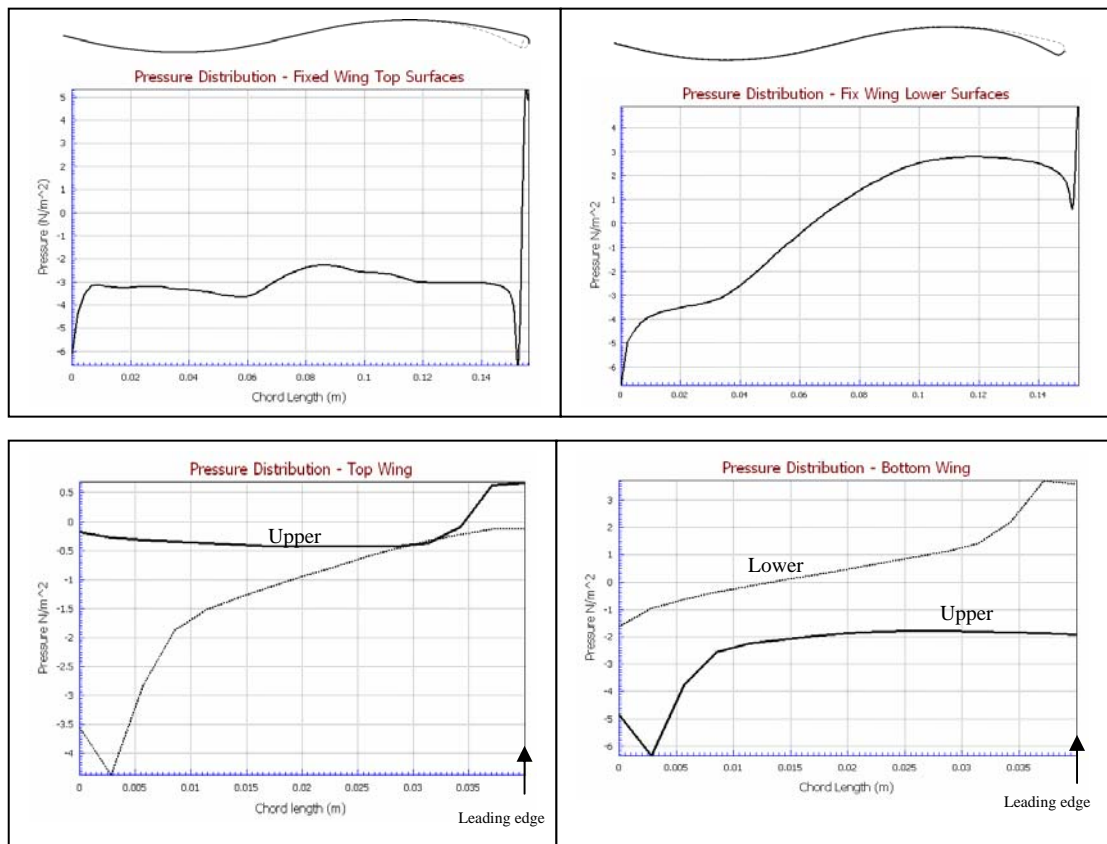


Figure 19. Pressure Distribution of the Fixed and Flapping Wing Surfaces (Transient Solution at 1000th step, $U_\infty=3\text{m/s}$, $\alpha=10^\circ$, $f=0\text{Hz}$)

Figure 18 shows the pressure distribution/contour plot. As expected, higher pressure is experienced near the leading edge on the lower surface of the fixed wing. Flow field interaction between the wake of the fixed wing and the top wing caused large variation in pressure distribution on the top wing surfaces. Figure 19 shows the pressure distribution with respect to wing chord for the various wings. It should be noted that these results only correspond to the particular snap shot at 1000th time step. The actual flow behavior is very unsteady. The following detailed analysis exemplifies this flow phenomenon.

1. Lift and Drag History of Non-Flapping Case

The presented lift and drag are the summation of all of the vertical and horizontal forces respectively that are experienced by the walls of the wings when the MAV is subjected to the nominal forward speed of 3m/s at a 10° angle of attack; this includes the pressure and shear forces. It should be noted that the convention used for the “lift” and “drag” forces in this report is with respect to the modeling coordinate system’s vertical and horizontal direction respectively, and that the free stream velocity is inclined, instead of horizontal. The presented forces are for 1m-span wings. These force components can be output to an ASCII file at the end of the simulation through activating the force summary features prior to the solution generation process. The plots show periodic fluctuations ($f = 21\text{Hz}$) which are typical of transient forces caused by unsteady vortex shedding from the wing surfaces. In this case, the flapping wings are located at the neutral position as shown in Figure 20. Figure 21 shows the lift variation with respect to time due to the various wings. As expected, the fixed wing provided a relatively significant amount of lift. The combined effect of the top and bottom flapping wings further contributed to the overall lift, thereby resulting in an increase in the combined lift magnitude. Figure 22 shows that for the non-flapping case, the combined drag is positive and that the drag induced by the bottom wing is the least. This is logical as the bottom wing is situated at location relatively undisturbed by the wake of the fixed wing.



Figure 20. Simulation Model of Non-Flapping Case

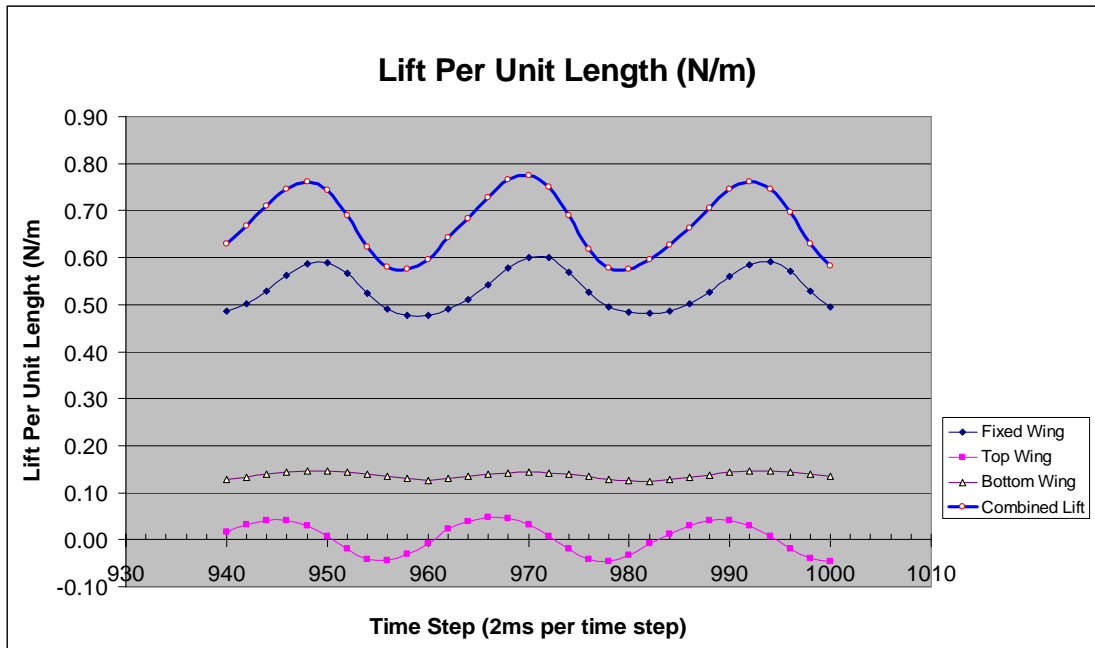


Figure 21. Lift per Unit Length ($U_\infty=3\text{m/s}$, $\alpha=10^\circ$, $f=0\text{Hz}$)

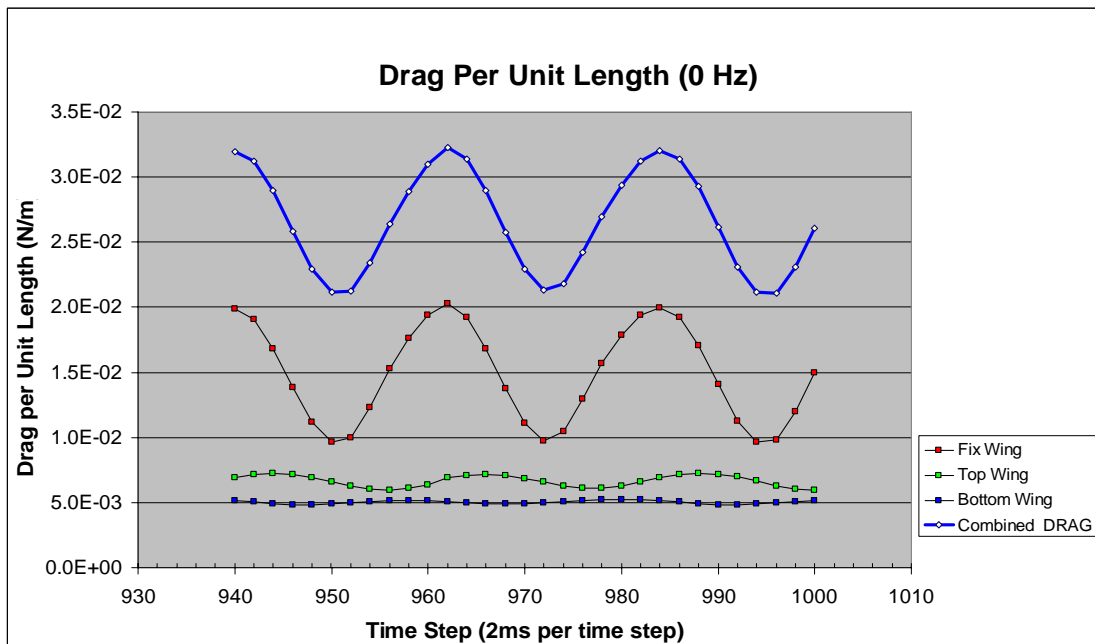


Figure 22. Drag per Unit Length ($U_\infty=3\text{m/s}$,)

2. Flow Visualization for Non-Flapping Case

The non-flapping test case simulation solution for the spray problem was studied qualitatively. Figure 23 shows the streaklines at the 1000th time step. The wake structure and the re-circulated motion of the spray particles at the separation zones seems to agree with experimental observations (wrt. Figure 24, extracted from [2]).

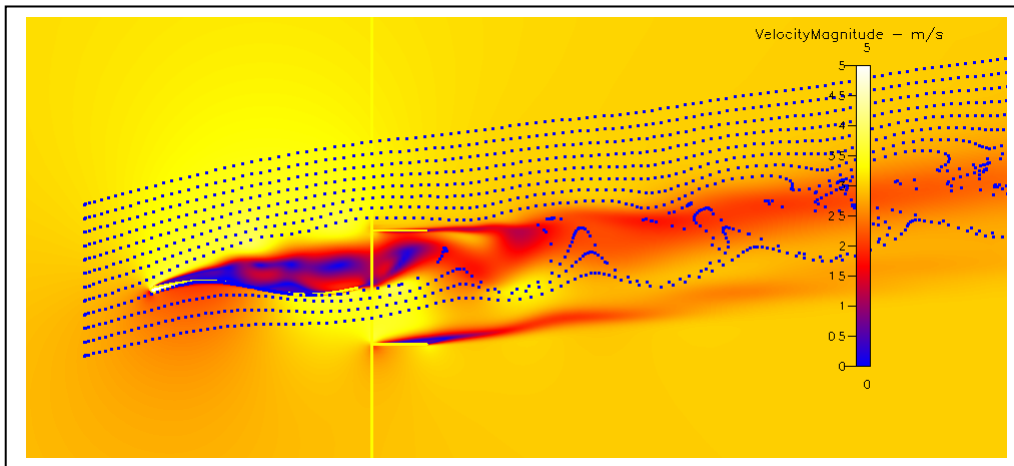


Figure 23. Flow Visualization Simulations - Shows Streaklines at 1000th Time Step ($U_\infty = 3\text{m/s}$, $\alpha=10^\circ$, $f=0\text{Hz}$)

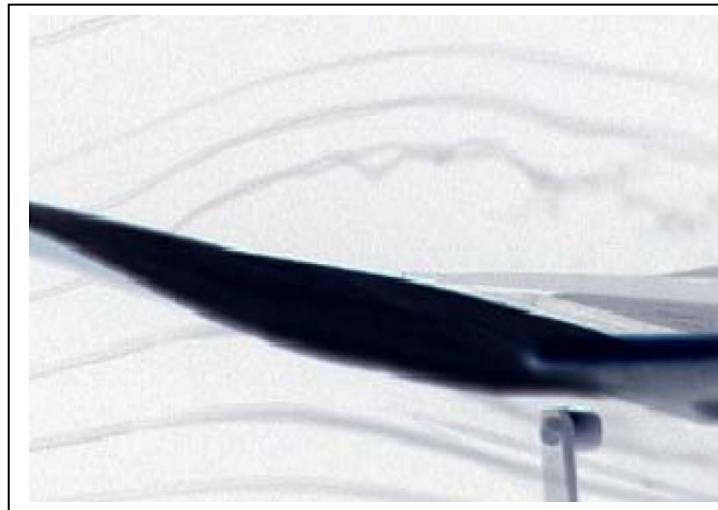


Figure 24. Experimental Flow Visualization - Showing Flow Separation Immediately After Leading Edge for the case of $U_\infty = 2\text{m/s}$, $\alpha=15^\circ$, $f=0\text{Hz}$. (From: [2]).

C. SIMULATION TEST CASE: ZERO INLET VELOCITY

The following test case was performed with $U_\infty=0$ while the flapping wings were set to flap with frequency 25Hz, pitch amplitude 10° , plunge amplitude 15mm, and 90° phase angle between pitch/plunge. The lift and drag history plots are shown in Figures 25 and 26 respectively. A net negative drag is equivalent to a positive thrust due to the effect of the flapping motion.

1. Lift and Drag History of Flapping Case with $U_\infty=0$

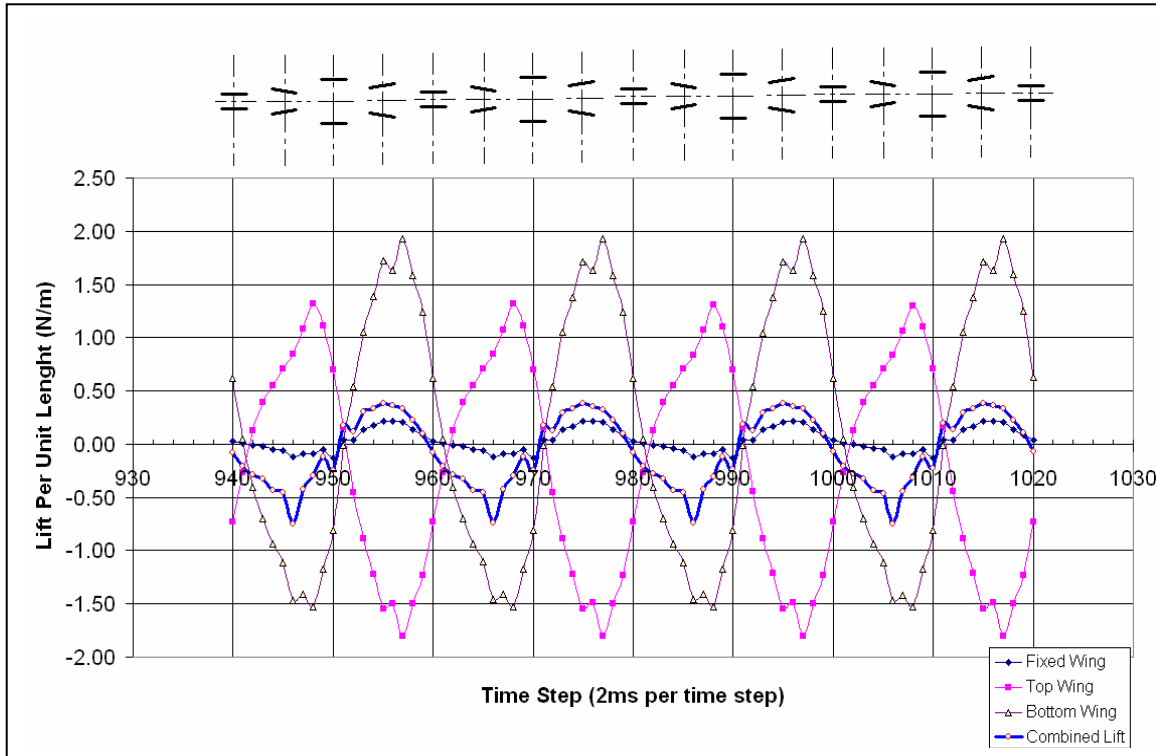


Figure 25. Lift History with $U_\infty=0$, $f=25\text{Hz}$, $\Phi=10^\circ$, $H=15\text{mm}$, Pitch/Plunge 90° Out of Phase.

It was noted that the lift profile generated by the top and bottom wing are almost mirror image of each other since they are performing symmetrical motions. This however would not be the case when subjected to non-zero free stream velocity due to wake interference on the upper wing. It was noted also that the main wing is producing a small lift in this case, due only to flow entrained by the flapping wings.

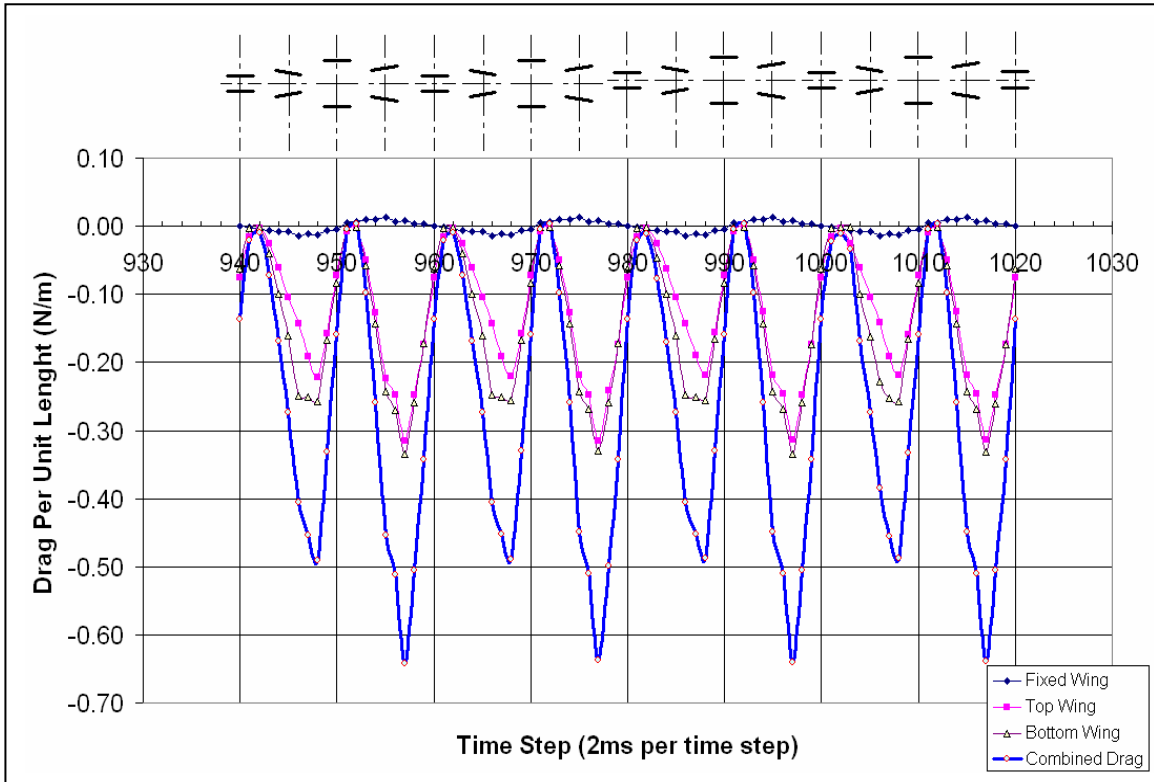


Figure 26. Drag History with $U_\infty=0$, $f=25\text{Hz}$, $\Phi=10^\circ$, $H=15\text{mm}$, Pitch/Plunge 90° Out of Phase.

The drag shown in Figure 26 indicates that the drag induced by the top and bottom wings is almost the same. Again, a different behavior should be observed in the case of non-zero free stream velocity. Also it was noted that more thrust is produced as the wings come together than when they pull apart. This might indicate some optimization possibility with a slight change in mean angle of attack of the flapping wings.

2. Flow Visualization for Flapping Case with $U_\infty=0$

Flow visualization shows that the flapping motion created a suction force to induce the spray particles which are released with zero velocity, to flow over the fixed wing. This is indicative of a lift generation on the fixed wing. On the other hand, the C-shaped structures in the wake are indicative of higher ‘exhaust velocity’ resulting from thrust production.

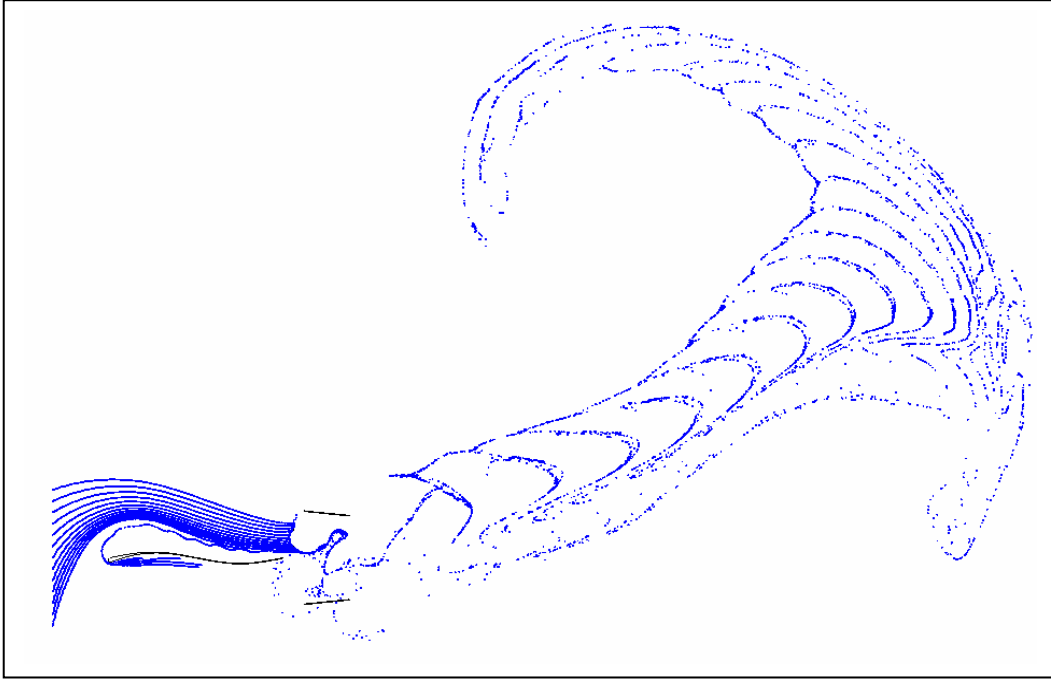


Figure 27. Flow Visualization for the Case of $U_{\infty}=0$, $f=25\text{Hz}$, $\Phi=10^\circ$, $H=15\text{mm}$, Pitch/Plunge 90° Out of Phase.

D. FULL SIMULATION RESULTS

The following section presents the full simulation results which involves the complete Navier-Stokes flow, spray and moving/grid solutions.

1. Full Flapping Wing Configuration: $U_{\infty}=3\text{m/s}$, $\alpha=10^\circ$, $f=25\text{Hz}$, $H=15\text{mm}$, $\Phi=10^\circ$, Pitch/Plunge Out of Phase

The results are shown in Figures 28 to 30. Various trends were noted as follows:

- Lift and drag peaks at the same time.
- Lift generated by the upper and lower flapping wings are nearly mirror images of each other but the lower wing performs better since it has a cleaner inflow.
- Thrust generated by the lower flapping wing is higher than that of the upper flapping wing.
- Lift from the fixed wing is significantly higher when the flapping wings are producing thrust, with peak lift corresponding to peak thrust.
- Larger streaklines turn angle as compared to the non flapping case.

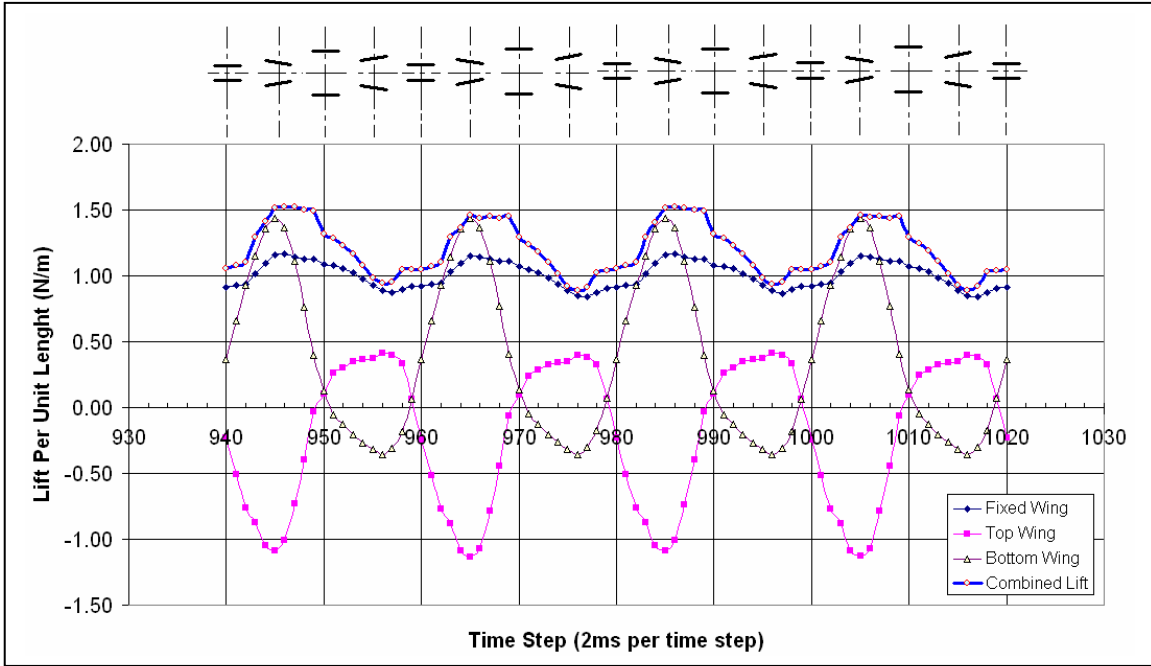


Figure 28. Lift History: $U_{\infty}= 3\text{m/s}$, $\alpha=10^{\circ}$, $f=25\text{Hz}$, $H=15\text{MM}$, $\Phi=10^{\circ}$, Out of Phase.

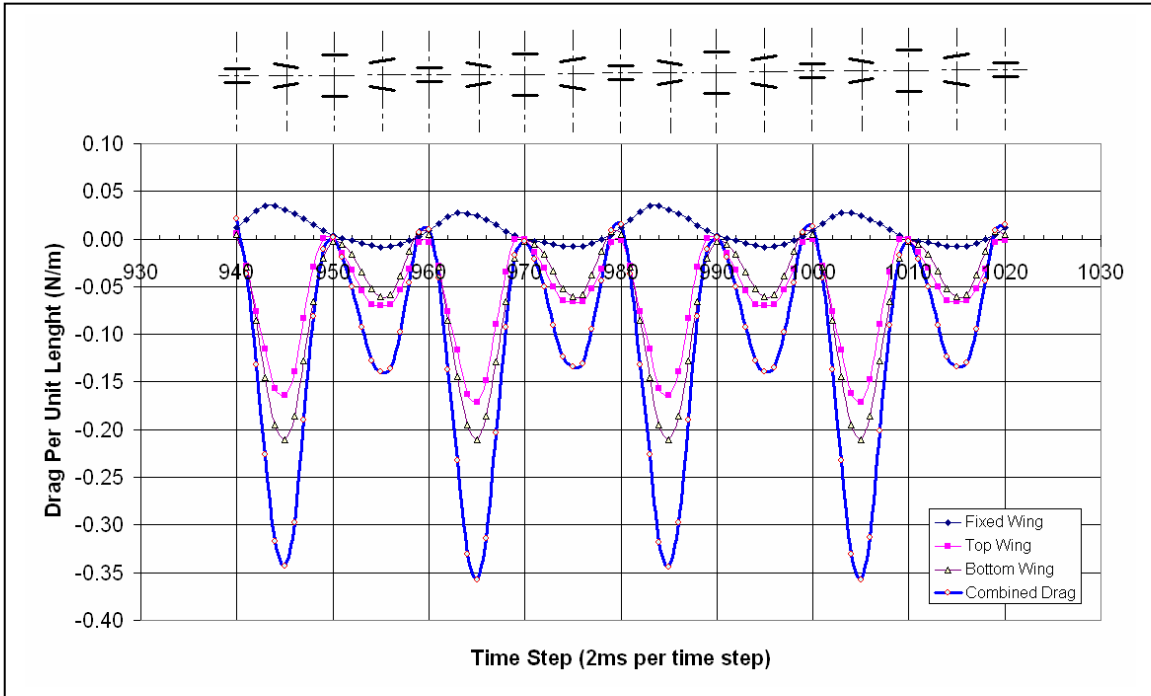


Figure 29. Drag History: $U_{\infty}= 3\text{m/s}$, $\alpha=10^{\circ}$, $f=25\text{Hz}$, $H=15\text{MM}$, $\Phi=10^{\circ}$, Out of Phase.

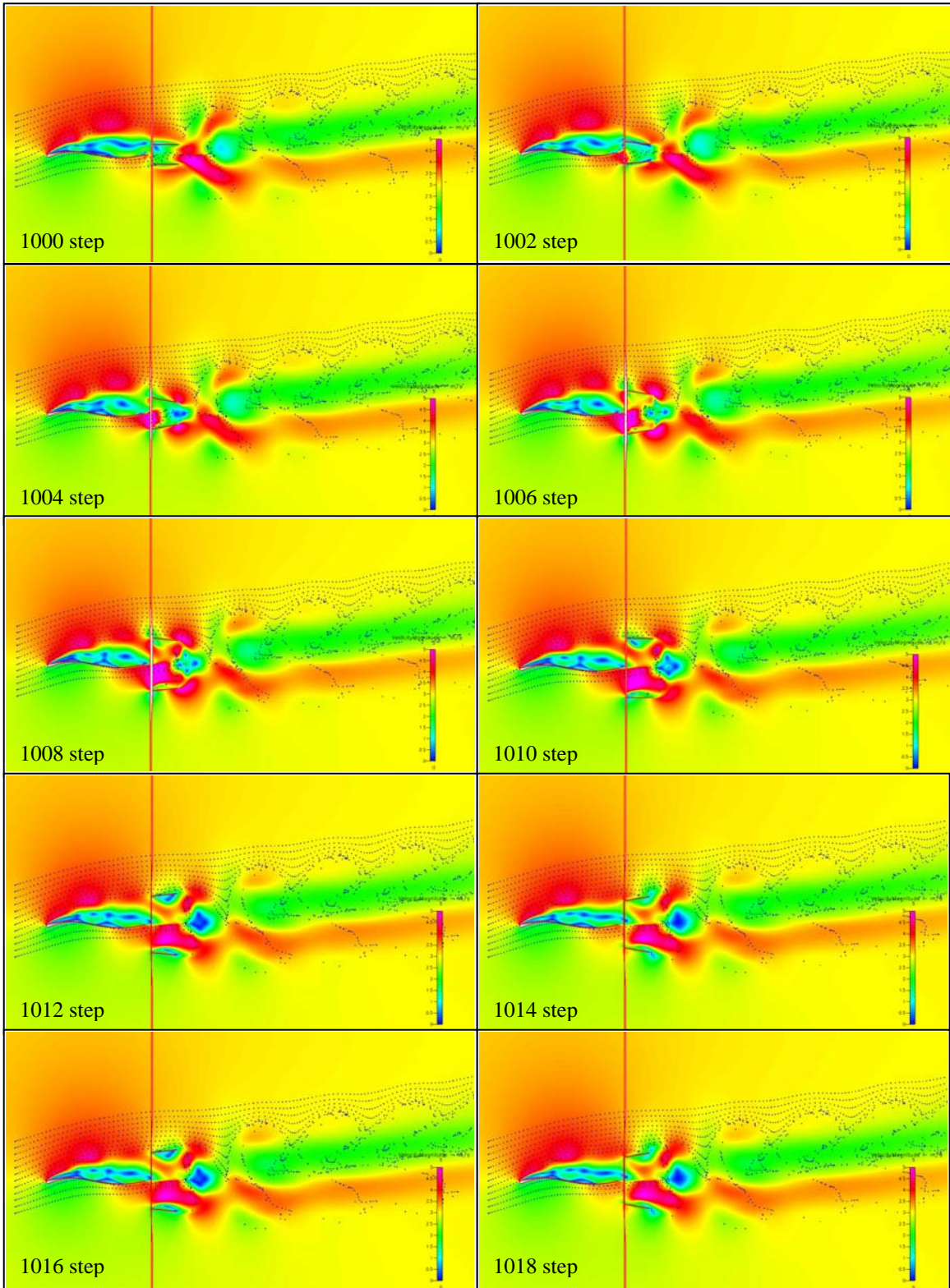


Figure 30. Velocity Field with Streaklines from Time Step 1000 - 1018: ($U_{\infty}= 3\text{m/s}$, $\alpha=10^\circ$, $f=25\text{Hz}$, $H=15\text{MM}$, $\Phi=10^\circ$, Out of Phase.)

2. Full Flapping Wing Configuration: $U_\infty=3\text{m/s}$, $\alpha=10^\circ$, $f=25\text{Hz}$, $H=15\text{mm}$, $\Phi=15^\circ$, Pitch/Plunge Out of Phase

The results are shown in Figures 31 to 33. Almost identical behavior was observed in the force histories, but now with slightly higher peaks. The streakline turning angles appears to be slightly greater. The velocity magnitude fields have also intensified.

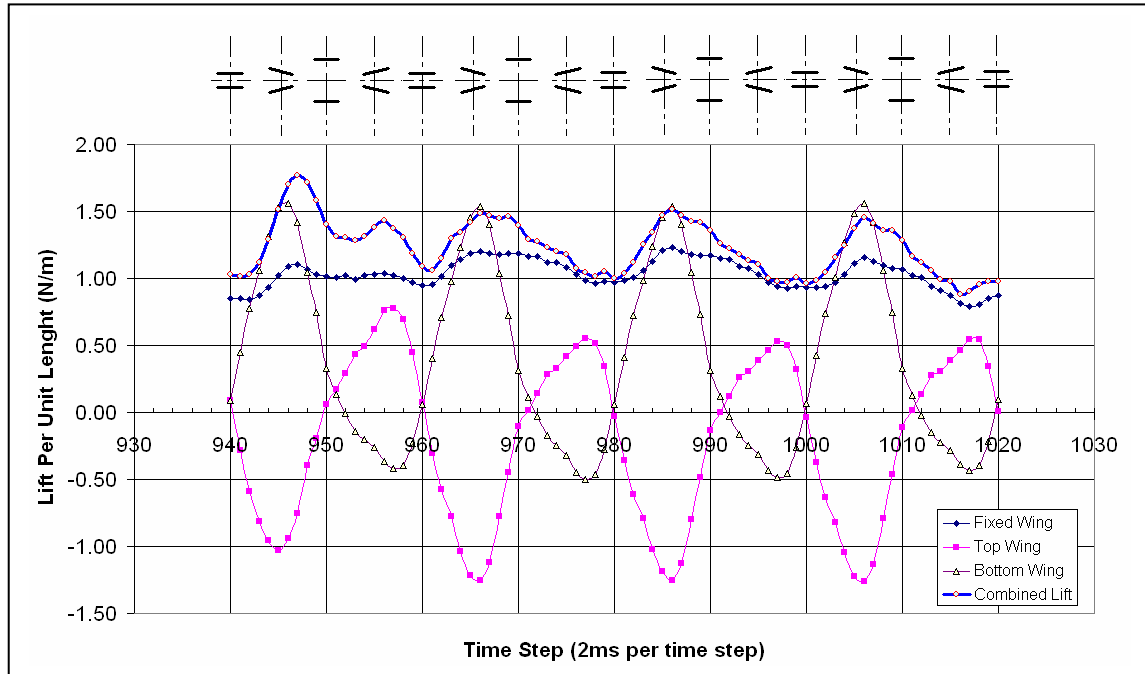


Figure 31. Lift History: $U_\infty= 3\text{m/s}$, $\alpha=10^\circ$, $f=25\text{Hz}$, $H=15\text{MM}$, $\Phi=15^\circ$, Out of Phase.

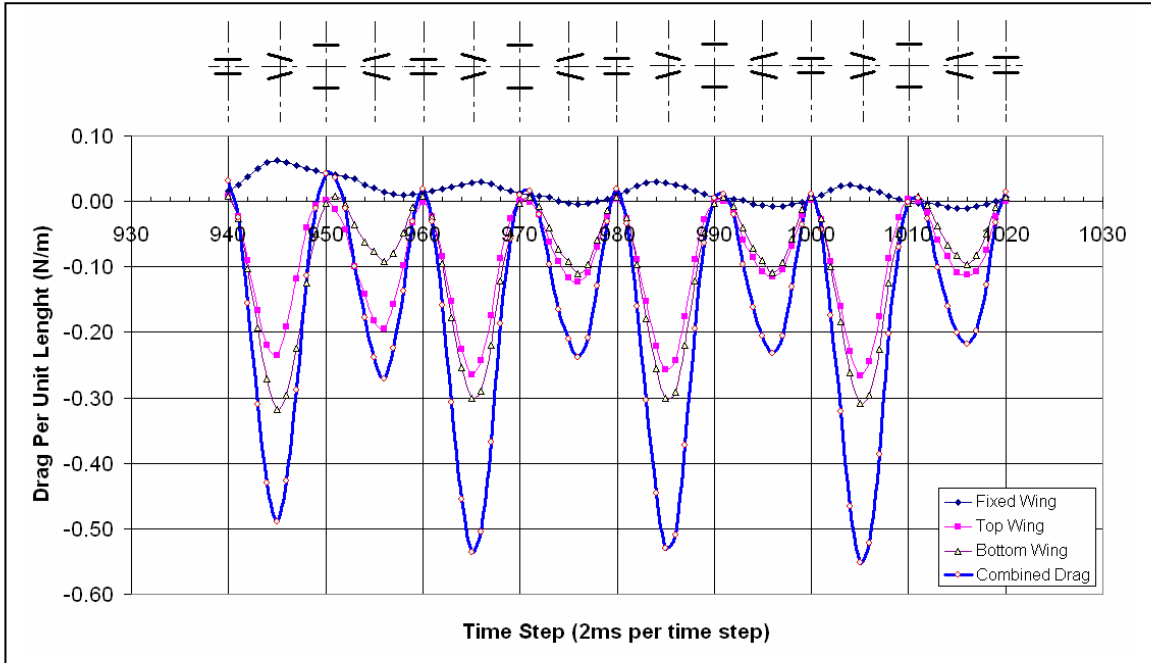


Figure 32. Drag History: $U_{\infty}= 3\text{m/s}$, $\alpha=10^{\circ}$, $f=25\text{Hz}$, $H=15\text{MM}$, $\Phi=15^{\circ}$, Out of Phase.

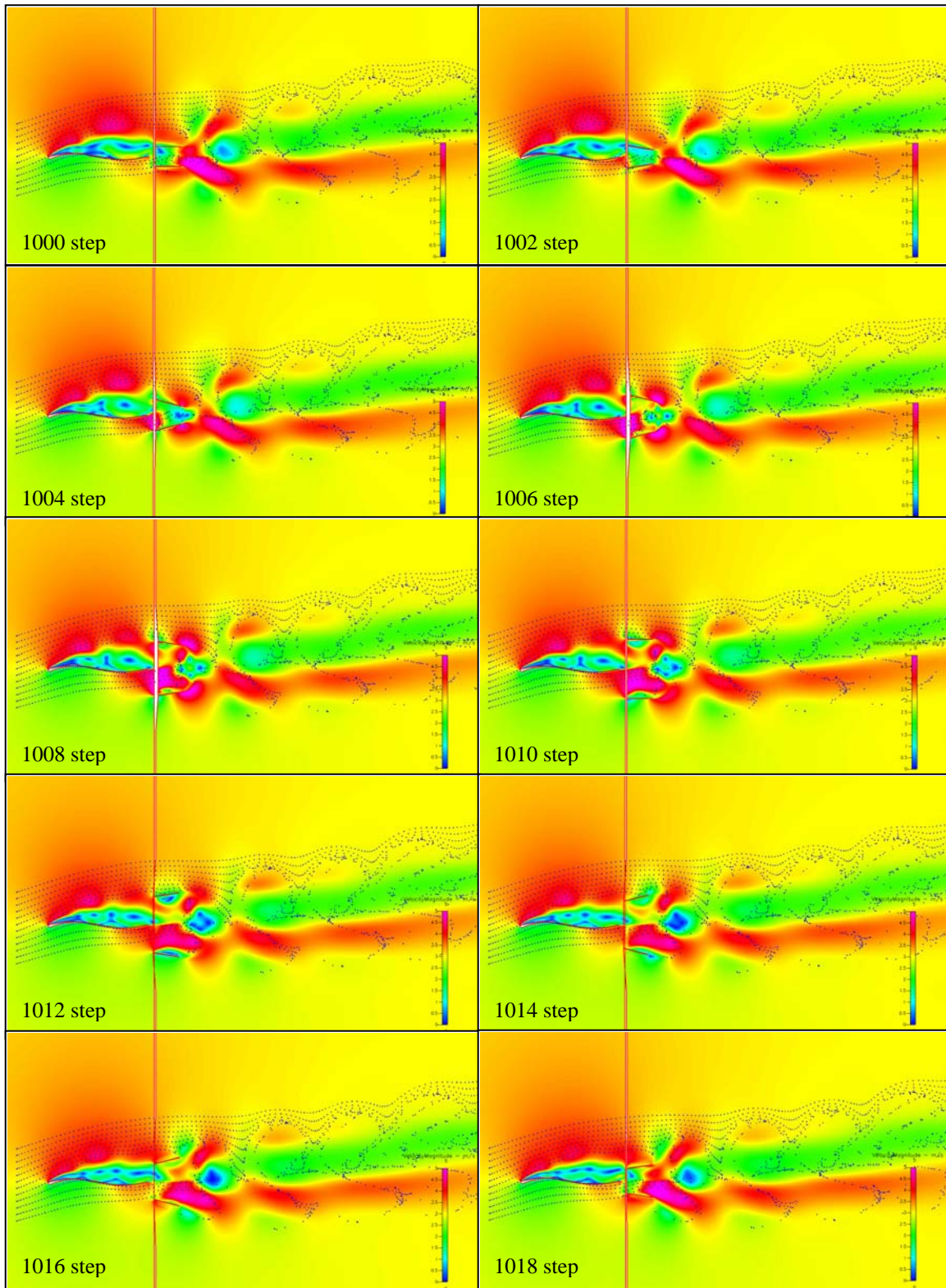


Figure 33. Velocity Field with Streaklines from Time Step 1000 - 1018: ($U_{\infty}= 3\text{m/s}$, $\alpha=10^\circ$, $f=25\text{Hz}$, $H=15\text{MM}$, $\Phi=15^\circ$, Out of Phase.)

3. Full Flapping Wing Configuration: $U_\infty=3\text{m/s}$, $\alpha=10^\circ$, $f=25\text{Hz}$, $H=15\text{mm}$, $\Phi=20^\circ$, Pitch/Plunge Out of Phase

The results are shown in Figures 34 to 36. This time, much higher peaks are observed. In particular, the positive cycle of the lift generated from the top flapping wing is significantly higher as compared to the previous two cases. The lift experienced by the fixed wing is noted to consist of two-stroke oscillations. This might well be caused by the favorable interaction of the flow fields generated from the flapping wings. The net result observed, is a much ‘flatter’ combined lift history. This might have suggested a more stable lift generation.

A distinctive increase in thrust production is also observed. While the general trend shows a similar increase in thrust during the opening stroke than in the closing stroke, the peak value of the combined drag is noted to be 150% higher than that of the earlier case with $\Phi=10^\circ$.

The streakline turning angle in this case is also much greater. The top most streakline almost levels out. The velocity magnitude distribution is also observed to be much intensified.

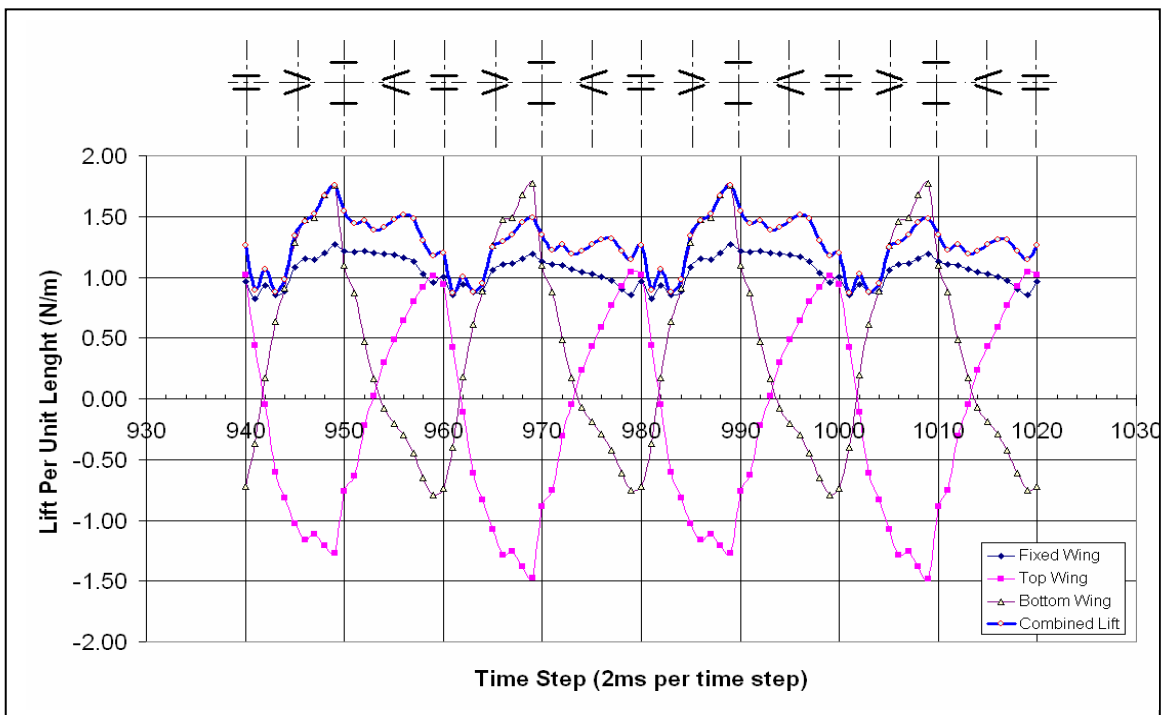


Figure 34. Lift History: $U_\infty= 3\text{m/s}$, $\alpha=10^\circ$, $f=25\text{Hz}$, $H=15\text{MM}$, $\Phi=20^\circ$, Out of Phase.

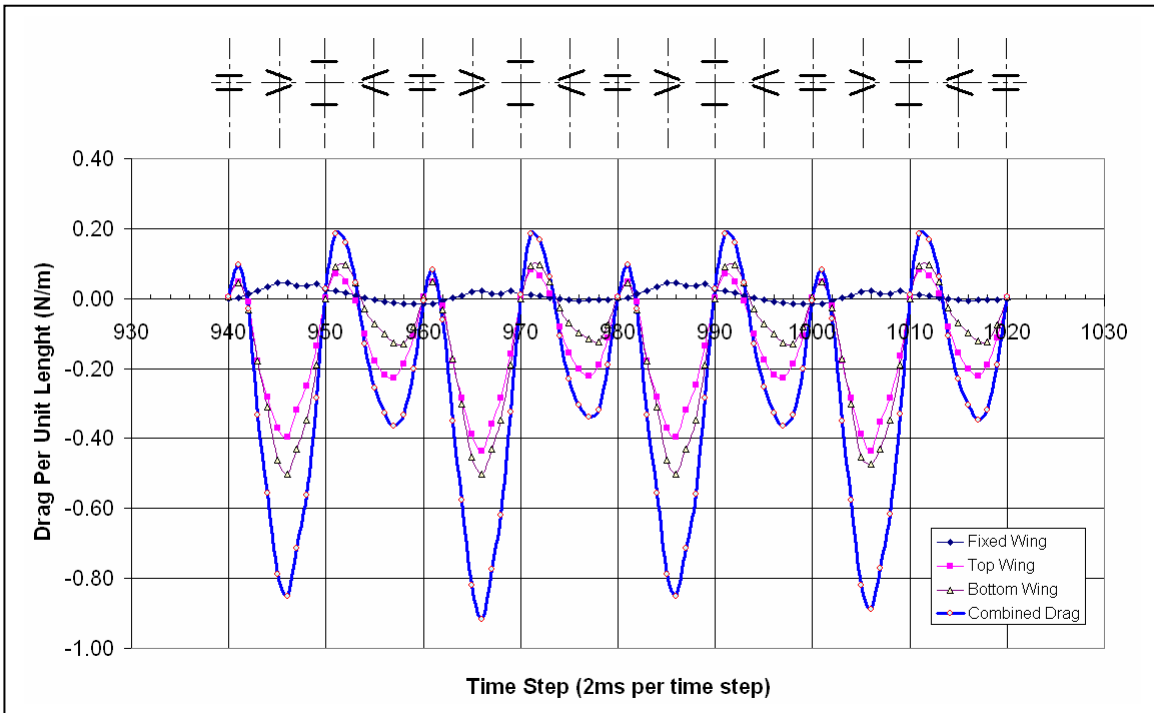


Figure 35. Drag History: $U_{\infty}= 3\text{m/s}$, $\alpha=10^{\circ}$, $f=25\text{Hz}$, $H=15\text{MM}$, $\Phi=20^{\circ}$, Out of Phase.

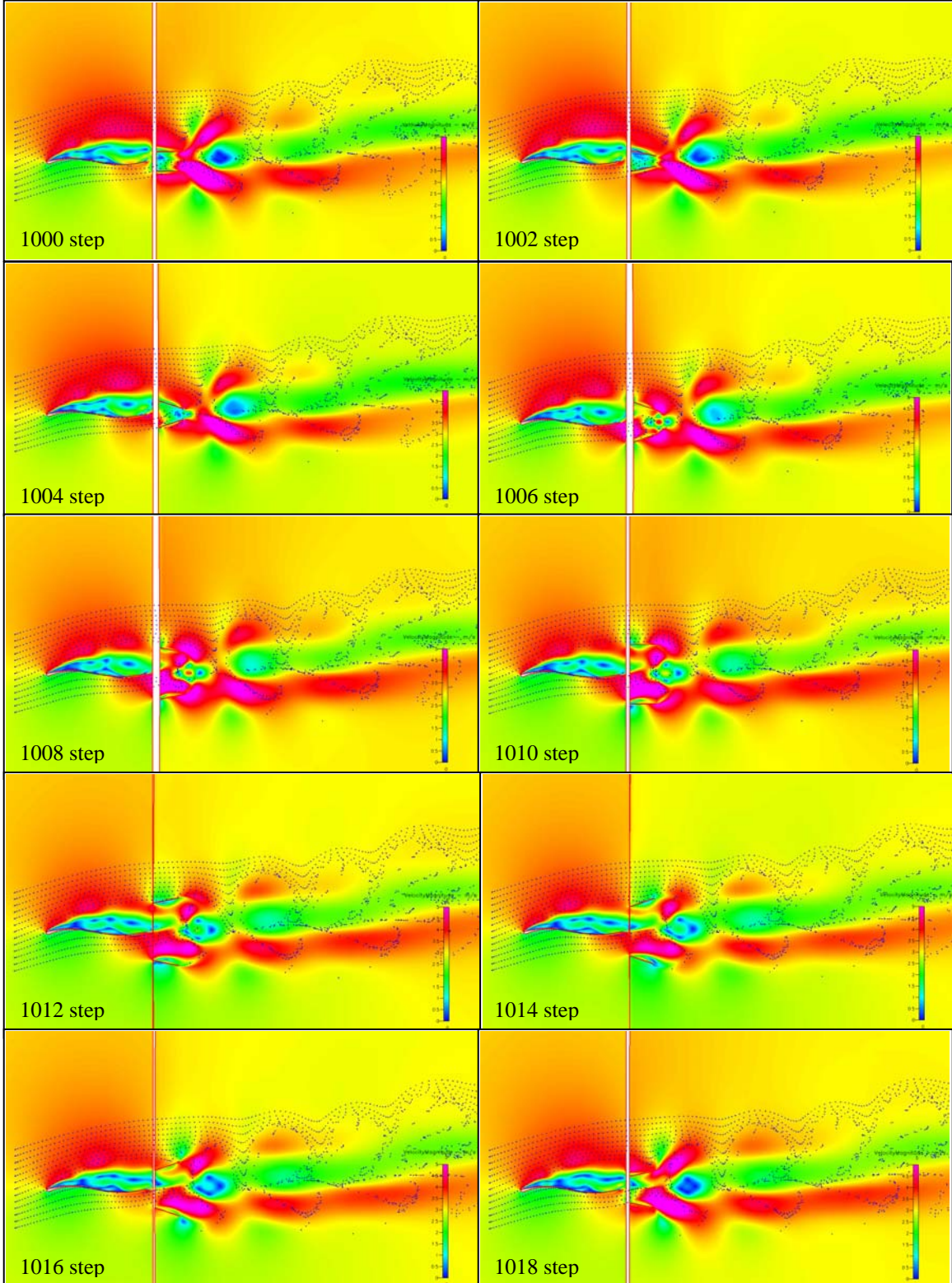


Figure 36. Velocity Field with Streaklines from Time Step 1000 - 1018: ($U_{\infty}= 3\text{m/s}$, $\alpha=10^{\circ}$, $f=25\text{Hz}$, $H=15\text{MM}$, $\Phi=20^{\circ}$, Out of Phase.)

3. Full Flapping Wing Configuration: $U_\infty=3\text{m/s}$, $\alpha=10^\circ$, $f=25\text{Hz}$, $H=15\text{mm}$, $\Phi=10^\circ$, Pitch/Plunge In-Phase ($\psi=0^\circ$)

The results are shown in Figures 37 to 39. Generally, it was observed that force histories exhibited chaotic behavior. The combined lift is much lower with greater fluctuation. In addition, the combined drag is largely positive which is undesirable.

It was also observed that the velocity magnitude distribution and particle traces in the wake do not portray well defined vortices common to all the earlier pitch/plunge out of phase cases.

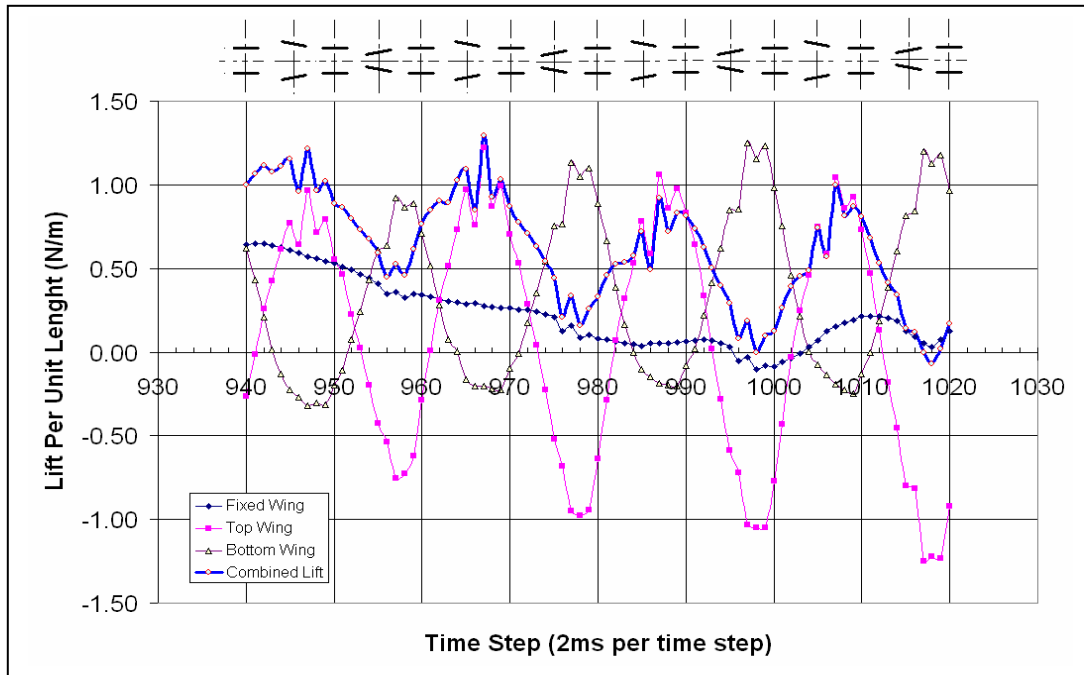


Figure 37. Lift History: $U_\infty= 3\text{m/s}$, $\alpha=10^\circ$, $f=25\text{Hz}$, $H=15\text{MM}$, $\Phi=10^\circ$, In- Phase.

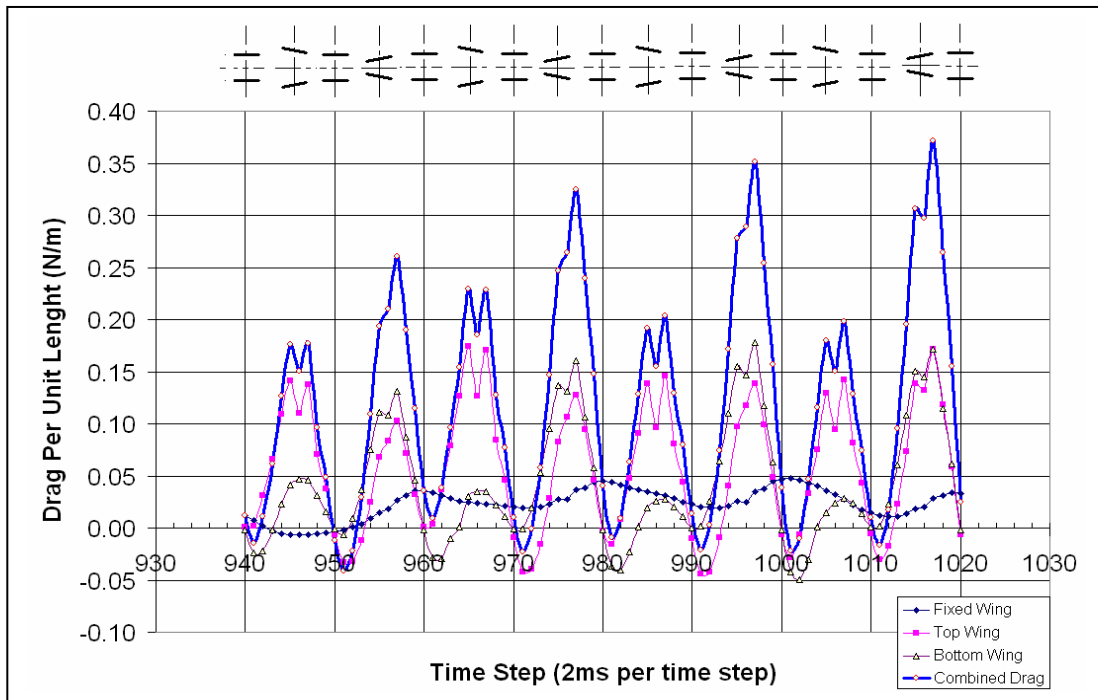


Figure 38. Drag History: $U_\infty = 3\text{m/s}$, $\alpha = 10^\circ$, $f = 25\text{Hz}$, $H = 15\text{MM}$, $\Phi = 10^\circ$, In-Phase.

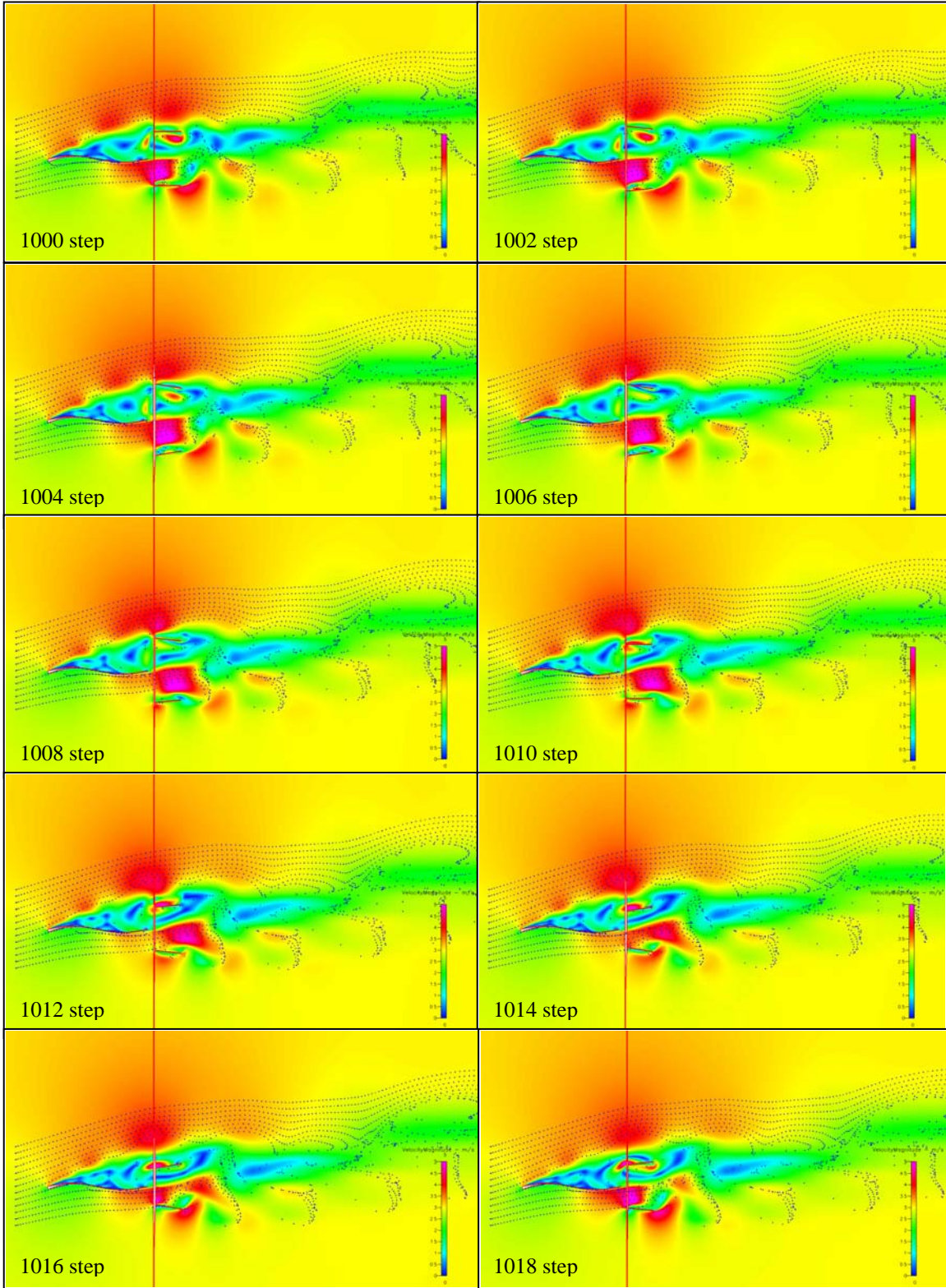


Figure 39. Velocity Field with Streaklines from Time Step 1000 - 1018: ($U_{\infty}= 3\text{m/s}$, $\alpha=10^{\circ}$, $f=25\text{Hz}$, $H=15\text{MM}$, $\Phi=10^{\circ}$, In-Phase.)

VI. DISCUSSION

A. COMPARISON OF FORCE HISTORIES: CASE OF IN-PHASE VS OUT-OF-PHASE PITCH/PLUNGE MOTION

In the earlier section, qualitative observations were noted. The following figures quantitatively compare and contrast the lift and drag forces induced on the individual wings and also the combined effects for the case of pitch/plunge flapping motion between the in-phase and out-of-phase configurations. The pitch amplitude is 10° . The non flapping case is also included for reference. Although all cases resulted in positive lift, the case with pitch/plunge 90° out of phase resulted in much higher lift. In addition, it induced negative drag (ie., net positive thrust) in contrast to the pitch/plunge in phase case.

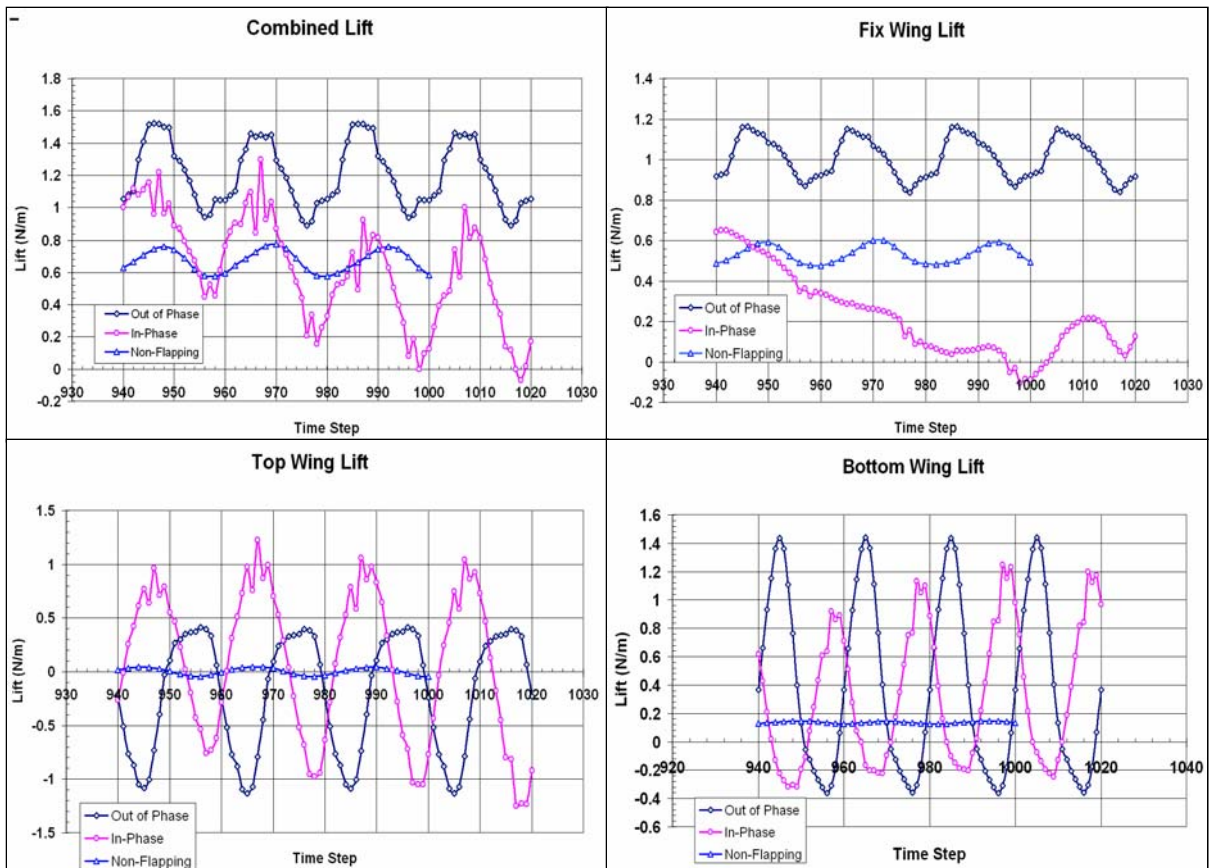


Figure 40. Time History of Drag: Comparison between Pitch/Plunge In-Phase and Out-of-Phase ($U_\infty = 3\text{m/s}$, $\alpha = 10^\circ$, $f = 25\text{Hz}$, $H = 15\text{mm}$, $\Phi = 10^\circ$) with Reference to the Non-Flapping Case

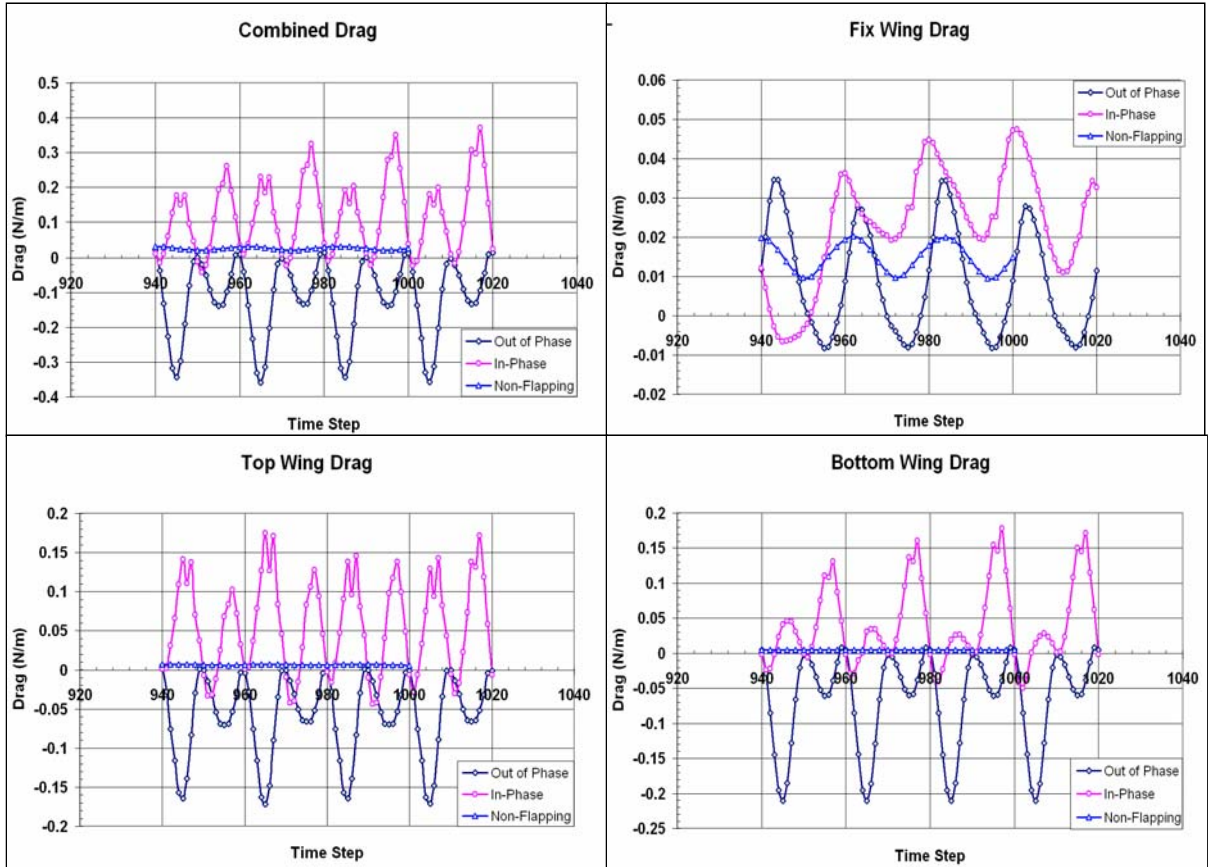


Figure 41. Time History of Lift: Comparison between Pitch/Plunge In-Phase and Out-of-Phase ($U_\infty = 3\text{m/s}$, $\alpha = 10^\circ$, $f = 25\text{Hz}$, $H = 15\text{mm}$, $\Phi = 10^\circ$) with Reference to the Non-Flapping Case

General comparison on the lift and drag history indicates a much lesser periodicity on the in-phase solution. This provides evidence of a more chaotic solution caused by more severe stall for the in-phase case.

B. PITCH AMPLITUDE EFFECTS ON FORCES HISTORY: CASE OF OUT-OF-PHASE PITCH/PLUNGE MOTION

The results presented in section V (D1 to D3) show some consistent trends which are summarized as follows:

- The lift profile generated by the top and bottom wings is almost in opposite phase. The bottom wing however does better.
- The thrust producing capability for the top and bottom wings is almost equal in magnitude. More thrust is observed as the wings pull apart.

The following figures (42-48) compare and contrast the lift and drag force histories due to the effects of pitch amplitude. Based on the last 4 cycles of the results (i.e., corresponding to the 940th to 1020th time step) as presented in section V, the sample mean and standard deviations of the forces are tabulated in Appendix B for all three cases of pitch amplitudes, namely, 10°, 15° and 20°. The results show higher overall lift and thrust (i.e., negative drag) with increasing pitch amplitude. This trend is consistent with previous experimental and numerical studies. From the summary plots of Figures 45 and 46, it is apparent that:

- The fixed wing is responsible for significant lift generation. Due to the asymmetrical wake production from the fixed wing trailing edge, the bottom flapping wing also assisted in lift generation while the top wing induced a slight negative lift. However, the overall lift increases as the pitch amplitude increases from 10° to 20°. In this case, the increase in lift due to the top wing is more significant compared with that of the bottom wing. (See results in Figures 43 and 44).
- Overall thrust increases significantly as pitch amplitude increases from 10° to 20°. This trend is also evident from the intensity of the velocity field distribution and the streakline patterns presented in section V Figures 30, 33 and 36. In this case, higher velocity magnitude and stronger vortical wake structures are indicative of higher thrust. This contrast is more pronounced when comparing the in-phase case with any of the out-of-phase cases.

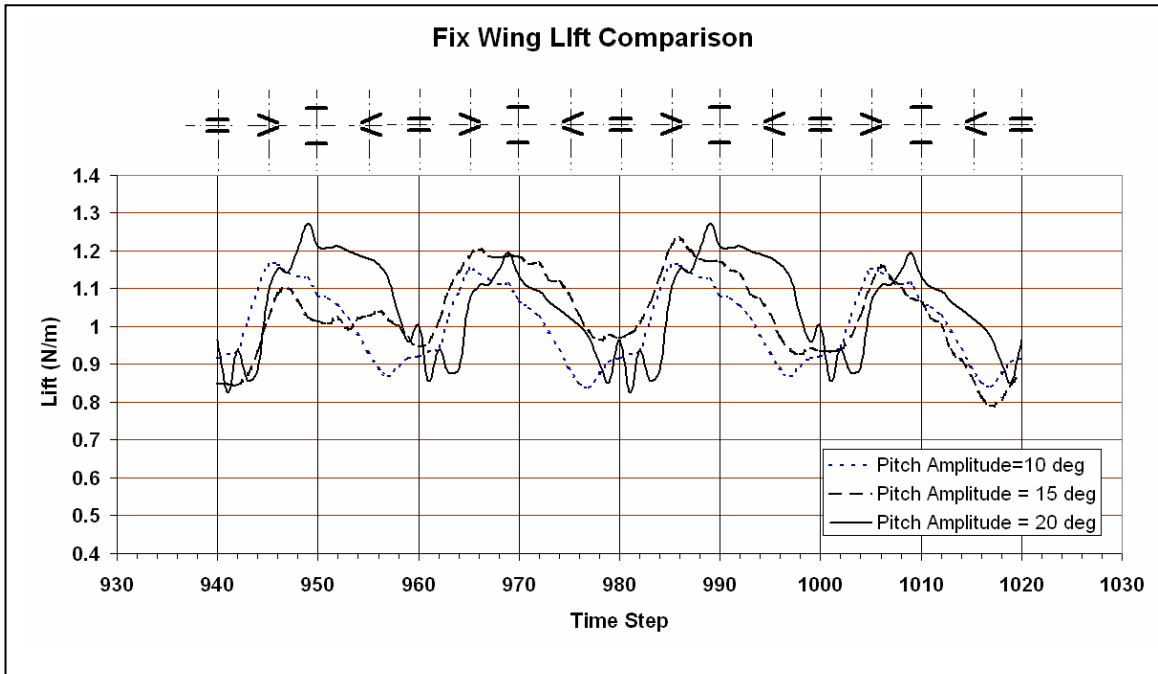


Figure 42. Effects of Pitch Amplitude on Lift of Fixed Wing (Case of Pitch/Plunge Out-of-Phase. $U_\infty = 3\text{m/s}$, $\alpha = 10^\circ$, $f = 25\text{Hz}$, $H = 15\text{mm}$, $\Phi = 10^\circ, 15^\circ, 20^\circ$)

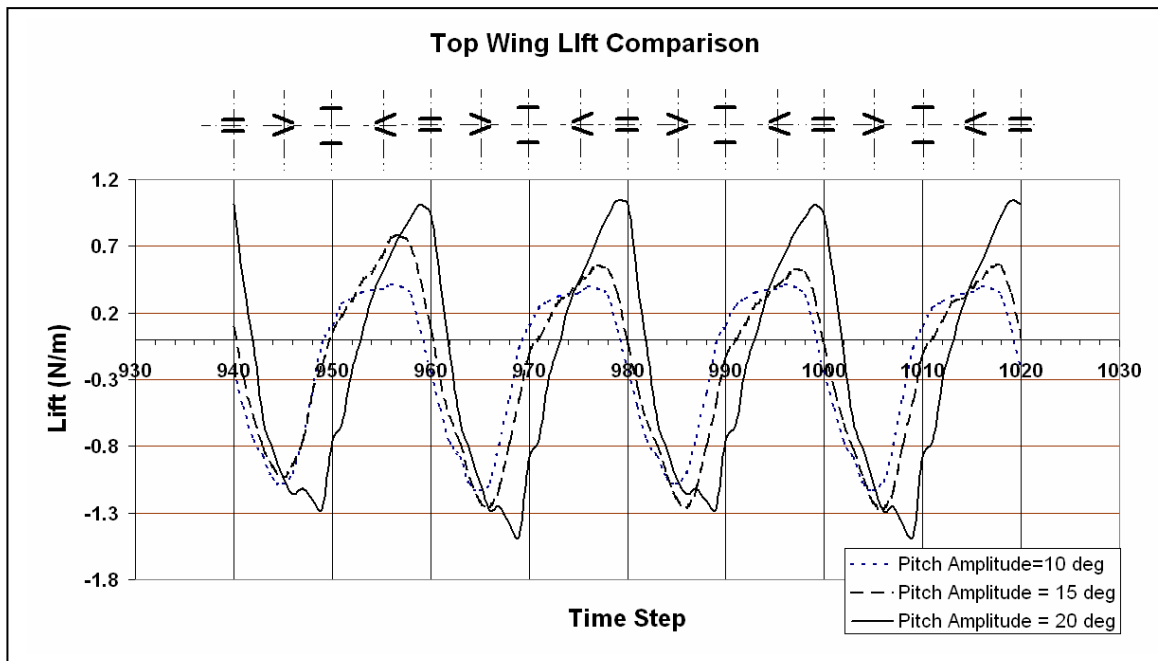


Figure 43. Effects of Pitch Amplitude on Lift of Top Wing (Case of Pitch/Plunge Out-of-Phase. $U_\infty = 3\text{m/s}$, $\alpha = 10^\circ$, $f = 25\text{Hz}$, $H = 15\text{mm}$, $\Phi = 10^\circ, 15^\circ, 20^\circ$)

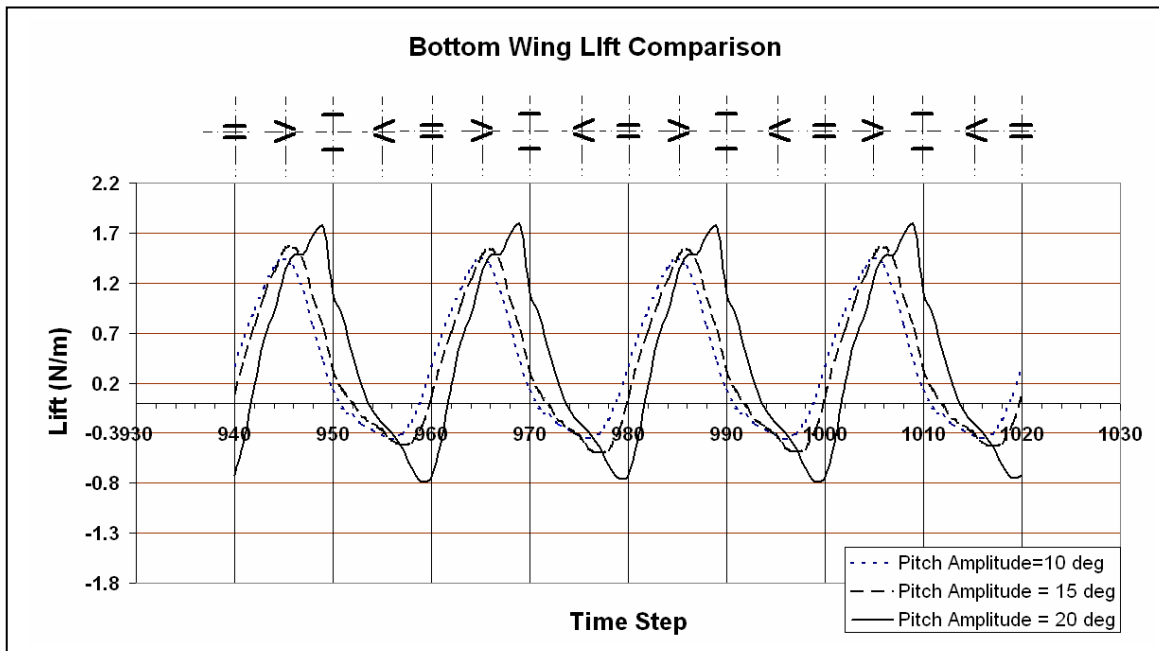


Figure 44. Effects of Pitch Amplitude on Lift of Bottom Wing (Case of Pitch/Plunge Out-of-Phase. ($U_\infty=3\text{m/s}$, $\alpha=10^\circ$, $f=25\text{Hz}$, $H=15\text{mm}$, $\Phi=10^\circ, 15^\circ, 20^\circ$))

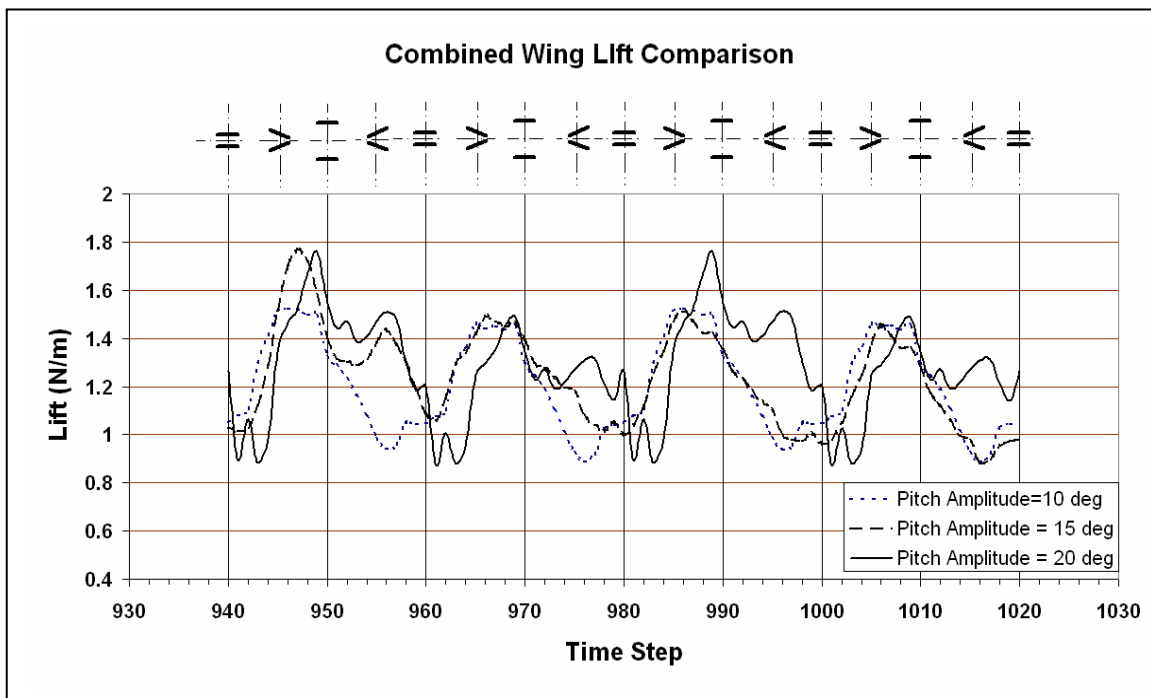


Figure 45. Effects of Pitch Amplitude on Overall Lift (Case of Pitch/Plunge Out-of-Phase. ($U_\infty=3\text{m/s}$, $\alpha=10^\circ$, $f=25\text{Hz}$, $H=15\text{mm}$, $\Phi=10^\circ, 15^\circ, 20^\circ$))

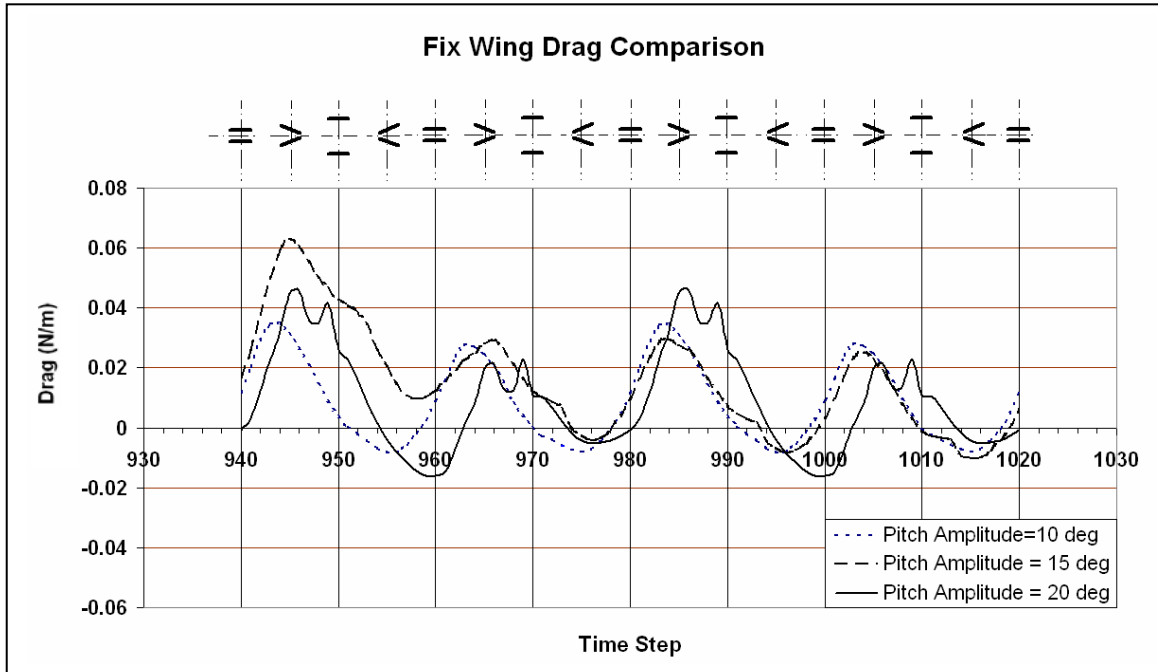


Figure 46. Effects of Pitch Amplitude on Drag of Fixed Wing (Case of Pitch/Plunge Out-of-Phase). ($U_\infty = 3\text{m/s}$, $\alpha = 10^\circ$, $f = 25\text{Hz}$, $H = 15\text{mm}$, $\Phi = 10^\circ, 15^\circ, 20^\circ$)

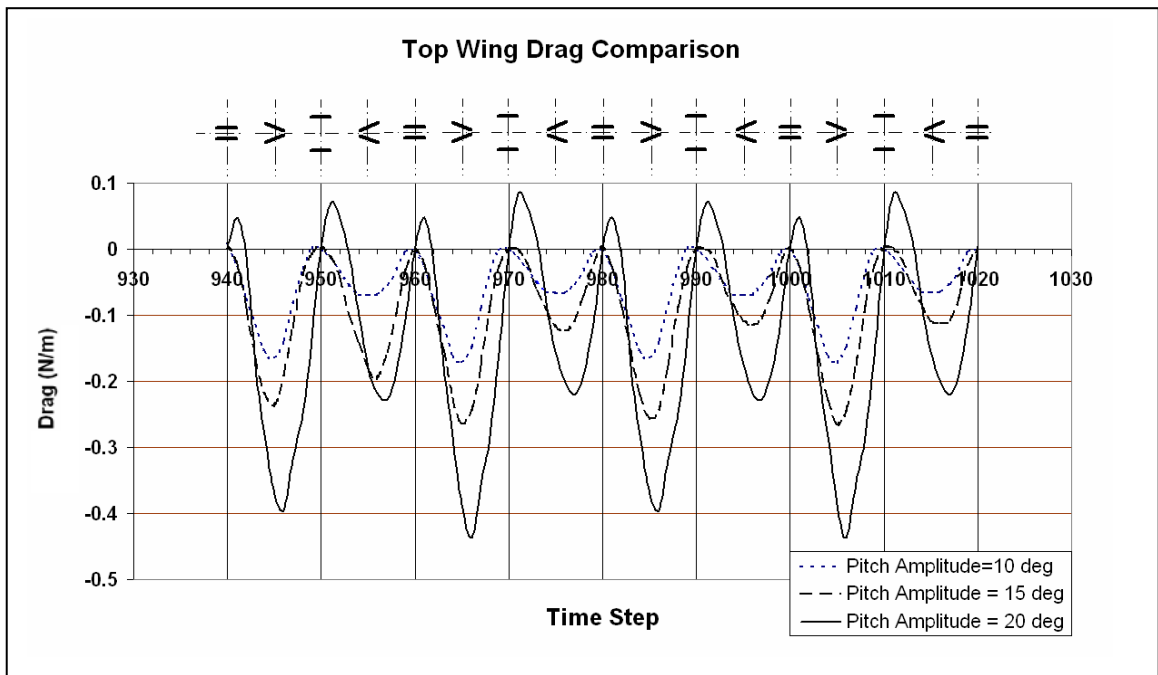


Figure 47. Effects of Pitch Amplitude on Drag of Top Wing (Case of Pitch/Plunge Out-of-Phase). ($U_\infty = 3\text{m/s}$, $\alpha = 10^\circ$, $f = 25\text{Hz}$, $H = 15\text{mm}$, $\Phi = 10^\circ, 15^\circ, 20^\circ$)

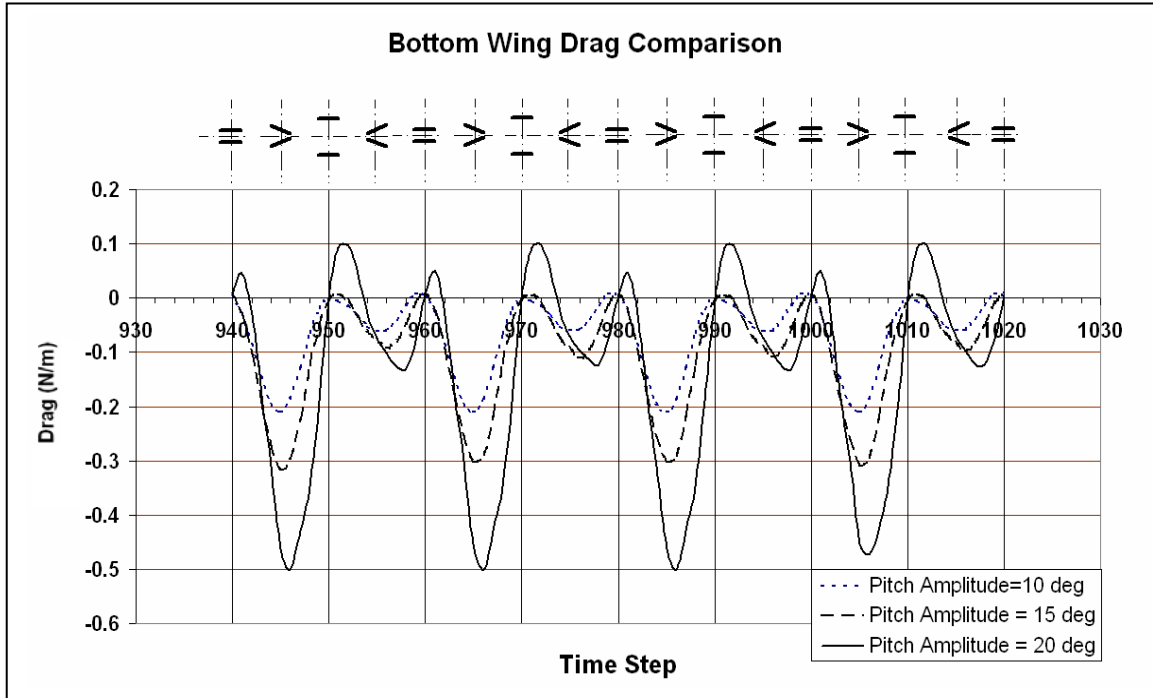


Figure 48. Effects of Pitch Amplitude on Drag of Bottom Wing (Case of Pitch/Plunge Out-of-Phase. ($U_\infty=3\text{m/s}$, $\alpha=10^\circ$, $f=25\text{Hz}$, $H=15\text{mm}$, $\Phi=10^\circ$, 15° , 20°))

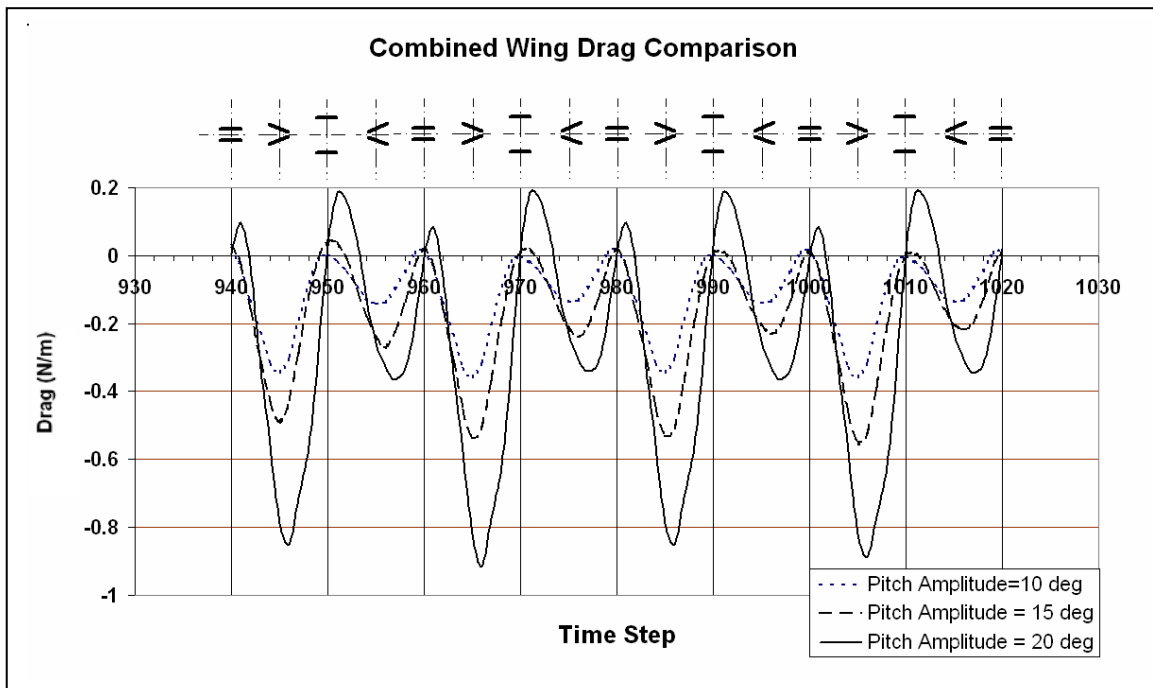


Figure 49. Effects of Pitch Amplitude on Overall Drag (Case of Pitch/Plunge Out-of-Phase. ($U_\infty=3\text{m/s}$, $\alpha=10^\circ$, $f=25\text{Hz}$, $H=15\text{mm}$, $\Phi=10^\circ$, 15° , 20°))

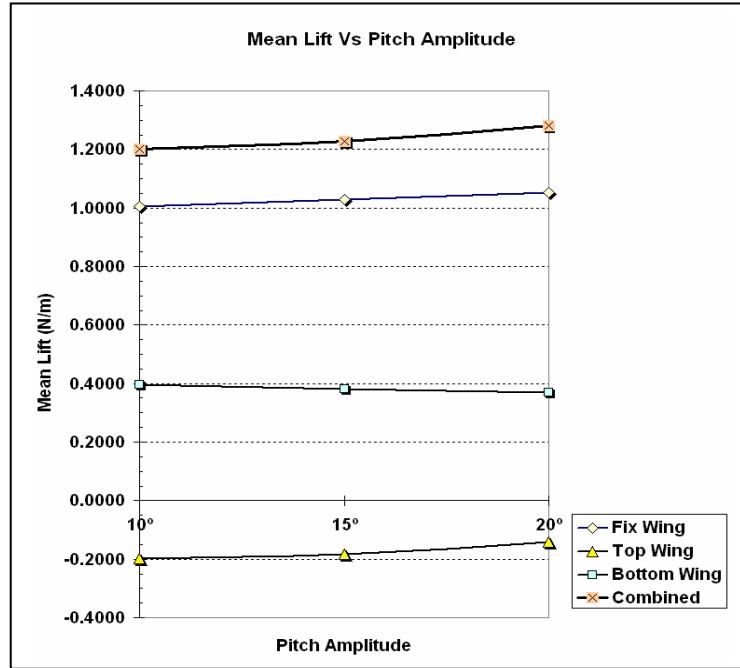


Figure 50. Mean Lift Vs Pitch Amplitude (Case of Pitch/Plunge Out-of-Phase. ($U_{\infty}=3\text{m/s}$, $\alpha=10^\circ$, $f=25\text{Hz}$, $H=15\text{mm}$, $\Phi=10^\circ, 15^\circ, 20^\circ$))

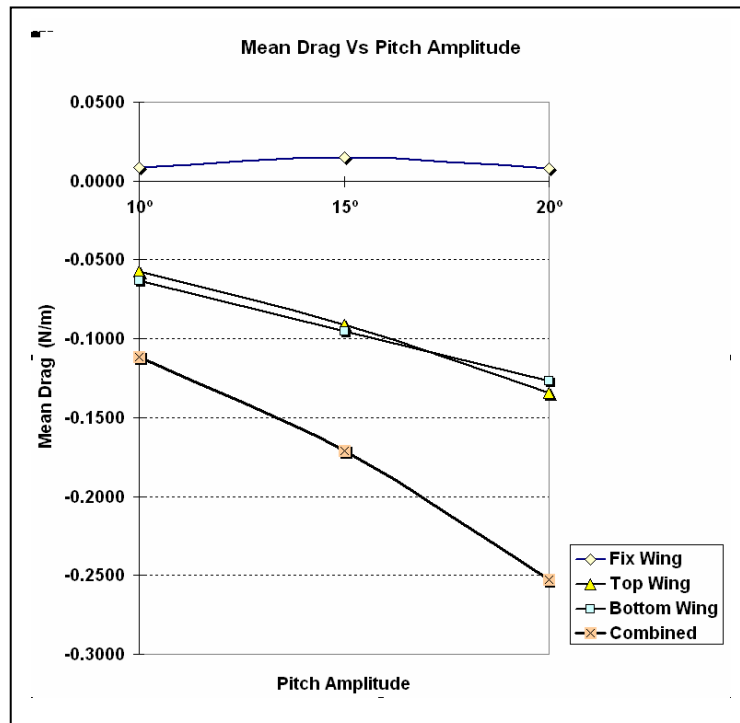


Figure 51. Mean Drag Vs Pitch Amplitude (Case of Pitch/Plunge Out-of-Phase. ($U_{\infty}=3\text{m/s}$, $\alpha=10^\circ$, $f=25\text{Hz}$, $H=15\text{mm}$, $\Phi=10^\circ, 15^\circ, 20^\circ$))

C. EFFECTS OF PITCH/PLUNGE HEAVING MOTION: FROM PERSPECTIVE OF FLOW VISUALIZATION RESULTS

The flow visualization simulation result shown in Figure 27 for the case of $U_\infty = 0$ indicates the phenomenon of flapping wing propulsion. Spray particles which are released with zero velocities are being induced to flow over the fixed wing and 'ejected' at higher velocity aft of the flapping wings. This not only resulted in thrust (negative drag) but also has the effect of producing lift on the fixed wing (refer to results in Figures 25 and 49).

At $U_\infty = 3\text{m/s}$ and 10° AOA, these effects continue to exist. The following figures depict the flow visualization simulation results of

- $f=0$ Hz (i.e., non-flapping case) at $U_\infty = 3\text{m/s}$, $\alpha=10^\circ$
- $f=25$ Hz, Pitch/Plunge Out-of-Phase at $U_\infty = 3\text{m/s}$, $\alpha=10^\circ$

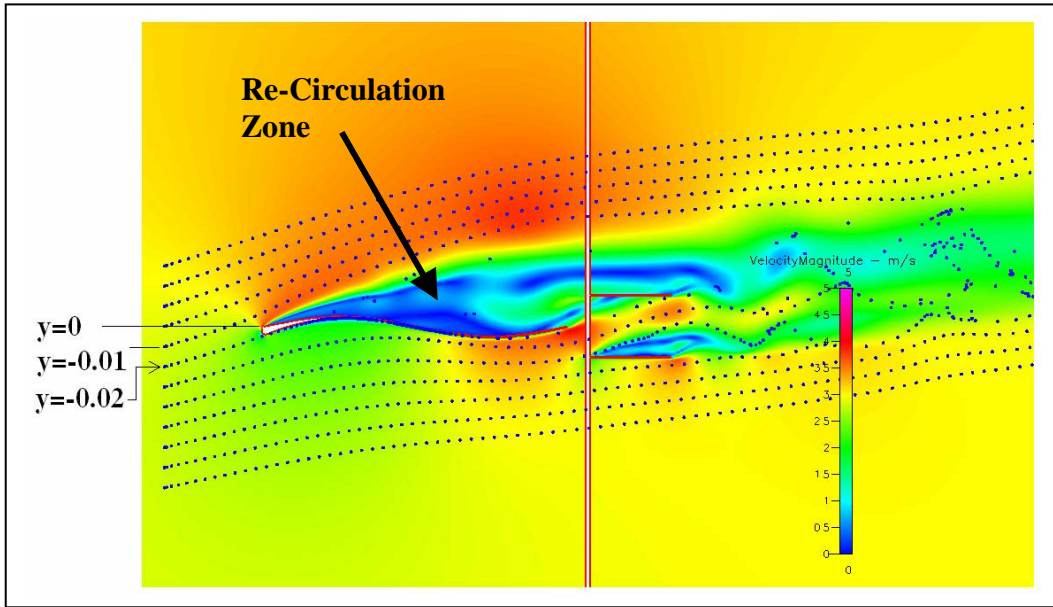


Figure 52. Flow Visualization Simulation Results at 1000th Time Step: ($U_\infty= 3\text{m/s}$, $\alpha=10^\circ$, $f=0\text{ Hz}$, $H=15\text{mm}$, $\Phi=10^\circ, 15^\circ, 20^\circ$)

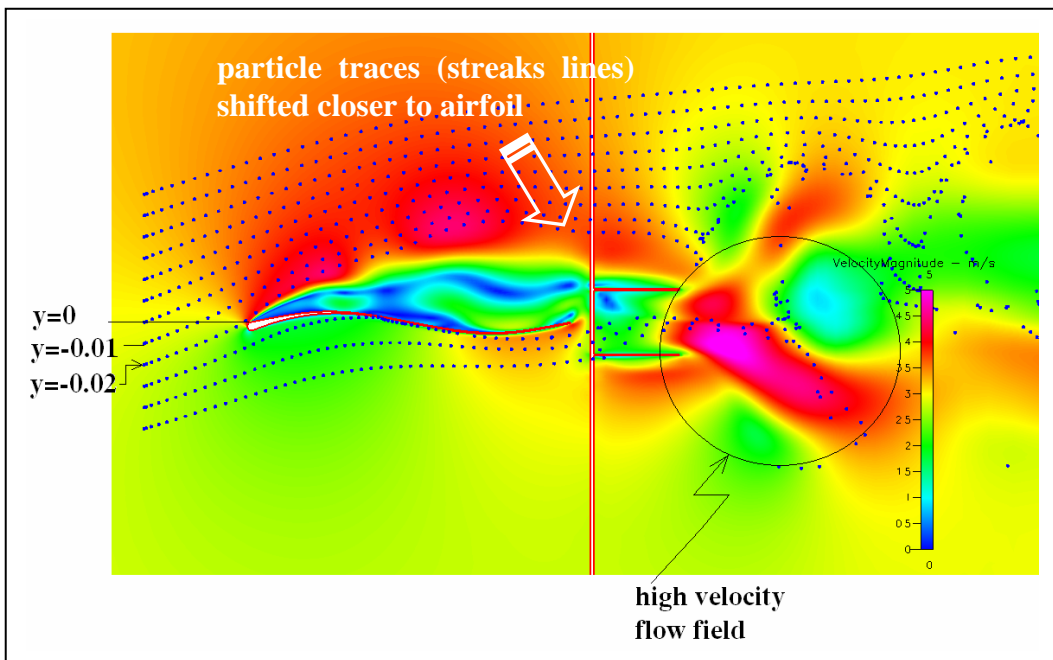


Figure 53. Flow Visualization Simulation Results at 1000th Time Step: ($U_\infty= 3\text{m/s}$, $\alpha=10^\circ$, $f=25\text{Hz}$, $H=15\text{mm}$, $\Phi=10^\circ$ Pitch/Plunge Out-of-Phase)

Flow field analysis from Figures 51 and 52 and observations of the transient video clip (30fps from time step up to 1020th) for the two cases show strong evidence of the following:

- Flow separation and re-circulation zones (in blue) are significantly reduced for the flapping case.
- The streaklines that is traced from particles released at $y=-0.02$ went under the wing at $f=0\text{Hz}$ and went over the wing at $f=25\text{Hz}$, which indicates increased circulation and lift over main wing .
- Particle trajectories (streaks lines at both upper and lower sides) are being induced to flow closer to the fixed wing surfaces.
- Pulses of high velocity flow fields are ‘ejected’ aft of the flapping wings.

Incidentally, past experimental flow visualization results show somewhat similar behavior (see Figures 1a and 1b).

THIS PAGE INTENTIONALLY LEFT BLANK

VII. CONCLUSIONS

The dynamic mesh model of the complete NPS multi-wing MAV was developed and the low Reynolds number, unsteady aerodynamic solutions were presented and analyzed for various cases of pitch/plunge heaving motion. The characteristics resulting from the flapping wing propulsion, which include the 2D flow visualization simulations of the transient flow fields, and time dependant force, were compared and contrasted. Resulting time dependant variation trends and flow phenomenon suggest similarity to past findings and experimental observations. This has provided much encouragement and impetus to future CFD simulations and optimization studies in NPS on-going research on multi-wing MAV configuration design.

THIS PAGE INTENTIONALLY LEFT BLANK

VIII. RECOMMENDATIONS

The equations of motion of the flapping wings in this study assumed rigid body kinematics in linear translation and angular rotation. Thus the effects of structural elasticity are neglected. Although the current version of the CFD code allows for fluid-structural interaction computation, there is still no parallel processing capability for the structural module at this point in time. In future versions, however, this feature might be incorporated. A three dimensional moving grid, coupled with elastic structural interaction with the unsteady flow fields would give the ultimate numerical solutions in the flapping-wing problem.

In addition, optimization simulations can be conducted on several key parameters which include the flapping wing mean separation distance, plunge/pitch phase difference, plunge and pitch amplitudes, the flapping frequency, etc.

THIS PAGE INTENTIONALLY LEFT BLANK

APPENDIX A. SIMULATION DATA

A. $U_\infty=0$, $f=25\text{HZ}$, $\Phi=10^\circ$, PITCH/PLUNGE OUT OF PHASE

Time step							TOTAL Lift (N/m)
	Fix wing total Lift N/3MM	Fix Wing Lift (N/M)	Top wing total Lift N/3MM	Top Wing Lift (N/M)	Bot wing total Lift N/3MM	Bottom Wing Lift (N/M)	
940	9.12E-05	3.040E-02	-2.18E-03	-7.266E-01	1.86E-03	6.210E-01	-7.526E-02
941	1.83E-05	6.106E-03	-8.04E-04	-2.678E-01	1.53E-04	5.091E-02	-2.108E-01
942	-3.20E-05	-1.067E-02	3.94E-04	1.313E-01	-1.21E-03	-4.045E-01	-2.839E-01
943	-7.18E-05	-2.393E-02	1.19E-03	3.951E-01	-2.09E-03	-6.975E-01	-3.263E-01
944	-1.40E-04	-4.665E-02	1.65E-03	5.494E-01	-2.82E-03	-9.398E-01	-4.370E-01
945	-1.74E-04	-5.792E-02	2.13E-03	7.111E-01	-3.33E-03	-1.109E+00	-4.563E-01
946	-3.66E-04	-1.219E-01	2.53E-03	8.426E-01	-4.40E-03	-1.465E+00	-7.447E-01
947	-2.68E-04	-8.938E-02	3.23E-03	1.078E+00	-4.23E-03	-1.411E+00	-4.227E-01
948	-2.63E-04	-8.770E-02	3.95E-03	1.316E+00	-4.58E-03	-1.528E+00	-2.994E-01
949	-1.64E-04	-5.466E-02	3.33E-03	1.110E+00	-3.53E-03	-1.175E+00	-1.195E-01
950	-3.95E-04	-1.316E-01	2.10E-03	7.009E-01	-2.44E-03	-8.132E-01	-2.439E-01
951	1.07E-04	3.559E-02	4.63E-04	1.542E-01	-3.43E-05	-1.142E-02	1.784E-01
952	1.08E-04	3.593E-02	-1.35E-03	-4.516E-01	1.61E-03	5.369E-01	1.212E-01
953	4.10E-04	1.367E-01	-2.67E-03	-8.902E-01	3.16E-03	1.053E+00	2.996E-01
954	5.14E-04	1.714E-01	-3.66E-03	-1.219E+00	4.15E-03	1.384E+00	3.359E-01
955	6.40E-04	2.134E-01	-4.65E-03	-1.551E+00	5.17E-03	1.722E+00	3.839E-01
956	6.52E-04	2.174E-01	-4.48E-03	-1.495E+00	4.91E-03	1.638E+00	3.602E-01
957	6.21E-04	2.071E-01	-5.42E-03	-1.806E+00	5.79E-03	1.930E+00	3.305E-01
958	4.05E-04	1.351E-01	-4.49E-03	-1.496E+00	4.75E-03	1.584E+00	2.237E-01
959	2.51E-04	8.360E-02	-3.69E-03	-1.229E+00	3.73E-03	1.244E+00	9.805E-02
960	9.11E-05	3.036E-02	-2.18E-03	-7.282E-01	1.86E-03	6.197E-01	-7.820E-02
961	2.11E-05	7.040E-03	-8.07E-04	-2.690E-01	1.51E-04	5.019E-02	-2.118E-01
962	-3.00E-05	-1.001E-02	3.91E-04	1.305E-01	-1.21E-03	-4.042E-01	-2.837E-01
963	-7.09E-05	-2.364E-02	1.18E-03	3.944E-01	-2.09E-03	-6.964E-01	-3.256E-01
964	-1.39E-04	-4.631E-02	1.65E-03	5.486E-01	-2.81E-03	-9.371E-01	-4.348E-01
965	-1.73E-04	-5.767E-02	2.13E-03	7.097E-01	-3.32E-03	-1.108E+00	-4.558E-01
966	-3.64E-04	-1.212E-01	2.52E-03	8.415E-01	-4.38E-03	-1.461E+00	-7.408E-01
967	-2.67E-04	-8.896E-02	3.23E-03	1.076E+00	-4.22E-03	-1.408E+00	-4.209E-01
968	-2.61E-04	-8.702E-02	3.94E-03	1.314E+00	-4.57E-03	-1.523E+00	-2.966E-01
969	-1.61E-04	-5.367E-02	3.32E-03	1.108E+00	-3.52E-03	-1.172E+00	-1.177E-01
970	-3.90E-04	-1.300E-01	2.09E-03	6.983E-01	-2.43E-03	-8.114E-01	-2.431E-01
971	1.13E-04	3.767E-02	4.57E-04	1.524E-01	-3.26E-05	-1.086E-02	1.792E-01
972	1.13E-04	3.764E-02	-1.35E-03	-4.513E-01	1.61E-03	5.359E-01	1.223E-01
973	4.09E-04	1.363E-01	-2.66E-03	-8.883E-01	3.15E-03	1.049E+00	2.973E-01
974	5.10E-04	1.699E-01	-3.65E-03	-1.218E+00	4.14E-03	1.381E+00	3.325E-01
975	6.33E-04	2.111E-01	-4.64E-03	-1.548E+00	5.15E-03	1.717E+00	3.802E-01
976	6.44E-04	2.145E-01	-4.47E-03	-1.491E+00	4.90E-03	1.632E+00	3.554E-01
977	6.13E-04	2.044E-01	-5.41E-03	-1.803E+00	5.78E-03	1.926E+00	3.273E-01
978	3.99E-04	1.330E-01	-4.48E-03	-1.493E+00	4.75E-03	1.583E+00	2.227E-01

Time step							TOTAL Lift (N/m)
	Fix wing total Lift N/3MM	Fix Wing Lift (N/M)	Top wing total Lift N/3MM	Top Wing Lift (N/M)	Bot wing total Lift N/3MM	Bottom Wing Lift (N/M)	
979	2.50E-04	8.327E-02	-3.69E-03	-1.229E+00	3.73E-03	1.244E+00	9.773E-02
980	9.64E-05	3.214E-02	-2.19E-03	-7.289E-01	1.86E-03	6.203E-01	-7.649E-02
981	2.97E-05	9.885E-03	-8.09E-04	-2.698E-01	1.52E-04	5.056E-02	-2.093E-01
982	-2.21E-05	-7.359E-03	3.89E-04	1.297E-01	-1.21E-03	-4.040E-01	-2.817E-01
983	-6.40E-05	-2.135E-02	1.18E-03	3.935E-01	-2.09E-03	-6.971E-01	-3.249E-01
984	-1.32E-04	-4.401E-02	1.64E-03	5.473E-01	-2.81E-03	-9.371E-01	-4.339E-01
985	-1.68E-04	-5.583E-02	2.12E-03	7.067E-01	-3.33E-03	-1.110E+00	-4.588E-01
986	-3.59E-04	-1.198E-01	2.51E-03	8.375E-01	-4.39E-03	-1.462E+00	-7.442E-01
987	-2.67E-04	-8.909E-02	3.21E-03	1.070E+00	-4.23E-03	-1.410E+00	-4.287E-01
988	-2.63E-04	-8.763E-02	3.92E-03	1.308E+00	-4.57E-03	-1.522E+00	-3.022E-01
989	-1.60E-04	-5.325E-02	3.32E-03	1.106E+00	-3.51E-03	-1.169E+00	-1.165E-01
990	-3.83E-04	-1.278E-01	2.10E-03	7.008E-01	-2.42E-03	-8.077E-01	-2.347E-01
991	1.21E-04	4.030E-02	4.70E-04	1.567E-01	-2.65E-05	-8.830E-03	1.882E-01
992	1.18E-04	3.944E-02	-1.34E-03	-4.478E-01	1.61E-03	5.359E-01	1.276E-01
993	4.07E-04	1.358E-01	-2.66E-03	-8.863E-01	3.14E-03	1.047E+00	2.966E-01
994	5.09E-04	1.695E-01	-3.65E-03	-1.215E+00	4.13E-03	1.378E+00	3.326E-01
995	6.32E-04	2.105E-01	-4.63E-03	-1.544E+00	5.14E-03	1.714E+00	3.805E-01
996	6.43E-04	2.143E-01	-4.46E-03	-1.487E+00	4.89E-03	1.630E+00	3.573E-01
997	6.12E-04	2.039E-01	-5.40E-03	-1.800E+00	5.78E-03	1.927E+00	3.310E-01
998	3.98E-04	1.327E-01	-4.48E-03	-1.493E+00	4.75E-03	1.585E+00	2.241E-01
999	2.53E-04	8.422E-02	-3.69E-03	-1.229E+00	3.74E-03	1.246E+00	1.012E-01
1000	1.03E-04	3.431E-02	-2.19E-03	-7.292E-01	1.87E-03	6.231E-01	-7.176E-02
1002	-1.36E-05	-4.518E-03	3.88E-04	1.293E-01	-1.21E-03	-4.044E-01	-2.796E-01
1003	-5.56E-05	-1.854E-02	1.18E-03	3.928E-01	-2.10E-03	-6.985E-01	-3.243E-01
1004	-1.24E-04	-4.127E-02	1.64E-03	5.458E-01	-2.82E-03	-9.399E-01	-4.354E-01
1005	-1.61E-04	-5.363E-02	2.11E-03	7.040E-01	-3.34E-03	-1.115E+00	-4.642E-01
1006	-3.56E-04	-1.185E-01	2.50E-03	8.335E-01	-4.39E-03	-1.464E+00	-7.489E-01
1007	-2.69E-04	-8.951E-02	3.20E-03	1.065E+00	-4.25E-03	-1.416E+00	-4.400E-01
1008	-2.67E-04	-8.896E-02	3.91E-03	1.302E+00	-4.58E-03	-1.525E+00	-3.121E-01
1009	-1.60E-04	-5.339E-02	3.32E-03	1.106E+00	-3.51E-03	-1.169E+00	-1.161E-01
1010	-3.78E-04	-1.259E-01	2.12E-03	7.057E-01	-2.41E-03	-8.043E-01	-2.245E-01
1011	1.26E-04	4.212E-02	4.90E-04	1.633E-01	-1.97E-05	-6.561E-03	1.988E-01
1012	1.21E-04	4.045E-02	-1.33E-03	-4.437E-01	1.61E-03	5.368E-01	1.336E-01
1013	4.08E-04	1.361E-01	-2.66E-03	-8.854E-01	3.14E-03	1.048E+00	2.988E-01
1014	5.12E-04	1.706E-01	-3.64E-03	-1.213E+00	4.13E-03	1.378E+00	3.362E-01
1015	6.37E-04	2.122E-01	-4.63E-03	-1.542E+00	5.15E-03	1.715E+00	3.852E-01
1016	6.51E-04	2.171E-01	-4.46E-03	-1.485E+00	4.90E-03	1.633E+00	3.649E-01
1017	6.19E-04	2.064E-01	-5.40E-03	-1.799E+00	5.79E-03	1.932E+00	3.385E-01
1018	4.03E-04	1.343E-01	-4.48E-03	-1.494E+00	4.77E-03	1.589E+00	2.299E-01

Time step							TOTAL Lift (N/m)
	Fix wing total Lift N/3MM	Fix Wing Lift (N/M)	Top wing total Lift N/3MM	Top Wing Lift (N/M)	Bot wing total Lift N/3MM	Bottom Wing Lift (N/M)	
1019	2.57E-04	8.555E-02	-3.69E-03	-1.229E+00	3.75E-03	1.250E+00	1.058E-01
1020	1.06E-04	3.524E-02	-2.19E-03	-7.293E-01	1.88E-03	6.262E-01	-6.782E-02

Time step							TOTAL Drag (N/m)
	Fix wing total Drag N/3MM	Fix Wing Drag (N/M)	Top wing total Drag N/3MM	Top Wing Drag (N/M)	Bot wing total Drag N/3MM	Bottom Wing Drag (N/M)	
940	2.26E-06	7.548E-04	-2.26E-04	-7.519E-02	-1.85E-04	-6.182E-02	-1.363E-01
941	-5.49E-06	-1.831E-03	-4.95E-05	-1.649E-02	-8.29E-06	-2.765E-03	-2.109E-02
942	-1.48E-05	-4.948E-03	-1.02E-05	-3.389E-03	-5.25E-06	-1.750E-03	-1.009E-02
943	-1.73E-05	-5.774E-03	-7.67E-05	-2.555E-02	-1.22E-04	-4.057E-02	-7.190E-02
944	-2.21E-05	-7.367E-03	-1.82E-04	-6.082E-02	-3.01E-04	-1.002E-01	-1.684E-01
945	-2.39E-05	-7.967E-03	-3.14E-04	-1.047E-01	-4.84E-04	-1.612E-01	-2.739E-01
946	-4.23E-05	-1.411E-02	-4.31E-04	-1.435E-01	-7.46E-04	-2.486E-01	-4.062E-01
947	-3.38E-05	-1.127E-02	-5.73E-04	-1.910E-01	-7.53E-04	-2.509E-01	-4.532E-01
948	-3.62E-05	-1.208E-02	-6.64E-04	-2.214E-01	-7.71E-04	-2.570E-01	-4.905E-01
949	-1.84E-05	-6.134E-03	-4.72E-04	-1.572E-01	-5.02E-04	-1.672E-01	-3.306E-01
950	-1.33E-05	-4.446E-03	-2.15E-04	-7.168E-02	-2.51E-04	-8.375E-02	-1.599E-01
951	1.53E-05	5.113E-03	-2.53E-05	-8.429E-03	-3.22E-06	-1.074E-03	-4.391E-03
952	1.81E-05	6.019E-03	-2.33E-06	-7.756E-04	-3.21E-06	-1.070E-03	4.173E-03
953	2.86E-05	9.534E-03	-1.48E-04	-4.924E-02	-1.75E-04	-5.833E-02	-9.804E-02
954	3.11E-05	1.037E-02	-3.79E-04	-1.264E-01	-4.30E-04	-1.434E-01	-2.594E-01
955	3.81E-05	1.270E-02	-6.69E-04	-2.230E-01	-7.30E-04	-2.435E-01	-4.537E-01
956	1.85E-05	6.155E-03	-7.43E-04	-2.478E-01	-8.10E-04	-2.701E-01	-5.117E-01
957	2.30E-05	7.664E-03	-9.46E-04	-3.153E-01	-1.00E-03	-3.343E-01	-6.419E-01
958	8.44E-06	2.814E-03	-7.44E-04	-2.480E-01	-7.79E-04	-2.596E-01	-5.048E-01
959	1.23E-05	4.099E-03	-5.21E-04	-1.735E-01	-5.18E-04	-1.726E-01	-3.420E-01
960	2.33E-06	7.779E-04	-2.25E-04	-7.511E-02	-1.85E-04	-6.179E-02	-1.361E-01
961	-5.61E-06	-1.871E-03	-4.97E-05	-1.658E-02	-8.46E-06	-2.821E-03	-2.127E-02
962	-1.50E-05	-5.007E-03	-1.02E-05	-3.409E-03	-5.50E-06	-1.833E-03	-1.025E-02
963	-1.75E-05	-5.828E-03	-7.66E-05	-2.554E-02	-1.22E-04	-4.059E-02	-7.196E-02
964	-2.22E-05	-7.405E-03	-1.82E-04	-6.076E-02	-3.00E-04	-1.000E-01	-1.682E-01
965	-2.41E-05	-8.032E-03	-3.14E-04	-1.045E-01	-4.83E-04	-1.610E-01	-2.736E-01
966	-4.24E-05	-1.414E-02	-4.30E-04	-1.433E-01	-7.44E-04	-2.479E-01	-4.054E-01
967	-3.40E-05	-1.133E-02	-5.72E-04	-1.907E-01	-7.51E-04	-2.504E-01	-4.525E-01
968	-3.89E-05	-1.297E-02	-6.60E-04	-2.200E-01	-7.69E-04	-2.562E-01	-4.892E-01
969	-1.86E-05	-6.189E-03	-4.71E-04	-1.569E-01	-5.00E-04	-1.667E-01	-3.298E-01
970	-1.36E-05	-4.548E-03	-2.14E-04	-7.143E-02	-2.51E-04	-8.352E-02	-1.595E-01
971	1.49E-05	4.965E-03	-2.50E-05	-8.348E-03	-2.94E-06	-9.812E-04	-4.364E-03
972	1.76E-05	5.864E-03	-2.35E-06	-7.833E-04	-3.00E-06	-1.000E-03	4.080E-03
973	2.82E-05	9.384E-03	-1.47E-04	-4.914E-02	-1.74E-04	-5.806E-02	-9.782E-02
974	3.09E-05	1.030E-02	-3.79E-04	-1.263E-01	-4.29E-04	-1.430E-01	-2.590E-01
975	3.79E-05	1.265E-02	-6.58E-04	-2.194E-01	-7.28E-04	-2.427E-01	-4.495E-01
976	1.83E-05	6.092E-03	-7.42E-04	-2.472E-01	-8.08E-04	-2.692E-01	-5.103E-01
977	2.30E-05	7.673E-03	-9.44E-04	-3.147E-01	-9.90E-04	-3.301E-01	-6.371E-01
978	8.66E-06	2.887E-03	-7.25E-04	-2.417E-01	-7.78E-04	-2.595E-01	-4.983E-01
979	1.26E-05	4.197E-03	-5.21E-04	-1.735E-01	-5.18E-04	-1.727E-01	-3.420E-01
980	2.44E-06	8.118E-04	-2.26E-04	-7.545E-02	-1.86E-04	-6.194E-02	-1.366E-01
981	-5.68E-06	-1.893E-03	-4.99E-05	-1.662E-02	-8.74E-06	-2.915E-03	-2.143E-02
982	-1.51E-05	-5.043E-03	-1.02E-05	-3.416E-03	-5.70E-06	-1.901E-03	-1.036E-02

Time step							TOTAL Drag (N/m)
	Fix wing total Drag N/3MM	Fix Wing Drag (N/M)	Top wing total Drag N/3MM	Top Wing Drag (N/M)	Bot wing total Drag N/3MM	Bottom Wing Drag (N/M)	
983	-1.76E-05	-5.867E-03	-7.65E-05	-2.550E-02	-1.37E-04	-4.583E-02	-7.719E-02
984	-2.23E-05	-7.439E-03	-1.87E-04	-6.225E-02	-3.00E-04	-1.001E-01	-1.698E-01
985	-2.43E-05	-8.103E-03	-3.12E-04	-1.041E-01	-4.84E-04	-1.613E-01	-2.735E-01
986	-4.26E-05	-1.419E-02	-4.28E-04	-1.427E-01	-7.44E-04	-2.480E-01	-4.049E-01
987	-3.43E-05	-1.143E-02	-5.69E-04	-1.897E-01	-7.52E-04	-2.507E-01	-4.519E-01
988	-3.65E-05	-1.218E-02	-6.57E-04	-2.190E-01	-7.68E-04	-2.560E-01	-4.872E-01
989	-1.87E-05	-6.235E-03	-4.70E-04	-1.566E-01	-4.99E-04	-1.664E-01	-3.293E-01
990	-1.38E-05	-4.599E-03	-2.15E-04	-7.164E-02	-2.49E-04	-8.312E-02	-1.594E-01
991	1.46E-05	4.852E-03	-2.56E-05	-8.541E-03	-2.51E-06	-8.382E-04	-4.527E-03
992	1.72E-05	5.718E-03	-2.27E-06	-7.573E-04	-2.86E-06	-9.536E-04	4.007E-03
993	2.77E-05	9.237E-03	-1.47E-04	-4.902E-02	-1.74E-04	-5.788E-02	-9.767E-02
994	3.06E-05	1.019E-02	-3.78E-04	-1.259E-01	-4.28E-04	-1.427E-01	-2.585E-01
995	3.76E-05	1.254E-02	-6.57E-04	-2.189E-01	-7.27E-04	-2.423E-01	-4.487E-01
996	1.79E-05	5.981E-03	-7.40E-04	-2.465E-01	-8.06E-04	-2.688E-01	-5.093E-01
997	2.28E-05	7.602E-03	-9.42E-04	-3.141E-01	-1.00E-03	-3.338E-01	-6.403E-01
998	8.54E-06	2.848E-03	-7.43E-04	-2.476E-01	-7.79E-04	-2.598E-01	-5.045E-01
999	1.25E-05	4.178E-03	-5.20E-04	-1.735E-01	-5.19E-04	-1.730E-01	-3.423E-01
1000	2.37E-06	7.904E-04	-2.26E-04	-7.547E-02	-1.87E-04	-6.223E-02	-1.369E-01
1001	-5.78E-06	-1.927E-03	-4.99E-05	-1.663E-02	-8.99E-06	-2.996E-03	-2.155E-02
1002	-1.53E-05	-5.091E-03	-1.02E-05	-3.416E-03	-5.76E-06	-1.919E-03	-1.043E-02
1003	-1.78E-05	-5.926E-03	-7.64E-05	-2.546E-02	-5.76E-06	-1.919E-03	-3.330E-02
1004	-2.25E-05	-7.508E-03	-1.81E-04	-6.049E-02	-3.01E-04	-1.004E-01	-1.684E-01
1005	-2.46E-05	-8.201E-03	-3.11E-04	-1.037E-01	-4.86E-04	-1.621E-01	-2.740E-01
1006	-4.29E-05	-1.430E-02	-4.26E-04	-1.420E-01	-6.83E-04	-2.278E-01	-3.841E-01
1007	-3.47E-05	-1.156E-02	-5.76E-04	-1.918E-01	-7.55E-04	-2.517E-01	-4.552E-01
1008	-3.69E-05	-1.229E-02	-6.54E-04	-2.180E-01	-7.72E-04	-2.574E-01	-4.876E-01
1009	-1.89E-05	-6.301E-03	-4.79E-04	-1.597E-01	-4.99E-04	-1.663E-01	-3.323E-01
1010	-1.39E-05	-4.636E-03	-2.16E-04	-7.207E-02	-2.48E-04	-8.277E-02	-1.595E-01
1011	1.43E-05	4.769E-03	-2.65E-05	-8.833E-03	-2.12E-06	-7.066E-04	-4.771E-03
1012	1.68E-05	5.606E-03	-2.15E-06	-7.155E-04	-2.80E-06	-9.340E-04	3.956E-03
1013	2.74E-05	9.129E-03	-1.47E-04	-4.895E-02	-1.74E-04	-5.791E-02	-9.773E-02
1014	3.02E-05	1.006E-02	-3.77E-04	-1.257E-01	-4.28E-04	-1.427E-01	-2.583E-01
1015	3.72E-05	1.241E-02	-6.56E-04	-2.187E-01	-7.27E-04	-2.424E-01	-4.487E-01
1016	1.75E-05	5.846E-03	-7.39E-04	-2.462E-01	-8.08E-04	-2.692E-01	-5.096E-01
1017	2.24E-05	7.472E-03	-9.42E-04	-3.140E-01	-9.96E-04	-3.320E-01	-6.386E-01
1018	8.10E-06	2.701E-03	-7.43E-04	-2.477E-01	-7.81E-04	-2.605E-01	-5.055E-01
1019	1.21E-05	4.045E-03	-5.21E-04	-1.735E-01	-5.21E-04	-1.735E-01	-3.430E-01
1020	2.12E-06	7.083E-04	-2.26E-04	-7.549E-02	-1.88E-04	-6.251E-02	-1.373E-01

B. $U_{\infty}=3\text{M/S}$, $\alpha = 10^\circ$, $f = 0\text{HZ}$, WING SEPARATION: 82.5MM

Time step	Fix Wing		Top Wing		Bottom Wing		TOTAL LIFT (N/M)
	X	Fix Wing Drag (N/M)	Top wing total Lift N/3MM	Top Wing Lift (N/M)	Bot wing total Lift N/3MM	Bottom Wing Lift (N/M)	
940	0.0014597	0.4865716	4.5811E-05	0.0152703	0.000384	0.1279348	0.629777
942	0.0015057	0.5019021	9.5779E-05	0.0319263	0.000399	0.132984133	0.666813
944	0.0015853	0.5284353	0.00012552	0.0418416	0.000416	0.138673533	0.70895
946	0.0016839	0.5612916	0.00012454	0.0415126	0.00043	0.143400567	0.746205
948	0.0017572	0.5857431	8.7404E-05	0.0291346	0.000438	0.146125667	0.761003
950	0.0017693	0.5897532	1.9373E-05	0.0064578	0.000439	0.146292867	0.742504
952	0.0016978	0.5659458	-6.1647E-05	-0.0205491	0.000432	0.1438901	0.689287
954	0.0015715	0.523843	-0.00012323	-0.0410781	0.000418	0.139480287	0.622245
956	0.0014731	0.491033	-0.00013382	-0.044606	0.000402	0.134137603	0.580565
958	0.0014335	0.4778363	-9.161E-05	-0.0305366	0.000388	0.129432933	0.576733
960	0.0014298	0.4765936	-2.2967E-05	-0.0076557	0.000381	0.1270441	0.595982
962	0.0014698	0.4899324	7.2445E-05	0.0241482	0.000388	0.129361233	0.643442
964	0.0015322	0.510724	0.00011791	0.0393018	0.000401	0.1338253	0.683851
966	0.0016265	0.5421824	0.00014177	0.047256	0.000416	0.138689233	0.728128
968	0.0017321	0.5773611	0.00013513	0.0450418	0.000427	0.1423665	0.764769
970	0.001801	0.60034	9.4655E-05	0.0315515	0.000432	0.143847033	0.775739
972	0.0017994	0.5998089	2.4369E-05	0.0081231	0.000428	0.142679233	0.750611
974	0.0017087	0.5695627	-5.9194E-05	-0.0197313	0.000417	0.139116967	0.688948
976	0.001576	0.5253303	-0.00012388	-0.0412936	0.000402	0.134057337	0.618094
978	0.0014869	0.4956384	-0.00013683	-0.0456112	0.000387	0.12885225	0.578879
980	0.0014495	0.4831832	-9.5549E-05	-0.0318497	0.000376	0.125205803	0.576539
982	0.0014434	0.4811365	-2.7509E-05	-0.0091697	0.000374	0.12451439	0.596481
984	0.0014589	0.486286	3.8872E-05	0.0129572	0.000382	0.127181867	0.626425
986	0.0015021	0.5007079	9.0911E-05	0.0303038	0.000397	0.1323028	0.663315
988	0.0015796	0.5265236	0.00012336	0.0411194	0.000414	0.138148733	0.705792
990	0.0016787	0.5595693	0.00012566	0.0418859	0.000429	0.143094933	0.74455
992	0.0017568	0.5856159	9.1479E-05	0.0304929	0.000438	0.146070467	0.762179
994	0.0017754	0.5917978	2.53E-05	0.0084334	0.00044	0.1465024	0.746734
996	0.0017108	0.570266	-5.607E-05	-0.0186899	0.000433	0.1443327	0.695909
998	0.0015859	0.5286221	-0.00012106	-0.040352	0.00042	0.140074333	0.628344
1000	0.0014819	0.4939766	-0.0001367	-0.0455678	0.000404	0.134763937	0.583173

Time step	Fix Wing		Top Wing		Bottom Wing		TOTAL DRAG (N/M)
	Fix wing total Drag (N/3MM)	Fix Wing Drag (N/M)	Top Wing Drag (N/3MM)	Top Wing Drag (N/M)	Bot wing drag N/3MM	Bot Wing Drag (N/M)	
940	5.966E-05	0.0198876	2.069E-05	0.0068967	1.54E-05	0.005139458	0.031924
942	5.709E-05	0.019031	2.139E-05	0.0071301	1.51E-05	0.005034822	0.031196
944	5.048E-05	0.0168268	2.1694E-05	0.0072315	1.48E-05	0.004931507	0.02899
946	4.148E-05	0.0138271	2.1507E-05	0.0071689	1.46E-05	0.004861962	0.025858
948	3.35E-05	0.0111678	2.0814E-05	0.0069381	1.45E-05	0.004846831	0.022953
950	2.889E-05	0.0096294	1.9812E-05	0.0066039	1.47E-05	0.004887632	0.021121
952	2.996E-05	0.0099882	1.8833E-05	0.0062777	1.49E-05	0.004968359	0.021234
954	3.705E-05	0.0123489	1.8085E-05	0.0060283	1.52E-05	0.005060334	0.023438
956	4.579E-05	0.015262	1.7858E-05	0.0059525	1.54E-05	0.005137493	0.026352
958	5.286E-05	0.0176188	1.8288E-05	0.0060959	1.55E-05	0.005183277	0.028898
960	5.808E-05	0.0193593	1.9185E-05	0.0063949	1.56E-05	0.005186124	0.03094
962	6.077E-05	0.0202578	2.0644E-05	0.0068813	1.53E-05	0.005106302	0.032245
964	5.767E-05	0.0192231	2.1298E-05	0.0070993	1.51E-05	0.005018672	0.031341
966	5.051E-05	0.0168381	2.1542E-05	0.0071807	1.48E-05	0.004938169	0.028957
968	4.125E-05	0.0137495	2.131E-05	0.0071034	1.47E-05	0.004895685	0.025749
970	3.341E-05	0.0111351	2.0618E-05	0.0068726	1.47E-05	0.004908415	0.022916
972	2.924E-05	0.0097453	1.9693E-05	0.0065645	1.49E-05	0.004973992	0.021284
974	3.13E-05	0.0104339	1.8863E-05	0.0062875	1.52E-05	0.005071138	0.021793
976	3.885E-05	0.0129505	1.8293E-05	0.0060976	1.55E-05	0.005167545	0.024216
978	4.695E-05	0.0156512	1.824E-05	0.00608	1.57E-05	0.005237086	0.026968
980	5.356E-05	0.0178526	1.8795E-05	0.0062649	1.58E-05	0.005263373	0.029381
982	5.82E-05	0.0193998	1.9728E-05	0.0065761	1.57E-05	0.005236834	0.031213
984	5.994E-05	0.0199808	2.0691E-05	0.0068969	1.55E-05	0.005159928	0.032038
986	5.767E-05	0.0192233	2.1413E-05	0.0071378	1.52E-05	0.00505148	0.031413
988	5.124E-05	0.0170815	2.1747E-05	0.007249	1.48E-05	0.004942286	0.029273
990	4.219E-05	0.0140638	2.1591E-05	0.0071971	1.46E-05	0.004865545	0.026127
992	3.388E-05	0.0112928	2.0924E-05	0.0069747	1.45E-05	0.004843201	0.023111
994	2.885E-05	0.0096153	1.9924E-05	0.0066412	1.46E-05	0.00487811	0.021135
996	2.936E-05	0.009786	1.8925E-05	0.0063083	1.49E-05	0.004955295	0.02105
998	3.606E-05	0.0120198	1.8138E-05	0.0060459	1.51E-05	0.005046525	0.023112
1000	4.489E-05	0.0149629	1.7852E-05	0.0059505	1.54E-05	0.005125047	0.026038

C. $U_\infty=3\text{M/S}$, $f=25\text{HZ}$, $\Phi=10^\circ$, PITCH/PLUNGE IN-PHASE

Time step							TOTAL Lift (N/m)
	Fix wing total Lift N/3MM	Fix Wing Lift (N/M)	Top wing total Lift N/3MM	Top Wing Lift (N/M)	Bot wing total Lift N/3MM	Bottom Wing Lift (N/M)	
940	1.93E-03	6.424E-01	-7.85E-04	-2.617E-01	1.86E-03	6.184E-01	9.991E-01
941	1.95E-03	6.498E-01	-4.07E-05	-1.357E-02	1.29E-03	4.291E-01	1.065E+00
942	1.95E-03	6.494E-01	7.75E-04	2.583E-01	6.33E-04	2.109E-01	1.119E+00
943	1.92E-03	6.385E-01	1.27E-03	4.238E-01	5.00E-05	1.668E-02	1.079E+00
944	1.88E-03	6.251E-01	1.85E-03	6.158E-01	-3.91E-04	-1.302E-01	1.111E+00
945	1.82E-03	6.081E-01	2.31E-03	7.700E-01	-6.72E-04	-2.240E-01	1.154E+00
946	1.77E-03	5.905E-01	1.92E-03	6.410E-01	-8.12E-04	-2.706E-01	9.609E-01
947	1.71E-03	5.685E-01	2.90E-03	9.660E-01	-9.53E-04	-3.176E-01	1.217E+00
948	1.67E-03	5.567E-01	2.14E-03	7.126E-01	-9.17E-04	-3.056E-01	9.636E-01
949	1.64E-03	5.451E-01	2.38E-03	7.937E-01	-9.50E-04	-3.167E-01	1.022E+00
950	1.59E-03	5.304E-01	1.66E-03	5.536E-01	-5.85E-04	-1.949E-01	8.891E-01
951	1.53E-03	5.099E-01	1.40E-03	4.670E-01	-3.28E-04	-1.092E-01	8.677E-01
952	1.47E-03	4.912E-01	6.82E-04	2.272E-01	2.33E-04	7.760E-02	7.960E-01
953	1.39E-03	4.636E-01	7.30E-05	2.433E-02	7.33E-04	2.442E-01	7.321E-01
954	1.32E-03	4.409E-01	-5.91E-04	-1.971E-01	1.29E-03	4.315E-01	6.752E-01
955	1.23E-03	4.117E-01	-1.28E-03	-4.282E-01	1.83E-03	6.091E-01	5.925E-01
956	1.05E-03	3.495E-01	-1.61E-03	-5.375E-01	1.91E-03	6.358E-01	4.478E-01
957	1.08E-03	3.616E-01	-2.27E-03	-7.565E-01	2.76E-03	9.199E-01	5.250E-01
958	9.69E-04	3.231E-01	-2.19E-03	-7.286E-01	2.59E-03	8.627E-01	4.572E-01
959	1.04E-03	3.453E-01	-1.86E-03	-6.207E-01	2.67E-03	8.903E-01	6.149E-01
960	1.02E-03	3.396E-01	-8.54E-04	-2.848E-01	2.13E-03	7.090E-01	7.637E-01
961	9.91E-04	3.305E-01	2.45E-05	8.173E-03	1.54E-03	5.123E-01	8.509E-01
962	9.48E-04	3.160E-01	9.31E-04	3.104E-01	8.35E-04	2.783E-01	9.047E-01
963	9.11E-04	3.037E-01	1.55E-03	5.157E-01	2.25E-04	7.484E-02	8.942E-01
964	8.88E-04	2.959E-01	2.19E-03	7.304E-01	4.11E-07	1.369E-04	1.026E+00
965	8.62E-04	2.874E-01	2.92E-03	9.733E-01	-4.98E-04	-1.660E-01	1.095E+00
966	8.70E-04	2.901E-01	2.28E-03	7.585E-01	-6.06E-04	-2.021E-01	8.464E-01
967	8.21E-04	2.736E-01	3.67E-03	1.224E+00	-6.06E-04	-2.021E-01	1.296E+00
968	8.14E-04	2.714E-01	2.62E-03	8.725E-01	-6.52E-04	-2.172E-01	9.267E-01
969	7.86E-04	2.621E-01	2.98E-03	9.940E-01	-6.68E-04	-2.227E-01	1.033E+00
970	7.85E-04	2.617E-01	2.11E-03	7.037E-01	-2.90E-04	-9.683E-02	8.686E-01
971	7.64E-04	2.548E-01	1.59E-03	5.299E-01	-2.37E-05	-7.896E-03	7.768E-01
972	7.52E-04	2.508E-01	8.66E-04	2.886E-01	5.19E-04	1.730E-01	7.124E-01
973	7.23E-04	2.411E-01	1.21E-04	4.048E-02	1.06E-03	3.519E-01	6.336E-01
974	6.82E-04	2.273E-01	-6.83E-04	-2.276E-01	1.63E-03	5.443E-01	5.439E-01
975	6.30E-04	2.099E-01	-1.56E-03	-5.199E-01	2.26E-03	7.523E-01	4.423E-01
976	3.79E-04	1.263E-01	-2.05E-03	-6.831E-01	2.30E-03	7.676E-01	2.108E-01
977	4.70E-04	1.566E-01	-2.85E-03	-9.510E-01	3.39E-03	1.131E+00	3.368E-01
978	2.60E-04	8.664E-02	-2.93E-03	-9.783E-01	3.15E-03	1.050E+00	1.580E-01
979	3.01E-04	1.002E-01	-2.82E-03	-9.412E-01	3.30E-03	1.100E+00	2.593E-01
980	2.37E-04	7.890E-02	-1.91E-03	-6.366E-01	2.66E-03	8.864E-01	3.287E-01
981	2.31E-04	7.692E-02	-8.57E-04	-2.856E-01	2.00E-03	6.673E-01	4.586E-01
982	1.87E-04	6.247E-02	2.14E-04	7.127E-02	1.17E-03	3.895E-01	5.233E-01
983	1.58E-04	5.269E-02	9.59E-04	3.198E-01	4.88E-04	1.628E-01	5.353E-01

Time step							TOTAL Lift (N/m)
	Fix wing total Lift N/3MM	Fix Wing Lift (N/M)	Top wing total Lift N/3MM	Top Wing Lift (N/M)	Bot wing total Lift N/3MM	Bottom Wing Lift (N/M)	
984	1.37E-04	4.551E-02	1.60E-03	5.325E-01	-6.33E-06	-2.110E-03	5.759E-01
985	1.12E-04	3.732E-02	2.35E-03	7.845E-01	-3.01E-04	-1.004E-01	7.215E-01
986	1.64E-04	5.460E-02	1.76E-03	5.867E-01	-4.45E-04	-1.485E-01	4.928E-01
987	1.56E-04	5.191E-02	3.17E-03	1.058E+00	-5.62E-04	-1.874E-01	9.228E-01
988	1.67E-04	5.560E-02	2.57E-03	8.582E-01	-5.85E-04	-1.949E-01	7.189E-01
989	1.73E-04	5.756E-02	2.93E-03	9.773E-01	-6.05E-04	-2.016E-01	8.332E-01
990	1.95E-04	6.510E-02	2.50E-03	8.334E-01	-2.45E-04	-8.160E-02	8.169E-01
991	2.12E-04	7.059E-02	1.93E-03	6.447E-01	6.44E-05	2.148E-02	7.368E-01
992	2.26E-04	7.529E-02	1.00E-03	3.348E-01	6.55E-04	2.185E-01	6.286E-01
993	2.05E-04	6.818E-02	5.48E-05	1.826E-02	1.25E-03	4.172E-01	5.037E-01
994	1.60E-04	5.349E-02	-8.35E-04	-2.785E-01	1.87E-03	6.229E-01	3.979E-01
995	9.44E-05	3.147E-02	-1.77E-03	-5.897E-01	2.54E-03	8.477E-01	2.894E-01
996	-1.58E-04	-5.274E-02	-2.16E-03	-7.209E-01	2.57E-03	8.557E-01	8.213E-02
997	-9.63E-05	-3.210E-02	-3.09E-03	-1.031E+00	3.75E-03	1.248E+00	1.858E-01
998	-3.13E-04	-1.044E-01	-3.15E-03	-1.049E+00	3.46E-03	1.152E+00	-1.167E-03
999	-2.50E-04	-8.340E-02	-3.15E-03	-1.051E+00	3.69E-03	1.231E+00	9.684E-02
1000	-2.61E-04	-8.700E-02	-2.31E-03	-7.695E-01	2.95E-03	9.833E-01	1.269E-01
1001	-1.78E-04	-5.941E-02	-1.30E-03	-4.331E-01	2.26E-03	7.548E-01	2.623E-01
1002	-1.05E-04	-3.484E-02	-9.21E-05	-3.069E-02	1.37E-03	4.570E-01	3.915E-01
1003	-1.68E-05	-5.594E-03	7.37E-04	2.458E-01	6.45E-04	2.150E-01	4.553E-01
1004	9.30E-05	3.098E-02	1.37E-03	4.564E-01	4.78E-07	1.593E-04	4.876E-01
1005	2.01E-04	6.712E-02	2.24E-03	7.471E-01	-2.21E-04	-7.369E-02	7.406E-01
1006	3.74E-04	1.246E-01	1.76E-03	5.870E-01	-4.16E-04	-1.386E-01	5.730E-01
1007	4.58E-04	1.527E-01	3.13E-03	1.042E+00	-5.80E-04	-1.932E-01	1.002E+00
1008	5.32E-04	1.773E-01	2.59E-03	8.625E-01	-6.73E-04	-2.245E-01	8.153E-01
1009	5.80E-04	1.934E-01	2.78E-03	9.270E-01	-7.40E-04	-2.466E-01	8.738E-01
1010	6.35E-04	2.118E-01	2.19E-03	7.309E-01	-3.91E-04	-1.302E-01	8.124E-01
1011	6.48E-04	2.160E-01	1.40E-03	4.677E-01	-3.61E-07	-1.202E-04	6.836E-01
1012	6.46E-04	2.153E-01	3.92E-04	1.306E-01	5.60E-04	1.865E-01	5.324E-01
1013	6.11E-04	2.037E-01	-5.37E-04	-1.789E-01	1.17E-03	3.889E-01	4.137E-01
1014	5.63E-04	1.876E-01	-1.36E-03	-4.527E-01	1.82E-03	6.057E-01	3.407E-01
1015	3.70E-04	1.235E-01	-2.40E-03	-7.996E-01	2.45E-03	8.173E-01	1.411E-01
1016	2.69E-04	8.959E-02	-2.44E-03	-8.127E-01	2.52E-03	8.413E-01	1.183E-01
1017	1.52E-04	5.065E-02	-3.75E-03	-1.250E+00	3.59E-03	1.198E+00	-1.752E-03
1018	9.52E-05	3.174E-02	-3.67E-03	-1.224E+00	3.37E-03	1.124E+00	-6.826E-02
1019	2.21E-04	7.358E-02	-3.69E-03	-1.230E+00	3.52E-03	1.174E+00	1.796E-02
1020	3.74E-04	1.247E-01	-2.77E-03	-9.220E-01	2.90E-03	9.675E-01	1.702E-01

Time step	Fix wing total DRAG N/3MM	Fix Wing Drag (N/M)	Top wing total Drag N/3MM	Top Wing Drag (N/M)	Bot wing total Drag N/3MM	Bottom Wing Drag (N/M)	TOTAL Drag (N/M)
940	3.6157E-05	0.012052	3.41E-06	0.001135	-5E-06	-0.00166	0.01153
941	2.1291E-05	0.007097	6.59E-06	0.002196	-7.2E-05	-0.02408	-0.01479
942	5.033E-06	0.001678	9.33E-05	0.031085	-6.6E-05	-0.022	0.010766
943	-7.947E-06	-0.00265	0.000198	0.066114	-5.5E-06	-0.00184	0.061627
944	-1.608E-05	-0.00536	0.000328	0.109184	6.92E-05	0.023083	0.126906
945	-1.956E-05	-0.00652	0.000423	0.141126	0.000123	0.041095	0.1757
946	-1.943E-05	-0.00648	0.000331	0.110248	0.000139	0.046341	0.150111
947	-1.837E-05	-0.00612	0.000412	0.137324	0.000136	0.045459	0.17666
948	-1.638E-05	-0.00546	0.000212	0.070568	9.23E-05	0.030774	0.095882
949	-1.479E-05	-0.00493	0.000113	0.037556	4.69E-05	0.015624	0.04825
950	-1.025E-05	-0.00342	-2.1E-05	-0.00684	-3.7E-06	-0.00122	-0.01148
951	-6.311E-06	-0.0021	-9.9E-05	-0.03304	-1.9E-05	-0.00635	-0.0415
952	2.5558E-06	0.000852	-9.5E-05	-0.0317	2.63E-05	0.008751	-0.0221
953	1.2042E-05	0.004014	-3.5E-05	-0.01177	0.000111	0.036954	0.0292
954	2.6198E-05	0.008733	7.52E-05	0.025079	0.000227	0.075592	0.109404
955	4.4508E-05	0.014836	0.000205	0.068242	0.000333	0.110947	0.194024
956	5.3963E-05	0.017987	0.000251	0.083749	0.000326	0.108714	0.21045
957	8.0696E-05	0.026898	0.000308	0.102615	0.000393	0.130946	0.26046
958	9.2927E-05	0.030975	0.000215	0.071791	0.000262	0.087417	0.190183
959	0.00010772	0.035905	9.73E-05	0.032419	0.000138	0.046033	0.114356
960	0.0001087	0.036233	3.64E-06	0.001214	-5.8E-06	-0.00192	0.035529
961	0.00010302	0.034338	1.07E-05	0.003563	-8.6E-05	-0.02881	0.009093
962	9.3134E-05	0.031044	0.00011	0.036533	-8.8E-05	-0.02918	0.038401
963	8.4471E-05	0.028157	0.000236	0.078703	-3.1E-05	-0.0104	0.096461
964	7.7797E-05	0.025932	0.000381	0.126931	2.45E-06	0.000817	0.153681
965	7.3568E-05	0.024522	0.000523	0.174438	9.16E-05	0.030533	0.229493
966	7.1494E-05	0.023831	0.000381	0.127016	0.000104	0.034629	0.185476
967	6.8965E-05	0.022988	0.000513	0.170908	0.000104	0.034629	0.228525
968	6.5301E-05	0.021767	0.000252	0.083986	6.53E-05	0.021778	0.127532
969	6.2626E-05	0.020875	0.000137	0.045633	3.24E-05	0.010784	0.077292
970	6.1193E-05	0.020397	-2.8E-05	-0.00928	-2.9E-06	-0.00097	0.010149
971	5.7909E-05	0.019303	-0.00013	-0.04183	-1.5E-06	-0.00049	-0.02302
972	5.8696E-05	0.019565	-0.00012	-0.03967	5.79E-05	0.019299	-0.00081
973	6.1234E-05	0.020411	-4.6E-05	-0.01537	0.00016	0.053207	0.058251
974	6.8234E-05	0.022745	8.67E-05	0.028894	0.000286	0.0954	0.147039
975	8.2491E-05	0.027497	0.000248	0.082808	0.00041	0.136793	0.247097
976	8.3037E-05	0.027679	0.000318	0.105993	0.000393	0.130913	0.264585
977	0.0001098	0.036598	0.000382	0.127419	0.000483	0.160868	0.324885
978	0.00011674	0.038914	0.000282	0.094126	0.00032	0.106554	0.239594
979	0.00013239	0.044131	0.000138	0.046101	0.000172	0.057358	0.14759
980	0.00013416	0.044721	-7.4E-06	-0.00247	-5.7E-06	-0.00188	0.040366
981	0.00013206	0.044021	-4.7E-05	-0.01572	-0.00011	-0.03712	-0.00881
982	0.0001237	0.041233	2.59E-05	0.008649	-0.00012	-0.04055	0.009336
983	0.00011637	0.038789	0.000143	0.047669	-6.9E-05	-0.02287	0.063586

Time step	Fix wing total DRAG N/3MM	Fix Wing Drag (N/M)	Top wing total Drag N/3MM	Top Wing Drag (N/M)	Bot wing total Drag N/3MM	Bottom Wing Drag (N/M)	TOTAL Drag (N/M)
984	0.0001095	0.036499	0.000273	0.090844	3.92E-06	0.001308	0.128651
985	0.00010406	0.034685	0.000415	0.138374	5.69E-05	0.01898	0.192039
986	9.9181E-05	0.03306	0.000288	0.096115	7.73E-05	0.025767	0.154943
987	9.2448E-05	0.030816	0.000437	0.145531	8.14E-05	0.027135	0.203481
988	8.3968E-05	0.027989	0.000243	0.081039	6.04E-05	0.020124	0.129152
989	7.5356E-05	0.025118	0.000132	0.044042	3.18E-05	0.010613	0.079774
990	6.9334E-05	0.023111	-3E-05	-0.00986	7.86E-07	0.000262	0.013514
991	6.192E-05	0.02064	-0.00013	-0.04359	5.05E-06	0.001684	-0.02127
992	5.9291E-05	0.019763	-0.00013	-0.0423	7.72E-05	0.025719	0.003186
993	5.8183E-05	0.019394	-2.8E-05	-0.00935	0.000193	0.064233	0.074277
994	6.2603E-05	0.020867	0.000121	0.040495	0.00033	0.110139	0.171501
995	7.5891E-05	0.025297	0.000293	0.097633	0.000465	0.15487	0.277799
996	7.5485E-05	0.025161	0.000352	0.117435	0.00044	0.146544	0.28914
997	0.00010427	0.034756	0.000415	0.13819	0.000534	0.178081	0.351027
998	0.0001136	0.037868	0.000297	0.099136	0.000352	0.117463	0.254467
999	0.00013417	0.044723	0.000145	0.048472	0.000191	0.063518	0.156713
1000	0.00014138	0.047125	-2E-05	-0.00668	-5.5E-06	-0.00183	0.038618
1001	0.00014229	0.047429	-8.4E-05	-0.02799	-0.00013	-0.04185	-0.02241
1002	0.00013898	0.046325	-1.8E-05	-0.00608	-0.00015	-0.0499	-0.00966
1003	0.00013069	0.043562	9.97E-05	0.033238	-9.1E-05	-0.03036	0.046439
1004	0.00011984	0.039945	0.000224	0.074795	2.85E-06	0.000951	0.115691
1005	0.00010832	0.036106	0.000387	0.129006	4.3E-05	0.014317	0.179429
1006	9.5835E-05	0.031945	0.000283	0.094345	7.28E-05	0.02428	0.15057
1007	8.1924E-05	0.027308	0.000428	0.142527	8.49E-05	0.028287	0.198121
1008	6.6878E-05	0.022292	0.000246	0.082062	7.11E-05	0.023708	0.128063
1009	5.287E-05	0.017623	0.00013	0.043353	4.13E-05	0.013765	0.074742
1010	4.3556E-05	0.014518	-1.8E-05	-0.00595	3.26E-06	0.001087	0.009655
1011	3.4813E-05	0.011604	-9E-05	-0.03006	6.68E-06	0.002227	-0.01623
1012	3.3028E-05	0.011009	-5.1E-05	-0.01701	6.94E-05	0.023138	0.017139
1013	3.3866E-05	0.011289	6.87E-05	0.022895	0.000183	0.060852	0.095035
1014	4.0801E-05	0.0136	0.000221	0.073632	0.000324	0.108062	0.195294
1015	5.4015E-05	0.018005	0.000414	0.138078	0.000452	0.150593	0.306676
1016	6.0679E-05	0.020226	0.000395	0.131743	0.000436	0.145236	0.297206
1017	8.4793E-05	0.028264	0.000514	0.171462	0.000515	0.171721	0.371447
1018	9.3405E-05	0.031135	0.000355	0.118441	0.000345	0.115086	0.264661
1019	0.00010285	0.034284	0.000176	0.058812	0.000185	0.061724	0.154821
1020	9.7902E-05	0.032634	-1.9E-05	-0.00627	-5.5E-06	-0.00185	0.024511

D. $U_\infty=3\text{M/S}$, $f=25\text{HZ}$, $\Phi=10^\circ$, PITCH/PLUNGE OUT OF PHASE

Time step	Fix wing		Top wing total		Bot wing		TOTAL Lift (N/m)
	total Lift N/3MM	Wing Lift (N/M)	Lift N/3MM	Wing Lift (N/M)	total Lift N/3MM	Bottom Wing Lift (N/M)	
940	2.75E-03	9.156E-01	-6.93E-04	-2.309E-01	1.10E-03	3.672E-01	1.052E+00
941	2.78E-03	9.268E-01	-1.53E-03	-5.092E-01	1.98E-03	6.609E-01	1.078E+00
942	2.80E-03	9.336E-01	-2.29E-03	-7.620E-01	2.80E-03	9.323E-01	1.104E+00
943	3.05E-03	1.017E+00	-2.62E-03	-8.726E-01	3.46E-03	1.153E+00	1.297E+00
944	3.29E-03	1.097E+00	-3.14E-03	-1.048E+00	4.08E-03	1.361E+00	1.409E+00
945	3.48E-03	1.161E+00	-3.25E-03	-1.084E+00	4.31E-03	1.438E+00	1.514E+00
946	3.49E-03	1.164E+00	-3.01E-03	-1.004E+00	4.09E-03	1.362E+00	1.522E+00
947	3.43E-03	1.144E+00	-2.20E-03	-7.331E-01	3.33E-03	1.109E+00	1.520E+00
948	3.39E-03	1.130E+00	-1.19E-03	-3.959E-01	2.29E-03	7.639E-01	1.498E+00
949	3.38E-03	1.126E+00	-9.08E-05	-3.028E-02	1.20E-03	3.995E-01	1.495E+00
950	3.25E-03	1.083E+00	3.21E-04	1.071E-01	3.90E-04	1.300E-01	1.321E+00
951	3.23E-03	1.076E+00	7.97E-04	2.656E-01	-1.59E-04	-5.314E-02	1.289E+00
952	3.17E-03	1.056E+00	9.07E-04	3.022E-01	-3.78E-04	-1.260E-01	1.232E+00
953	3.06E-03	1.021E+00	1.06E-03	3.521E-01	-6.25E-04	-2.085E-01	1.165E+00
954	2.94E-03	9.799E-01	1.10E-03	3.673E-01	-8.02E-04	-2.673E-01	1.080E+00
955	2.79E-03	9.308E-01	1.13E-03	3.761E-01	-9.60E-04	-3.199E-01	9.871E-01
956	2.67E-03	8.893E-01	1.24E-03	4.125E-01	-1.08E-03	-3.610E-01	9.407E-01
957	2.61E-03	8.695E-01	1.19E-03	3.965E-01	-9.31E-04	-3.104E-01	9.556E-01
958	2.69E-03	8.966E-01	9.99E-04	3.330E-01	-5.41E-04	-1.802E-01	1.049E+00
959	2.75E-03	9.173E-01	1.87E-04	6.236E-02	1.93E-04	6.429E-02	1.044E+00
960	2.77E-03	9.225E-01	-7.29E-04	-2.428E-01	1.10E-03	3.655E-01	1.045E+00
961	2.80E-03	9.348E-01	-1.55E-03	-5.179E-01	1.97E-03	6.576E-01	1.074E+00
962	2.83E-03	9.442E-01	-2.31E-03	-7.697E-01	2.78E-03	9.267E-01	1.101E+00
963	3.09E-03	1.028E+00	-2.64E-03	-8.805E-01	3.44E-03	1.145E+00	1.293E+00
964	3.29E-03	1.095E+00	-3.27E-03	-1.091E+00	4.08E-03	1.358E+00	1.363E+00
965	3.45E-03	1.151E+00	-3.40E-03	-1.133E+00	4.32E-03	1.440E+00	1.458E+00
966	3.43E-03	1.143E+00	-3.21E-03	-1.072E+00	4.10E-03	1.367E+00	1.438E+00
967	3.38E-03	1.126E+00	-2.37E-03	-7.895E-01	3.34E-03	1.114E+00	1.451E+00
968	3.33E-03	1.111E+00	-1.34E-03	-4.452E-01	2.31E-03	7.686E-01	1.435E+00
969	3.34E-03	1.112E+00	-1.93E-04	-6.422E-02	1.21E-03	4.035E-01	1.452E+00
970	3.21E-03	1.068E+00	2.84E-04	9.455E-02	3.97E-04	1.322E-01	1.295E+00
971	3.15E-03	1.052E+00	7.25E-04	2.415E-01	-1.54E-04	-5.150E-02	1.242E+00
972	3.08E-03	1.026E+00	8.54E-04	2.847E-01	-3.74E-04	-1.247E-01	1.186E+00
973	2.95E-03	9.850E-01	9.82E-04	3.274E-01	-6.22E-04	-2.072E-01	1.105E+00
974	2.82E-03	9.392E-01	1.02E-03	3.415E-01	-7.96E-04	-2.654E-01	1.015E+00
975	2.67E-03	8.891E-01	1.05E-03	3.503E-01	-9.50E-04	-3.168E-01	9.227E-01
976	2.55E-03	8.506E-01	1.18E-03	3.932E-01	-1.07E-03	-3.568E-01	8.870E-01
977	2.51E-03	8.383E-01	1.15E-03	3.830E-01	-9.15E-04	-3.050E-01	9.163E-01
978	2.63E-03	8.756E-01	9.81E-04	3.268E-01	-5.25E-04	-1.749E-01	1.028E+00
979	2.72E-03	9.055E-01	2.00E-04	6.664E-02	2.05E-04	6.817E-02	1.040E+00
980	2.75E-03	9.153E-01	-6.93E-04	-2.309E-01	1.10E-03	3.672E-01	1.052E+00
981	2.78E-03	9.266E-01	-1.53E-03	-5.092E-01	1.98E-03	6.609E-01	1.078E+00
982	2.80E-03	9.335E-01	-2.29E-03	-7.620E-01	2.80E-03	9.322E-01	1.104E+00

Time step							TOTAL Lift (N/m)
	Fix wing total Lift N/3MM	Fix Wing Lift (N/M)	Top wing total Lift N/3MM	Top Wing Lift (N/M)	Bot wing total Lift N/3MM	Bottom Wing Lift (N/M)	
983	3.05E-03	1.017E+00	-2.62E-03	-8.725E-01	3.46E-03	1.153E+00	1.297E+00
984	3.29E-03	1.096E+00	-3.15E-03	-1.049E+00	4.08E-03	1.361E+00	1.408E+00
985	3.48E-03	1.160E+00	-3.26E-03	-1.085E+00	4.31E-03	1.438E+00	1.513E+00
986	3.49E-03	1.163E+00	-3.02E-03	-1.005E+00	4.09E-03	1.362E+00	1.520E+00
987	3.43E-03	1.143E+00	-2.20E-03	-7.342E-01	3.33E-03	1.109E+00	1.519E+00
988	3.39E-03	1.130E+00	-1.19E-03	-3.970E-01	2.29E-03	7.641E-01	1.497E+00
989	3.38E-03	1.125E+00	-9.30E-05	-3.100E-02	1.20E-03	3.997E-01	1.494E+00
990	3.25E-03	1.083E+00	3.20E-04	1.067E-01	3.91E-04	1.302E-01	1.320E+00
991	3.23E-03	1.075E+00	7.95E-04	2.650E-01	-1.59E-04	-5.304E-02	1.287E+00
992	3.16E-03	1.054E+00	9.05E-04	3.017E-01	-3.78E-04	-1.259E-01	1.230E+00
993	3.06E-03	1.020E+00	1.05E-03	3.514E-01	-6.25E-04	-2.084E-01	1.163E+00
994	2.93E-03	9.781E-01	1.10E-03	3.664E-01	-8.01E-04	-2.671E-01	1.077E+00
995	2.79E-03	9.289E-01	1.13E-03	3.752E-01	-9.59E-04	-3.196E-01	9.845E-01
996	2.66E-03	8.875E-01	1.24E-03	4.118E-01	-1.08E-03	-3.607E-01	9.386E-01
997	2.60E-03	8.681E-01	1.19E-03	3.964E-01	-9.30E-04	-3.100E-01	9.544E-01
998	2.69E-03	8.956E-01	1.00E-03	3.332E-01	-5.40E-04	-1.799E-01	1.049E+00
999	2.75E-03	9.167E-01	1.89E-04	6.285E-02	1.94E-04	6.452E-02	1.044E+00
1000	2.77E-03	9.222E-01	-7.26E-04	-2.421E-01	1.10E-03	3.656E-01	1.046E+00
1001	2.80E-03	9.345E-01	-1.55E-03	-5.174E-01	1.97E-03	6.578E-01	1.075E+00
1002	2.83E-03	9.439E-01	-2.31E-03	-7.692E-01	2.78E-03	9.270E-01	1.102E+00
1003	3.08E-03	1.028E+00	-2.64E-03	-8.797E-01	3.44E-03	1.146E+00	1.294E+00
1004	3.29E-03	1.096E+00	-3.27E-03	-1.089E+00	4.08E-03	1.359E+00	1.365E+00
1005	3.46E-03	1.152E+00	-3.39E-03	-1.130E+00	4.32E-03	1.439E+00	1.461E+00
1006	3.43E-03	1.144E+00	-3.21E-03	-1.068E+00	4.10E-03	1.367E+00	1.442E+00
1007	3.38E-03	1.127E+00	-2.36E-03	-7.870E-01	3.34E-03	1.114E+00	1.454E+00
1008	3.34E-03	1.112E+00	-1.33E-03	-4.431E-01	2.31E-03	7.685E-01	1.437E+00
1009	3.34E-03	1.113E+00	-1.88E-04	-6.282E-02	1.21E-03	4.033E-01	1.454E+00
1010	3.21E-03	1.069E+00	2.85E-04	9.493E-02	3.96E-04	1.321E-01	1.296E+00
1011	3.16E-03	1.053E+00	7.27E-04	2.423E-01	-1.55E-04	-5.154E-02	1.243E+00
1012	3.08E-03	1.028E+00	8.55E-04	2.851E-01	-3.74E-04	-1.248E-01	1.188E+00
1013	2.96E-03	9.867E-01	9.85E-04	3.282E-01	-6.22E-04	-2.073E-01	1.108E+00
1014	2.82E-03	9.411E-01	1.03E-03	3.422E-01	-7.96E-04	-2.654E-01	1.018E+00
1015	2.67E-03	8.910E-01	1.05E-03	3.510E-01	-9.51E-04	-3.169E-01	9.251E-01
1016	2.56E-03	8.523E-01	1.18E-03	3.933E-01	-1.07E-03	-3.570E-01	8.887E-01
1017	2.52E-03	8.397E-01	1.15E-03	3.833E-01	-9.16E-04	-3.053E-01	9.178E-01
1018	2.63E-03	8.766E-01	9.81E-04	3.269E-01	-5.25E-04	-1.752E-01	1.028E+00
1019	2.72E-03	9.062E-01	1.99E-04	6.635E-02	2.04E-04	6.794E-02	1.040E+00
1020	2.75E-03	9.158E-01	-6.94E-04	-2.314E-01	1.10E-03	3.670E-01	1.051E+00

Time step							TOTAL Drag (N/m)
	Fix wing total Drag N/3MM	Fix Wing Drag (N/M)	Top wing total Drag N/3MM	Top Wing Drag (N/M)	Bot wing total Drag N/3MM	Bottom Wing Drag (N/M)	
940	3.52E-05	1.172E-02	1.60E-05	5.338E-03	1.40E-05	4.656E-03	2.171E-02
941	6.06E-05	2.021E-02	-8.37E-05	-2.790E-02	-8.73E-05	-2.909E-02	-3.679E-02
942	8.76E-05	2.919E-02	-2.27E-04	-7.557E-02	-2.56E-04	-8.529E-02	-1.317E-01
943	1.04E-04	3.461E-02	-3.47E-04	-1.157E-01	-4.35E-04	-1.449E-01	-2.259E-01
944	1.04E-04	3.469E-02	-4.70E-04	-1.567E-01	-5.87E-04	-1.955E-01	-3.175E-01
945	9.34E-05	3.113E-02	-4.92E-04	-1.640E-01	-6.32E-04	-2.106E-01	-3.435E-01
946	7.98E-05	2.659E-02	-4.16E-04	-1.386E-01	-5.57E-04	-1.856E-01	-2.976E-01
947	6.32E-05	2.107E-02	-2.48E-04	-8.282E-02	-3.85E-04	-1.282E-01	-1.899E-01
948	4.38E-05	1.461E-02	-8.87E-05	-2.955E-02	-1.97E-04	-6.574E-02	-8.068E-02
949	2.60E-05	8.656E-03	2.47E-06	8.245E-04	-6.11E-05	-2.037E-02	-1.089E-02
950	1.12E-05	3.731E-03	-2.53E-07	-8.440E-05	-6.72E-06	-2.241E-03	1.406E-03
951	1.93E-06	6.447E-04	-4.40E-05	-1.467E-02	-1.57E-05	-5.239E-03	-1.927E-02
952	-4.82E-06	-1.605E-03	-9.78E-05	-3.260E-02	-4.77E-05	-1.591E-02	-5.012E-02
953	-1.28E-05	-4.255E-03	-1.63E-04	-5.418E-02	-1.02E-04	-3.408E-02	-9.251E-02
954	-1.99E-05	-6.648E-03	-2.07E-04	-6.900E-02	-1.57E-04	-5.227E-02	-1.279E-01
955	-2.46E-05	-8.184E-03	-2.11E-04	-7.017E-02	-1.82E-04	-6.059E-02	-1.389E-01
956	-2.38E-05	-7.942E-03	-2.06E-04	-6.882E-02	-1.77E-04	-5.886E-02	-1.356E-01
957	-1.61E-05	-5.368E-03	-1.61E-04	-5.362E-02	-1.16E-04	-3.874E-02	-9.772E-02
958	-4.80E-06	-1.600E-03	-9.54E-05	-3.179E-02	-3.92E-05	-1.307E-02	-4.645E-02
959	8.16E-06	2.719E-03	-1.03E-05	-3.425E-03	2.37E-05	7.897E-03	7.191E-03
960	2.65E-05	8.817E-03	-1.15E-05	-3.847E-03	1.37E-05	4.582E-03	9.552E-03
961	4.85E-05	1.616E-02	-8.39E-05	-2.797E-02	-8.70E-05	-2.899E-02	-4.081E-02
962	7.09E-05	2.363E-02	-2.27E-04	-7.581E-02	-2.54E-04	-8.480E-02	-1.370E-01
963	8.28E-05	2.760E-02	-3.49E-04	-1.162E-01	-4.32E-04	-1.439E-01	-2.325E-01
964	8.10E-05	2.702E-02	-4.88E-04	-1.627E-01	-5.85E-04	-1.951E-01	-3.308E-01
965	7.24E-05	2.413E-02	-5.14E-04	-1.714E-01	-6.32E-04	-2.107E-01	-3.580E-01
966	6.11E-05	2.037E-02	-4.44E-04	-1.480E-01	-5.58E-04	-1.862E-01	-3.137E-01
967	4.62E-05	1.541E-02	-2.69E-04	-8.961E-02	-3.86E-04	-1.286E-01	-2.028E-01
968	2.40E-05	8.012E-03	-1.03E-04	-3.429E-02	-1.98E-04	-6.606E-02	-9.233E-02
969	1.20E-05	4.002E-03	-2.65E-06	-8.842E-04	-6.16E-05	-2.054E-02	-1.743E-02
970	-5.85E-07	-1.950E-04	-3.27E-07	-1.090E-04	-6.77E-06	-2.255E-03	-2.559E-03
971	-7.66E-06	-2.555E-03	-4.03E-05	-1.345E-02	-1.55E-05	-5.159E-03	-2.116E-02
972	-1.16E-05	-3.882E-03	-9.24E-05	-3.078E-02	-4.73E-05	-1.577E-02	-5.044E-02
973	-1.70E-05	-5.682E-03	-1.51E-04	-5.044E-02	-1.02E-04	-3.385E-02	-8.997E-02
974	-2.18E-05	-7.257E-03	-1.93E-04	-6.444E-02	-1.56E-04	-5.186E-02	-1.236E-01
975	-2.42E-05	-8.079E-03	-1.97E-04	-6.576E-02	-1.80E-04	-5.994E-02	-1.338E-01
976	-2.17E-05	-7.221E-03	-1.98E-04	-6.595E-02	-1.74E-04	-5.811E-02	-1.313E-01
977	-1.25E-05	-4.160E-03	-1.56E-04	-5.209E-02	-1.14E-04	-3.798E-02	-9.422E-02
978	-2.07E-07	-6.902E-05	-9.46E-05	-3.152E-02	-3.75E-05	-1.251E-02	-4.410E-02
979	1.42E-05	4.731E-03	-1.20E-05	-3.994E-03	2.44E-05	8.147E-03	8.884E-03
980	3.48E-05	1.161E-02	-3.75E-06	-1.249E-03	1.40E-05	4.657E-03	1.502E-02
981	6.02E-05	2.007E-02	-8.37E-05	-2.790E-02	-8.73E-05	-2.909E-02	-3.692E-02
982	8.70E-05	2.901E-02	-2.27E-04	-7.556E-02	-2.56E-04	-8.529E-02	-1.318E-01

Time step							TOTAL Drag (N/m)
	Fix wing total Drag N/3MM	Fix Wing Drag (N/M)	Top wing total Drag N/3MM	Top Wing Drag (N/M)	Bot wing total Drag N/3MM	Bottom Wing Drag (N/M)	
983	1.03E-04	3.439E-02	-3.47E-04	-1.157E-01	-4.35E-04	-1.449E-01	-2.261E-01
984	1.03E-04	3.446E-02	-4.70E-04	-1.568E-01	-5.87E-04	-1.955E-01	-3.179E-01
985	9.27E-05	3.091E-02	-4.92E-04	-1.642E-01	-6.32E-04	-2.106E-01	-3.438E-01
986	7.92E-05	2.639E-02	-4.16E-04	-1.388E-01	-5.57E-04	-1.856E-01	-2.980E-01
987	6.27E-05	2.089E-02	-2.49E-04	-8.296E-02	-3.85E-04	-1.282E-01	-1.903E-01
988	4.33E-05	1.443E-02	-8.90E-05	-2.966E-02	-1.97E-04	-6.576E-02	-8.098E-02
989	2.55E-05	8.498E-03	2.37E-06	7.885E-04	-6.11E-05	-2.038E-02	-1.109E-02
990	1.08E-05	3.594E-03	-2.57E-07	-8.571E-05	-6.72E-06	-2.241E-03	1.266E-03
991	1.59E-06	5.294E-04	-4.39E-05	-1.464E-02	-1.57E-05	-5.234E-03	-1.935E-02
992	-5.07E-06	-1.692E-03	-9.76E-05	-3.255E-02	-4.77E-05	-1.590E-02	-5.014E-02
993	-1.29E-05	-4.312E-03	-1.62E-04	-5.406E-02	-1.02E-04	-3.406E-02	-9.243E-02
994	-2.00E-05	-6.674E-03	-2.07E-04	-6.884E-02	-1.57E-04	-5.224E-02	-1.277E-01
995	-2.45E-05	-8.179E-03	-2.10E-04	-7.001E-02	-1.82E-04	-6.054E-02	-1.387E-01
996	-2.37E-05	-7.905E-03	-2.06E-04	-6.872E-02	-1.76E-04	-5.880E-02	-1.354E-01
997	-1.59E-05	-5.303E-03	-1.61E-04	-5.361E-02	-1.16E-04	-3.869E-02	-9.761E-02
998	-4.54E-06	-1.512E-03	-9.55E-05	-3.182E-02	-3.91E-05	-1.304E-02	-4.637E-02
999	8.50E-06	2.834E-03	-1.04E-05	-3.466E-03	2.37E-05	7.911E-03	7.280E-03
1000	2.69E-05	8.970E-03	-2.75E-06	-9.171E-04	1.38E-05	4.585E-03	1.264E-02
1001	4.91E-05	1.636E-02	-8.39E-05	-2.797E-02	-8.70E-05	-2.900E-02	-4.061E-02
1002	7.17E-05	2.389E-02	-2.27E-04	-7.579E-02	-2.54E-04	-8.482E-02	-1.367E-01
1003	8.37E-05	2.791E-02	-3.48E-04	-1.161E-01	-4.32E-04	-1.439E-01	-2.321E-01
1004	8.20E-05	2.734E-02	-4.87E-04	-1.624E-01	-5.85E-04	-1.951E-01	-3.302E-01
1005	7.33E-05	2.442E-02	-5.13E-04	-1.710E-01	-6.32E-04	-2.107E-01	-3.573E-01
1006	6.19E-05	2.064E-02	-4.43E-04	-1.475E-01	-5.58E-04	-1.861E-01	-3.130E-01
1007	4.69E-05	1.564E-02	-2.68E-04	-8.932E-02	-3.84E-04	-1.278E-01	-2.015E-01
1008	2.86E-05	9.521E-03	-1.02E-04	-3.410E-02	-1.98E-04	-6.605E-02	-9.063E-02
1009	1.26E-05	4.189E-03	-2.46E-06	-8.204E-04	-6.16E-05	-2.054E-02	-1.717E-02
1010	-1.19E-07	-3.960E-05	-3.29E-07	-1.096E-04	-6.76E-06	-2.255E-03	-2.404E-03
1011	-7.29E-06	-2.431E-03	-4.05E-05	-1.349E-02	-1.55E-05	-5.161E-03	-2.108E-02
1012	-1.14E-05	-3.795E-03	-9.25E-05	-3.083E-02	-4.73E-05	-1.578E-02	-5.041E-02
1013	-1.69E-05	-5.629E-03	-1.52E-04	-5.055E-02	-1.02E-04	-3.386E-02	-9.004E-02
1014	-2.17E-05	-7.236E-03	-1.94E-04	-6.456E-02	-1.56E-04	-5.187E-02	-1.237E-01
1015	-2.43E-05	-8.084E-03	-1.98E-04	-6.586E-02	-1.80E-04	-5.997E-02	-1.339E-01
1016	-2.17E-05	-7.249E-03	-1.94E-04	-6.479E-02	-1.74E-04	-5.814E-02	-1.302E-01
1017	-1.26E-05	-4.204E-03	-1.56E-04	-5.211E-02	-1.14E-04	-3.801E-02	-9.433E-02
1018	-3.72E-07	-1.242E-04	-9.45E-05	-3.151E-02	-3.76E-05	-1.254E-02	-4.417E-02
1019	1.40E-05	4.657E-03	-1.19E-05	-3.960E-03	2.44E-05	8.134E-03	8.831E-03
1020	3.45E-05	1.150E-02	-3.69E-06	-1.230E-03	1.40E-05	4.654E-03	1.493E-02

E. $U_{\infty}=3\text{M/S}$, $f=25\text{HZ}$, $\Phi=15^\circ$, PITCH/PLUNGE OUT OF PHASE

Time step							TOTAL Lift (N/m)
	Fix wing total Lift N/3MM	Fix Wing Lift (N/M)	Top wing total Lift N/3MM	Top Wing Lift (N/M)	Bot wing total Lift N/3MM	Bottom Wing Lift (N/M)	
940	2.55E-03	8.503E-01	2.62E-04	8.747E-02	2.76E-04	9.209E-02	1.030E+00
941	2.54E-03	8.482E-01	-8.43E-04	-2.809E-01	1.34E-03	4.462E-01	1.013E+00
942	2.54E-03	8.461E-01	-1.78E-03	-5.920E-01	2.33E-03	7.755E-01	1.030E+00
943	2.62E-03	8.734E-01	-2.44E-03	-8.148E-01	3.18E-03	1.061E+00	1.120E+00
944	2.80E-03	9.340E-01	-2.87E-03	-9.562E-01	3.94E-03	1.312E+00	1.290E+00
945	3.06E-03	1.020E+00	-3.10E-03	-1.032E+00	4.58E-03	1.527E+00	1.515E+00
946	3.26E-03	1.086E+00	-2.83E-03	-9.419E-01	4.67E-03	1.558E+00	1.702E+00
947	3.30E-03	1.101E+00	-2.26E-03	-7.539E-01	4.26E-03	1.419E+00	1.767E+00
948	3.20E-03	1.067E+00	-1.18E-03	-3.945E-01	3.14E-03	1.047E+00	1.720E+00
949	3.08E-03	1.027E+00	-5.75E-04	-1.917E-01	2.24E-03	7.467E-01	1.582E+00
950	3.04E-03	1.014E+00	1.73E-04	5.763E-02	9.84E-04	3.280E-01	1.400E+00
951	3.02E-03	1.008E+00	5.26E-04	1.753E-01	3.98E-04	1.327E-01	1.316E+00
952	3.07E-03	1.022E+00	8.66E-04	2.888E-01	-2.05E-05	-6.828E-03	1.304E+00
953	2.98E-03	9.932E-01	1.30E-03	4.335E-01	-4.21E-04	-1.403E-01	1.286E+00
954	3.06E-03	1.019E+00	1.48E-03	4.946E-01	-5.97E-04	-1.990E-01	1.315E+00
955	3.08E-03	1.027E+00	1.86E-03	6.192E-01	-7.94E-04	-2.647E-01	1.382E+00
956	3.12E-03	1.041E+00	2.29E-03	7.618E-01	-1.10E-03	-3.681E-01	1.434E+00
957	3.06E-03	1.020E+00	2.32E-03	7.741E-01	-1.26E-03	-4.194E-01	1.375E+00
958	3.00E-03	1.001E+00	2.09E-03	6.967E-01	-1.19E-03	-3.954E-01	1.302E+00
959	2.91E-03	9.697E-01	1.35E-03	4.498E-01	-6.90E-04	-2.300E-01	1.189E+00
960	2.84E-03	9.478E-01	2.30E-04	7.653E-02	1.90E-04	6.326E-02	1.088E+00
961	2.88E-03	9.586E-01	-9.17E-04	-3.057E-01	1.21E-03	4.039E-01	1.057E+00
962	3.04E-03	1.014E+00	-1.73E-03	-5.760E-01	2.13E-03	7.104E-01	1.149E+00
963	3.29E-03	1.096E+00	-2.33E-03	-7.755E-01	2.93E-03	9.765E-01	1.297E+00
964	3.43E-03	1.144E+00	-3.11E-03	-1.038E+00	3.70E-03	1.234E+00	1.340E+00
965	3.55E-03	1.183E+00	-3.66E-03	-1.219E+00	4.36E-03	1.453E+00	1.417E+00
966	3.61E-03	1.204E+00	-3.76E-03	-1.252E+00	4.61E-03	1.536E+00	1.488E+00
967	3.56E-03	1.186E+00	-3.35E-03	-1.117E+00	4.21E-03	1.402E+00	1.471E+00
968	3.55E-03	1.183E+00	-2.32E-03	-7.748E-01	3.12E-03	1.041E+00	1.449E+00
969	3.56E-03	1.186E+00	-1.35E-03	-4.510E-01	2.18E-03	7.269E-01	1.462E+00
970	3.55E-03	1.185E+00	-3.03E-04	-1.010E-01	9.37E-04	3.123E-01	1.396E+00
971	3.49E-03	1.164E+00	3.68E-05	1.228E-02	3.44E-04	1.146E-01	1.291E+00
972	3.50E-03	1.167E+00	4.31E-04	1.438E-01	-9.85E-05	-3.284E-02	1.278E+00
973	3.37E-03	1.123E+00	8.41E-04	2.804E-01	-5.09E-04	-1.696E-01	1.234E+00
974	3.35E-03	1.116E+00	9.94E-04	3.312E-01	-7.43E-04	-2.478E-01	1.199E+00
975	3.26E-03	1.085E+00	1.26E-03	4.191E-01	-9.65E-04	-3.215E-01	1.183E+00
976	3.08E-03	1.028E+00	1.48E-03	4.948E-01	-1.34E-03	-4.456E-01	1.077E+00
977	2.96E-03	9.872E-01	1.66E-03	5.525E-01	-1.49E-03	-4.975E-01	1.042E+00
978	2.89E-03	9.644E-01	1.55E-03	5.154E-01	-1.40E-03	-4.651E-01	1.015E+00
979	2.93E-03	9.769E-01	1.04E-03	3.460E-01	-8.19E-04	-2.731E-01	1.050E+00
980	2.91E-03	9.704E-01	-8.31E-05	-2.770E-02	1.69E-04	5.650E-02	9.992E-01
981	2.95E-03	9.832E-01	-1.06E-03	-3.546E-01	1.23E-03	4.112E-01	1.040E+00

Time step							TOTAL Lift (N/m)
	Fix wing total Lift N/3MM	Fix Wing Lift (N/M)	Top wing total Lift N/3MM	Top Wing Lift (N/M)	Bot wing total Lift N/3MM	Bottom Wing Lift (N/M)	
982	3.03E-03	1.009E+00	-1.83E-03	-6.103E-01	2.16E-03	7.213E-01	1.120E+00
983	3.19E-03	1.062E+00	-2.37E-03	-7.905E-01	2.95E-03	9.817E-01	1.253E+00
984	3.39E-03	1.130E+00	-3.06E-03	-1.021E+00	3.71E-03	1.237E+00	1.346E+00
985	3.62E-03	1.208E+00	-3.56E-03	-1.188E+00	4.36E-03	1.453E+00	1.473E+00
986	3.70E-03	1.232E+00	-3.77E-03	-1.257E+00	4.61E-03	1.537E+00	1.512E+00
987	3.60E-03	1.199E+00	-3.38E-03	-1.128E+00	4.20E-03	1.399E+00	1.471E+00
988	3.54E-03	1.180E+00	-2.40E-03	-7.985E-01	3.13E-03	1.044E+00	1.425E+00
989	3.52E-03	1.172E+00	-1.45E-03	-4.840E-01	2.19E-03	7.292E-01	1.417E+00
990	3.52E-03	1.172E+00	-3.93E-04	-1.311E-01	9.50E-04	3.166E-01	1.357E+00
991	3.45E-03	1.148E+00	-4.69E-06	-1.562E-03	3.51E-04	1.170E-01	1.264E+00
992	3.42E-03	1.140E+00	3.47E-04	1.158E-01	-8.89E-05	-2.962E-02	1.226E+00
993	3.26E-03	1.087E+00	7.83E-04	2.611E-01	-5.01E-04	-1.671E-01	1.181E+00
994	3.22E-03	1.072E+00	9.19E-04	3.063E-01	-7.29E-04	-2.431E-01	1.135E+00
995	3.10E-03	1.033E+00	1.17E-03	3.898E-01	-9.48E-04	-3.160E-01	1.107E+00
996	2.92E-03	9.734E-01	1.38E-03	4.608E-01	-1.31E-03	-4.361E-01	9.981E-01
997	2.81E-03	9.380E-01	1.58E-03	5.271E-01	-1.46E-03	-4.858E-01	9.793E-01
998	2.78E-03	9.258E-01	1.50E-03	4.993E-01	-1.36E-03	-4.526E-01	9.725E-01
999	2.83E-03	9.419E-01	9.72E-04	3.239E-01	-7.83E-04	-2.610E-01	1.005E+00
1000	2.80E-03	9.347E-01	-1.18E-04	-3.941E-02	1.99E-04	6.638E-02	9.617E-01
1001	2.80E-03	9.334E-01	-1.12E-03	-3.738E-01	1.27E-03	4.227E-01	9.824E-01
1002	2.82E-03	9.405E-01	-1.90E-03	-6.324E-01	2.21E-03	7.383E-01	1.046E+00
1003	2.91E-03	9.709E-01	-2.46E-03	-8.189E-01	3.02E-03	1.006E+00	1.158E+00
1004	3.08E-03	1.028E+00	-3.14E-03	-1.048E+00	3.80E-03	1.266E+00	1.246E+00
1005	3.33E-03	1.111E+00	-3.67E-03	-1.224E+00	4.46E-03	1.487E+00	1.374E+00
1006	3.48E-03	1.159E+00	-3.79E-03	-1.264E+00	4.68E-03	1.559E+00	1.454E+00
1007	3.38E-03	1.128E+00	-3.41E-03	-1.137E+00	4.26E-03	1.421E+00	1.412E+00
1008	3.29E-03	1.098E+00	-2.38E-03	-7.945E-01	3.17E-03	1.058E+00	1.361E+00
1009	3.23E-03	1.076E+00	-1.39E-03	-4.637E-01	2.24E-03	7.453E-01	1.358E+00
1010	3.19E-03	1.065E+00	-3.34E-04	-1.114E-01	9.88E-04	3.292E-01	1.282E+00
1011	3.07E-03	1.024E+00	4.52E-05	1.507E-02	3.86E-04	1.287E-01	1.167E+00
1012	3.02E-03	1.005E+00	4.06E-04	1.355E-01	-5.86E-05	-1.955E-02	1.121E+00
1013	2.81E-03	9.372E-01	8.18E-04	2.727E-01	-4.55E-04	-1.517E-01	1.058E+00
1014	2.74E-03	9.118E-01	9.18E-04	3.059E-01	-6.65E-04	-2.216E-01	9.961E-01
1015	2.62E-03	8.719E-01	1.17E-03	3.904E-01	-8.60E-04	-2.868E-01	9.755E-01
1016	2.44E-03	8.125E-01	1.38E-03	4.598E-01	-1.17E-03	-3.887E-01	8.836E-01
1017	2.37E-03	7.897E-01	1.63E-03	5.423E-01	-1.29E-03	-4.314E-01	9.006E-01
1018	2.42E-03	8.072E-01	1.63E-03	5.435E-01	-1.19E-03	-3.975E-01	9.533E-01
1019	2.55E-03	8.485E-01	1.02E-03	3.412E-01	-6.46E-04	-2.154E-01	9.743E-01
1020	2.61E-03	8.713E-01	2.89E-05	9.642E-03	2.90E-04	9.659E-02	9.776E-01

Time Steps	Fix wing total Drag N/3MM	Fix Wing Drag (N/M)	Top wing total Drag N/3MM	Top Wing Drag (N/M)	Bot wing total Drag N/3MM	Bottom Wing Drag (N/M)	Total Drag (N/m)
940	4.95E-05	1.652E-02	2.23E-05	7.430E-03	2.18E-05	7.269E-03	3.121E-02
941	7.71E-05	2.570E-02	-7.03E-05	-2.343E-02	-8.03E-05	-2.678E-02	-2.451E-02
942	1.12E-04	3.750E-02	-2.72E-04	-9.054E-02	-3.10E-04	-1.034E-01	-1.564E-01
943	1.50E-04	5.009E-02	-4.98E-04	-1.661E-01	-5.81E-04	-1.935E-01	-3.096E-01
944	1.79E-04	5.956E-02	-6.57E-04	-2.190E-01	-8.13E-04	-2.709E-01	-4.303E-01
945	1.89E-04	6.294E-02	-7.06E-04	-2.354E-01	-9.51E-04	-3.171E-01	-4.896E-01
946	1.81E-04	6.022E-02	-5.74E-04	-1.913E-01	-8.89E-04	-2.962E-01	-4.272E-01
947	1.66E-04	5.533E-02	-3.56E-04	-1.187E-01	-6.73E-04	-2.243E-01	-2.877E-01
948	1.50E-04	5.000E-02	-1.19E-04	-3.975E-02	-3.73E-04	-1.245E-01	-1.142E-01
949	1.39E-04	4.647E-02	-1.85E-05	-6.181E-03	-1.51E-04	-5.043E-02	-1.015E-02
950	1.29E-04	4.301E-02	6.76E-06	2.253E-03	-8.55E-06	-2.851E-03	4.241E-02
951	1.23E-04	4.089E-02	-3.80E-05	-1.265E-02	2.23E-05	7.432E-03	3.567E-02
952	1.15E-04	3.833E-02	-1.31E-04	-4.372E-02	-1.39E-05	-4.646E-03	-1.004E-02
953	1.04E-04	3.466E-02	-2.99E-04	-9.959E-02	-1.06E-04	-3.533E-02	-1.003E-01
954	7.78E-05	2.593E-02	-4.26E-04	-1.419E-01	-1.85E-04	-6.154E-02	-1.775E-01
955	6.13E-05	2.044E-02	-5.45E-04	-1.817E-01	-2.30E-04	-7.659E-02	-2.379E-01
956	4.43E-05	1.476E-02	-5.84E-04	-1.945E-01	-2.75E-04	-9.158E-02	-2.713E-01
957	3.28E-05	1.095E-02	-4.69E-04	-1.565E-01	-2.38E-04	-7.944E-02	-2.250E-01
958	2.91E-05	9.707E-03	-2.93E-04	-9.758E-02	-1.46E-04	-4.859E-02	-1.365E-01
959	3.14E-05	1.047E-02	-9.61E-05	-3.203E-02	-2.74E-05	-9.129E-03	-3.070E-02
960	3.78E-05	1.261E-02	-3.80E-06	-1.268E-03	2.22E-05	7.399E-03	1.874E-02
961	4.71E-05	1.570E-02	-7.07E-05	-2.356E-02	-7.14E-05	-2.380E-02	-3.166E-02
962	5.83E-05	1.945E-02	-2.54E-04	-8.468E-02	-2.83E-04	-9.427E-02	-1.595E-01
963	6.76E-05	2.252E-02	-4.57E-04	-1.522E-01	-5.32E-04	-1.773E-01	-3.070E-01
964	7.58E-05	2.526E-02	-6.78E-04	-2.261E-01	-7.61E-04	-2.536E-01	-4.545E-01
965	8.43E-05	2.810E-02	-7.92E-04	-2.641E-01	-9.02E-04	-3.006E-01	-5.367E-01
966	8.79E-05	2.931E-02	-7.30E-04	-2.435E-01	-8.71E-04	-2.903E-01	-5.044E-01
967	7.89E-05	2.630E-02	-5.25E-04	-1.751E-01	-6.58E-04	-2.193E-01	-3.681E-01
968	6.37E-05	2.124E-02	-2.60E-04	-8.655E-02	-3.64E-04	-1.214E-01	-1.867E-01
969	4.94E-05	1.648E-02	-7.70E-05	-2.567E-02	-1.43E-04	-4.761E-02	-5.680E-02
970	3.73E-05	1.242E-02	3.96E-07	1.320E-04	-7.36E-06	-2.452E-03	1.010E-02
971	3.07E-05	1.024E-02	-4.57E-06	-1.523E-03	1.93E-05	6.419E-03	1.514E-02
972	2.57E-05	8.582E-03	-6.10E-05	-2.032E-02	-2.32E-05	-7.744E-03	-1.948E-02
973	1.94E-05	6.477E-03	-1.88E-04	-6.271E-02	-1.21E-04	-4.020E-02	-9.644E-02
974	-1.98E-08	-6.611E-06	-2.76E-04	-9.210E-02	-2.20E-04	-7.330E-02	-1.654E-01
975	-7.04E-06	-2.348E-03	-3.51E-04	-1.169E-01	-2.75E-04	-9.168E-02	-2.110E-01
976	-1.30E-05	-4.343E-03	-3.70E-04	-1.233E-01	-3.33E-04	-1.111E-01	-2.388E-01
977	-9.74E-06	-3.245E-03	-3.28E-04	-1.092E-01	-2.88E-04	-9.583E-02	-2.083E-01
978	-1.17E-06	-3.896E-04	-2.08E-04	-6.943E-02	-1.78E-04	-5.941E-02	-1.292E-01
979	1.18E-05	3.941E-03	-6.57E-05	-2.189E-02	-3.94E-05	-1.314E-02	-3.109E-02
980	2.80E-05	9.336E-03	8.40E-06	2.800E-03	2.01E-05	6.712E-03	1.885E-02
981	4.90E-05	1.634E-02	-7.69E-05	-2.565E-02	-7.52E-05	-2.507E-02	-3.438E-02
982	7.08E-05	2.360E-02	-2.64E-04	-8.800E-02	-2.90E-04	-9.656E-02	-1.610E-01
983	8.62E-05	2.875E-02	-4.60E-04	-1.532E-01	-5.37E-04	-1.791E-01	-3.036E-01

Time Steps	Fix wing total Drag N/3MM	Fix Wing Drag (N/M)	Top wing total Drag N/3MM	Top Wing Drag (N/M)	Bot wing total Drag N/3MM	Bottom Wing Drag (N/M)	Total Drag (N/m)
984	8.90E-05	2.968E-02	-6.63E-04	-2.210E-01	-7.65E-04	-2.551E-01	-4.464E-01
985	8.34E-05	2.781E-02	-7.69E-04	-2.564E-01	-9.03E-04	-3.011E-01	-5.297E-01
986	7.71E-05	2.569E-02	-7.30E-04	-2.433E-01	-8.74E-04	-2.912E-01	-5.088E-01
987	6.60E-05	2.199E-02	-5.27E-04	-1.756E-01	-6.58E-04	-2.195E-01	-3.731E-01
988	4.92E-05	1.640E-02	-2.65E-04	-8.825E-02	-3.66E-04	-1.220E-01	-1.939E-01
989	3.46E-05	1.154E-02	-8.20E-05	-2.734E-02	-1.44E-04	-4.789E-02	-6.369E-02
990	2.15E-05	7.161E-03	9.49E-07	3.163E-04	-7.33E-06	-2.443E-03	5.034E-03
991	1.45E-05	4.821E-03	-1.62E-06	-5.404E-04	1.98E-05	6.596E-03	1.088E-02
992	9.51E-06	3.171E-03	-4.77E-05	-1.590E-02	-2.21E-05	-7.360E-03	-2.009E-02
993	4.33E-06	1.443E-03	-1.75E-04	-5.847E-02	-1.20E-04	-3.986E-02	-9.689E-02
994	-1.40E-05	-4.656E-03	-2.56E-04	-8.525E-02	-2.17E-04	-7.224E-02	-1.621E-01
995	-1.98E-05	-6.614E-03	-3.24E-04	-1.081E-01	-2.71E-04	-9.030E-02	-2.050E-01
996	-2.50E-05	-8.347E-03	-3.45E-04	-1.151E-01	-3.26E-04	-1.087E-01	-2.322E-01
997	-2.20E-05	-7.329E-03	-3.14E-04	-1.047E-01	-2.81E-04	-9.353E-02	-2.055E-01
998	-1.54E-05	-5.142E-03	-2.03E-04	-6.771E-02	-1.73E-04	-5.771E-02	-1.306E-01
999	-5.20E-06	-1.735E-03	-6.32E-05	-2.106E-02	-3.68E-05	-1.227E-02	-3.506E-02
1000	8.72E-06	2.906E-03	5.97E-06	1.988E-03	2.02E-05	6.750E-03	1.164E-02
1001	2.88E-05	9.600E-03	-8.36E-05	-2.788E-02	-7.75E-05	-2.584E-02	-4.412E-02
1002	5.16E-05	1.720E-02	-2.77E-04	-9.224E-02	-2.97E-04	-9.888E-02	-1.739E-01
1003	6.99E-05	2.329E-02	-4.81E-04	-1.603E-01	-5.51E-04	-1.836E-01	-3.206E-01
1004	7.52E-05	2.507E-02	-6.87E-04	-2.290E-01	-7.84E-04	-2.614E-01	-4.653E-01
1005	6.79E-05	2.263E-02	-7.99E-04	-2.662E-01	-9.26E-04	-3.087E-01	-5.523E-01
1006	5.62E-05	1.874E-02	-7.36E-04	-2.453E-01	-8.88E-04	-2.960E-01	-5.226E-01
1007	4.14E-05	1.379E-02	-5.26E-04	-1.752E-01	-6.75E-04	-2.251E-01	-3.865E-01
1008	2.35E-05	7.843E-03	-2.59E-04	-8.639E-02	-3.73E-04	-1.244E-01	-2.030E-01
1009	9.52E-06	3.174E-03	-7.19E-05	-2.397E-02	-1.48E-04	-4.939E-02	-7.019E-02
1010	-2.34E-06	-7.808E-04	8.49E-06	2.831E-03	-7.89E-06	-2.629E-03	-5.786E-04
1011	-7.61E-06	-2.536E-03	1.69E-06	5.627E-04	2.21E-05	7.355E-03	5.382E-03
1012	-9.97E-06	-3.322E-03	-5.01E-05	-1.669E-02	-1.86E-05	-6.200E-03	-2.621E-02
1013	-1.23E-05	-4.111E-03	-1.78E-04	-5.924E-02	-1.11E-04	-3.709E-02	-1.004E-01
1014	-2.78E-05	-9.276E-03	-2.52E-04	-8.404E-02	-2.01E-04	-6.695E-02	-1.603E-01
1015	-3.00E-05	-9.989E-03	-3.24E-04	-1.082E-01	-2.46E-04	-8.209E-02	-2.002E-01
1016	-3.02E-05	-1.008E-02	-3.36E-04	-1.120E-01	-2.90E-04	-9.665E-02	-2.188E-01
1017	-2.24E-05	-7.482E-03	-3.24E-04	-1.078E-01	-2.47E-04	-8.248E-02	-1.978E-01
1018	-1.21E-05	-4.046E-03	-2.23E-04	-7.432E-02	-1.50E-04	-4.985E-02	-1.282E-01
1019	3.36E-08	1.120E-05	-7.04E-05	-2.348E-02	-2.63E-05	-8.763E-03	-3.223E-02
1020	1.85E-05	6.157E-03	2.53E-06	8.433E-04	2.13E-05	7.115E-03	1.412E-02

F. $U_\infty=3\text{M/S}$, $f=25\text{HZ}$, $\Phi=20^\circ$, PITCH/PLUNGE OUT OF PHASE

Time step	Fix wing		Top wing total		Bot wing		TOTAL Lift (N/m)
	total Lift N/3MM	Wing Lift (N/M)	Lift N/3MM	Wing Lift (N/M)	total Lift N/3MM	Wing Lift (N/M)	
940	2.90E-03	9.657E-01	3.05E-03	1.017E+00	-2.15E-03	-7.183E-01	1.265E+00
941	2.47E-03	8.241E-01	1.32E-03	4.397E-01	-1.10E-03	-3.683E-01	8.955E-01
942	2.81E-03	9.368E-01	-1.48E-04	-4.932E-02	5.27E-04	1.757E-01	1.063E+00
943	2.57E-03	8.550E-01	-1.82E-03	-6.073E-01	1.90E-03	6.335E-01	8.813E-01
944	2.65E-03	8.843E-01	-2.45E-03	-8.158E-01	2.73E-03	9.114E-01	9.799E-01
945	3.26E-03	1.085E+00	-3.09E-03	-1.029E+00	3.85E-03	1.284E+00	1.340E+00
946	3.45E-03	1.151E+00	-3.48E-03	-1.160E+00	4.41E-03	1.471E+00	1.463E+00
947	3.44E-03	1.145E+00	-3.35E-03	-1.116E+00	4.47E-03	1.490E+00	1.520E+00
948	3.61E-03	1.203E+00	-3.62E-03	-1.206E+00	5.03E-03	1.677E+00	1.673E+00
949	3.82E-03	1.274E+00	-3.82E-03	-1.274E+00	5.28E-03	1.760E+00	1.759E+00
950	3.64E-03	1.213E+00	-2.28E-03	-7.606E-01	3.28E-03	1.094E+00	1.547E+00
951	3.63E-03	1.208E+00	-1.89E-03	-6.315E-01	2.60E-03	8.679E-01	1.445E+00
952	3.64E-03	1.213E+00	-6.60E-04	-2.198E-01	1.42E-03	4.735E-01	1.467E+00
953	3.60E-03	1.200E+00	7.95E-05	2.649E-02	4.84E-04	1.613E-01	1.388E+00
954	3.57E-03	1.191E+00	8.96E-04	2.985E-01	-2.35E-04	-7.831E-02	1.411E+00
955	3.54E-03	1.181E+00	1.47E-03	4.902E-01	-6.02E-04	-2.005E-01	1.471E+00
956	3.49E-03	1.164E+00	1.93E-03	6.440E-01	-8.91E-04	-2.970E-01	1.511E+00
957	3.38E-03	1.128E+00	2.40E-03	8.001E-01	-1.34E-03	-4.459E-01	1.482E+00
958	3.09E-03	1.031E+00	2.75E-03	9.160E-01	-1.94E-03	-6.478E-01	1.299E+00
959	2.88E-03	9.594E-01	3.04E-03	1.012E+00	-2.38E-03	-7.917E-01	1.180E+00
960	3.01E-03	1.003E+00	2.82E-03	9.401E-01	-2.22E-03	-7.405E-01	1.203E+00
961	2.57E-03	8.560E-01	1.26E-03	4.212E-01	-1.21E-03	-4.033E-01	8.739E-01
962	2.82E-03	9.388E-01	-3.34E-04	-1.113E-01	5.34E-04	1.780E-01	1.006E+00
963	2.64E-03	8.787E-01	-1.84E-03	-6.137E-01	1.84E-03	6.145E-01	8.794E-01
964	2.67E-03	8.890E-01	-2.49E-03	-8.301E-01	2.66E-03	8.875E-01	9.465E-01
965	3.18E-03	1.060E+00	-3.22E-03	-1.075E+00	3.78E-03	1.262E+00	1.247E+00
966	3.33E-03	1.110E+00	-3.85E-03	-1.285E+00	4.42E-03	1.472E+00	1.297E+00
967	3.33E-03	1.111E+00	-3.76E-03	-1.252E+00	4.48E-03	1.493E+00	1.352E+00
968	3.45E-03	1.151E+00	-4.14E-03	-1.380E+00	5.05E-03	1.682E+00	1.452E+00
969	3.58E-03	1.195E+00	-4.43E-03	-1.478E+00	5.31E-03	1.771E+00	1.487E+00
970	3.40E-03	1.132E+00	-2.65E-03	-8.842E-01	3.30E-03	1.099E+00	1.347E+00
971	3.31E-03	1.104E+00	-2.27E-03	-7.554E-01	2.63E-03	8.773E-01	1.226E+00
972	3.28E-03	1.094E+00	-9.16E-04	-3.053E-01	1.45E-03	4.837E-01	1.273E+00
973	3.20E-03	1.066E+00	-1.39E-04	-4.633E-02	5.17E-04	1.723E-01	1.192E+00
974	3.14E-03	1.045E+00	7.17E-04	2.390E-01	-2.02E-04	-6.721E-02	1.217E+00
975	3.08E-03	1.026E+00	1.30E-03	4.339E-01	-5.70E-04	-1.900E-01	1.270E+00
976	3.01E-03	1.003E+00	1.78E-03	5.921E-01	-8.60E-04	-2.867E-01	1.309E+00
977	2.92E-03	9.730E-01	2.30E-03	7.676E-01	-1.28E-03	-4.251E-01	1.316E+00
978	2.71E-03	9.037E-01	2.78E-03	9.265E-01	-1.85E-03	-6.156E-01	1.215E+00
979	2.56E-03	8.531E-01	3.13E-03	1.044E+00	-2.26E-03	-7.540E-01	1.143E+00
980	2.90E-03	9.656E-01	3.05E-03	1.017E+00	-2.15E-03	-7.183E-01	1.264E+00
981	2.47E-03	8.241E-01	1.32E-03	4.397E-01	-1.10E-03	-3.682E-01	8.955E-01
982	2.81E-03	9.367E-01	-1.48E-04	-4.929E-02	5.27E-04	1.757E-01	1.063E+00

Time step							TOTAL Lift (N/m)
	Fix wing total Lift N/3MM	Fix Wing Lift (N/M)	Top wing total Lift N/3MM	Top Wing Lift (N/M)	Bot wing total Lift N/3MM	Bottom Wing Lift (N/M)	
983	2.57E-03	8.550E-01	-1.82E-03	-6.072E-01	1.90E-03	6.337E-01	8.815E-01
984	2.65E-03	8.844E-01	-2.45E-03	-8.158E-01	2.73E-03	9.114E-01	9.801E-01
985	3.26E-03	1.086E+00	-3.09E-03	-1.029E+00	3.85E-03	1.284E+00	1.340E+00
986	3.45E-03	1.152E+00	-3.48E-03	-1.160E+00	4.41E-03	1.471E+00	1.463E+00
987	3.44E-03	1.145E+00	-3.35E-03	-1.115E+00	4.47E-03	1.490E+00	1.520E+00
988	3.61E-03	1.203E+00	-3.62E-03	-1.207E+00	5.03E-03	1.677E+00	1.673E+00
989	3.82E-03	1.274E+00	-3.82E-03	-1.274E+00	5.28E-03	1.760E+00	1.760E+00
990	3.64E-03	1.214E+00	-2.28E-03	-7.604E-01	3.28E-03	1.094E+00	1.548E+00
991	3.63E-03	1.209E+00	-1.89E-03	-6.312E-01	2.60E-03	8.679E-01	1.446E+00
992	3.64E-03	1.213E+00	-6.59E-04	-2.196E-01	1.42E-03	4.735E-01	1.467E+00
993	3.60E-03	1.200E+00	8.02E-05	2.673E-02	4.84E-04	1.612E-01	1.388E+00
994	3.58E-03	1.192E+00	8.96E-04	2.988E-01	-2.35E-04	-7.835E-02	1.412E+00
995	3.55E-03	1.182E+00	1.47E-03	4.887E-01	-6.02E-04	-2.006E-01	1.470E+00
996	3.49E-03	1.165E+00	1.93E-03	6.443E-01	-8.91E-04	-2.971E-01	1.512E+00
997	3.39E-03	1.129E+00	2.40E-03	8.004E-01	-1.34E-03	-4.460E-01	1.483E+00
998	3.09E-03	1.032E+00	2.75E-03	9.161E-01	-1.94E-03	-6.480E-01	1.300E+00
999	2.88E-03	9.600E-01	3.04E-03	1.012E+00	-2.38E-03	-7.919E-01	1.180E+00
1000	3.01E-03	1.003E+00	2.82E-03	9.399E-01	-2.22E-03	-7.407E-01	1.203E+00
1001	2.57E-03	8.561E-01	1.26E-03	4.211E-01	-1.21E-03	-4.035E-01	8.737E-01
1002	2.82E-03	9.389E-01	-3.35E-04	-1.116E-01	5.97E-04	1.990E-01	1.026E+00
1003	2.64E-03	8.789E-01	-1.84E-03	-6.138E-01	1.84E-03	6.144E-01	8.795E-01
1004	2.67E-03	8.892E-01	-2.49E-03	-8.303E-01	2.66E-03	8.874E-01	9.463E-01
1005	3.18E-03	1.060E+00	-3.23E-03	-1.075E+00	3.78E-03	1.261E+00	1.247E+00
1006	3.33E-03	1.110E+00	-3.86E-03	-1.285E+00	4.39E-03	1.462E+00	1.286E+00
1007	3.33E-03	1.111E+00	-3.77E-03	-1.256E+00	4.48E-03	1.493E+00	1.348E+00
1008	3.45E-03	1.150E+00	-4.14E-03	-1.381E+00	5.05E-03	1.682E+00	1.451E+00
1009	3.58E-03	1.195E+00	-4.44E-03	-1.479E+00	5.31E-03	1.771E+00	1.486E+00
1010	3.39E-03	1.132E+00	-2.65E-03	-8.844E-01	3.30E-03	1.099E+00	1.347E+00
1011	3.31E-03	1.104E+00	-2.27E-03	-7.555E-01	2.63E-03	8.773E-01	1.226E+00
1012	3.28E-03	1.094E+00	-9.16E-04	-3.054E-01	1.45E-03	4.837E-01	1.273E+00
1013	3.20E-03	1.065E+00	-1.39E-04	-4.633E-02	5.17E-04	1.723E-01	1.191E+00
1014	3.13E-03	1.045E+00	7.17E-04	2.390E-01	-2.02E-04	-6.721E-02	1.217E+00
1015	3.08E-03	1.026E+00	1.30E-03	4.339E-01	-5.70E-04	-1.900E-01	1.270E+00
1016	3.01E-03	1.003E+00	1.78E-03	5.921E-01	-8.60E-04	-2.867E-01	1.309E+00
1017	2.92E-03	9.729E-01	2.30E-03	7.677E-01	-1.28E-03	-4.272E-01	1.313E+00
1018	2.71E-03	9.036E-01	2.78E-03	9.267E-01	-1.85E-03	-6.156E-01	1.215E+00
1019	2.56E-03	8.530E-01	3.13E-03	1.044E+00	-2.26E-03	-7.540E-01	1.143E+00
1020	2.90E-03	9.656E-01	3.05E-03	1.017E+00	-2.15E-03	-7.183E-01	1.264E+00

Time step							TOTAL Drag (N/m)
	Fix wing total Drag N/3MM	Fix Wing Drag (N/M)	Top wing total Drag N/3MM	Top Wing Drag (N/M)	Bot wing total Drag N/3MM	Bottom Wing Drag (N/M)	
940	-2.39E-06	-7.955E-04	3.31E-06	1.103E-03	1.76E-05	5.865E-03	6.173E-03
941	9.35E-06	3.116E-03	1.44E-04	4.795E-02	1.36E-04	4.539E-02	9.646E-02
942	3.64E-05	1.214E-02	-3.22E-05	-1.073E-02	-9.33E-05	-3.109E-02	-2.969E-02
943	6.94E-05	2.312E-02	-5.31E-04	-1.769E-01	-5.36E-04	-1.785E-01	-3.323E-01
944	9.66E-05	3.220E-02	-8.41E-04	-2.804E-01	-9.28E-04	-3.093E-01	-5.576E-01
945	1.34E-04	4.472E-02	-1.11E-03	-3.714E-01	-1.39E-03	-4.618E-01	-7.885E-01
946	1.37E-04	4.572E-02	-1.19E-03	-3.953E-01	-1.51E-03	-5.021E-01	-8.517E-01
947	1.07E-04	3.578E-02	-9.58E-04	-3.193E-01	-1.29E-03	-4.289E-01	-7.125E-01
948	1.05E-04	3.504E-02	-7.48E-04	-2.494E-01	-1.04E-03	-3.471E-01	-5.615E-01
949	1.24E-04	4.126E-02	-4.06E-04	-1.352E-01	-5.69E-04	-1.898E-01	-2.838E-01
950	7.86E-05	2.621E-02	4.94E-06	1.646E-03	-2.30E-06	-7.680E-04	2.709E-02
951	6.82E-05	2.273E-02	2.09E-04	6.952E-02	2.76E-04	9.213E-02	1.844E-01
952	4.80E-05	1.600E-02	1.40E-04	4.673E-02	2.87E-04	9.582E-02	1.586E-01
953	2.55E-05	8.494E-03	-1.95E-05	-6.516E-03	1.32E-04	4.399E-02	4.597E-02
954	4.22E-06	1.408E-03	-3.02E-04	-1.008E-01	-8.67E-05	-2.891E-02	-1.283E-01
955	-1.22E-05	-4.053E-03	-5.38E-04	-1.794E-01	-2.20E-04	-7.335E-02	-2.568E-01
956	-2.46E-05	-8.194E-03	-6.54E-04	-2.179E-01	-3.03E-04	-1.010E-01	-3.271E-01
957	-3.43E-05	-1.143E-02	-6.84E-04	-2.279E-01	-3.79E-04	-1.262E-01	-3.655E-01
958	-4.34E-05	-1.446E-02	-5.61E-04	-1.869E-01	-3.90E-04	-1.301E-01	-3.315E-01
959	-4.78E-05	-1.593E-02	-3.20E-04	-1.065E-01	-2.40E-04	-8.004E-02	-2.025E-01
960	-4.76E-05	-1.587E-02	1.30E-05	4.342E-03	1.75E-05	5.836E-03	-5.693E-03
961	-4.35E-05	-1.451E-02	1.43E-04	4.756E-02	1.47E-04	4.906E-02	8.212E-02
962	-2.17E-05	-7.223E-03	-6.63E-05	-2.211E-02	-9.55E-05	-3.184E-02	-6.117E-02
963	3.37E-06	1.124E-03	-5.31E-04	-1.770E-01	-5.19E-04	-1.732E-01	-3.491E-01
964	2.50E-05	8.327E-03	-8.50E-04	-2.834E-01	-9.03E-04	-3.010E-01	-5.761E-01
965	5.93E-05	1.977E-02	-1.16E-03	-3.863E-01	-1.36E-03	-4.537E-01	-8.202E-01
966	6.46E-05	2.153E-02	-1.31E-03	-4.369E-01	-1.51E-03	-5.022E-01	-9.175E-01
967	3.93E-05	1.311E-02	-1.07E-03	-3.580E-01	-1.29E-03	-4.297E-01	-7.747E-01
968	3.80E-05	1.268E-02	-8.50E-04	-2.833E-01	-1.04E-03	-3.482E-01	-6.189E-01
969	6.86E-05	2.286E-02	-4.71E-04	-1.569E-01	-5.73E-04	-1.910E-01	-3.250E-01
970	3.24E-05	1.081E-02	5.27E-06	1.757E-03	-2.36E-06	-7.880E-04	1.178E-02
971	3.08E-05	1.027E-02	2.49E-04	8.290E-02	2.79E-04	9.309E-02	1.863E-01
972	1.99E-05	6.649E-03	1.93E-04	6.436E-02	2.94E-04	9.783E-02	1.688E-01
973	6.61E-06	2.202E-03	4.28E-05	1.428E-02	1.41E-04	4.705E-02	6.354E-02
974	-5.40E-06	-1.799E-03	-2.42E-04	-8.078E-02	-7.58E-05	-2.526E-02	-1.078E-01
975	-1.26E-05	-4.189E-03	-4.66E-04	-1.554E-01	-2.09E-04	-6.973E-02	-2.293E-01
976	-1.55E-05	-5.172E-03	-6.03E-04	-2.010E-01	-2.93E-04	-9.760E-02	-3.038E-01
977	-1.47E-05	-4.900E-03	-6.60E-04	-2.199E-01	-3.44E-04	-1.146E-01	-3.394E-01
978	-1.26E-05	-4.204E-03	-5.69E-04	-1.897E-01	-3.71E-04	-1.235E-01	-3.174E-01
979	-7.86E-06	-2.620E-03	-3.35E-04	-1.118E-01	-2.28E-04	-7.602E-02	-1.904E-01
980	-2.27E-06	-7.564E-04	3.30E-06	1.099E-03	1.76E-05	5.864E-03	6.206E-03
981	9.48E-06	3.159E-03	1.44E-04	4.795E-02	1.36E-04	4.538E-02	9.649E-02
982	3.66E-05	1.219E-02	-3.22E-05	-1.073E-02	-9.33E-05	-3.110E-02	-2.964E-02
983	6.95E-05	2.318E-02	-5.31E-04	-1.769E-01	-5.37E-04	-1.791E-01	-3.328E-01
984	9.68E-05	3.227E-02	-8.41E-04	-2.805E-01	-9.28E-04	-3.093E-01	-5.576E-01

Time step							TOTAL Drag (N/m)
	Fix wing total Drag N/3MM	Fix Wing Drag (N/M)	Top wing total Drag N/3MM	Top Wing Drag (N/M)	Bot wing total Drag N/3MM	Bottom Wing Drag (N/M)	
985	1.34E-04	4.479E-02	-1.11E-03	-3.713E-01	-1.39E-03	-4.618E-01	-7.883E-01
986	1.37E-04	4.580E-02	-1.19E-03	-3.952E-01	-1.51E-03	-5.021E-01	-8.515E-01
987	1.08E-04	3.586E-02	-9.58E-04	-3.193E-01	-1.29E-03	-4.289E-01	-7.123E-01
988	1.05E-04	3.512E-02	-7.43E-04	-2.478E-01	-1.04E-03	-3.471E-01	-5.598E-01
989	1.24E-04	4.134E-02	-4.06E-04	-1.352E-01	-5.69E-04	-1.898E-01	-2.836E-01
990	7.89E-05	2.629E-02	4.94E-06	1.646E-03	-2.30E-06	-7.679E-04	2.717E-02
991	6.84E-05	2.280E-02	2.08E-04	6.949E-02	2.76E-04	9.213E-02	1.844E-01
992	4.82E-05	1.605E-02	1.40E-04	4.668E-02	2.87E-04	9.581E-02	1.585E-01
993	2.56E-05	8.533E-03	-1.98E-05	-6.595E-03	1.32E-04	4.398E-02	4.592E-02
994	4.29E-06	1.430E-03	-3.03E-04	-1.009E-01	-8.68E-05	-2.892E-02	-1.284E-01
995	-1.22E-05	-4.051E-03	-5.24E-04	-1.746E-01	-2.20E-04	-7.337E-02	-2.520E-01
996	-2.46E-05	-8.215E-03	-6.54E-04	-2.180E-01	-3.03E-04	-1.010E-01	-3.272E-01
997	-3.44E-05	-1.147E-02	-6.84E-04	-2.279E-01	-3.79E-04	-1.262E-01	-3.656E-01
998	-4.36E-05	-1.453E-02	-5.61E-04	-1.869E-01	-3.90E-04	-1.302E-01	-3.316E-01
999	-4.80E-05	-1.601E-02	-3.20E-04	-1.065E-01	-2.40E-04	-8.006E-02	-2.026E-01
1000	-4.79E-05	-1.596E-02	8.44E-06	2.814E-03	1.75E-05	5.836E-03	-7.306E-03
1001	-4.38E-05	-1.460E-02	1.43E-04	4.756E-02	1.47E-04	4.909E-02	8.204E-02
1002	-2.19E-05	-7.309E-03	-6.65E-05	-2.217E-02	-8.24E-05	-2.746E-02	-5.694E-02
1003	3.11E-06	1.037E-03	-5.31E-04	-1.770E-01	-5.19E-04	-1.731E-01	-3.491E-01
1004	2.47E-05	8.244E-03	-8.50E-04	-2.834E-01	-9.03E-04	-3.010E-01	-5.762E-01
1005	5.91E-05	1.970E-02	-1.16E-03	-3.864E-01	-1.36E-03	-4.537E-01	-8.204E-01
1006	6.44E-05	2.147E-02	-1.31E-03	-4.371E-01	-1.42E-03	-4.730E-01	-8.886E-01
1007	3.92E-05	1.306E-02	-1.06E-03	-3.534E-01	-1.29E-03	-4.297E-01	-7.701E-01
1008	4.24E-05	1.413E-02	-8.50E-04	-2.834E-01	-1.04E-03	-3.482E-01	-6.175E-01
1009	6.85E-05	2.284E-02	-4.90E-04	-1.634E-01	-5.73E-04	-1.910E-01	-3.315E-01
1010	3.24E-05	1.080E-02	5.27E-06	1.757E-03	-2.36E-06	-7.880E-04	1.177E-02
1011	3.08E-05	1.026E-02	2.49E-04	8.292E-02	2.79E-04	9.309E-02	1.863E-01
1012	1.99E-05	6.649E-03	1.93E-04	6.437E-02	2.94E-04	9.784E-02	1.689E-01
1013	6.62E-06	2.206E-03	4.28E-05	1.428E-02	1.41E-04	4.706E-02	6.354E-02
1014	-5.38E-06	-1.792E-03	-2.42E-04	-8.078E-02	-7.58E-05	-2.526E-02	-1.078E-01
1015	-1.25E-05	-4.181E-03	-4.66E-04	-1.554E-01	-2.09E-04	-6.974E-02	-2.293E-01
1016	-1.55E-05	-5.161E-03	-6.03E-04	-2.010E-01	-2.93E-04	-9.762E-02	-3.038E-01
1017	-1.47E-05	-4.886E-03	-6.60E-04	-2.199E-01	-3.65E-04	-1.217E-01	-3.465E-01
1018	-1.26E-05	-4.187E-03	-5.73E-04	-1.909E-01	-3.71E-04	-1.235E-01	-3.186E-01
1019	-7.80E-06	-2.599E-03	-3.35E-04	-1.118E-01	-2.28E-04	-7.602E-02	-1.904E-01
1020	-2.20E-06	-7.347E-04	3.29E-06	1.096E-03	1.76E-05	5.863E-03	6.225E-03

THIS PAGE INTENTIONALLY LEFT BLANK

APPENDIX B. MEAN LIFT & DRAG VARIATION FOR CASE OF OUT-OF-PHASE PITCH/PLUNGE MOTION

Table 1. Mean Lift Variation for Case of Out-of-Phase Pitch/Plunge Motion

Pitch Amplitude	LIFT (N/m)						
	Wing	Mean				Sample Mean	Standard Deviation
		Cycle 1 940 - 960	Cycle 2 960 - 980	Cycle 3 980 - 1000	Cycle 4 1000 - 1020		
10°	Fixed	1.0122	0.9959	1.0114	0.9967	1.0041	0.0090
	Top	-0.1876	-0.2108	-0.1880	-0.2099	-0.1991	0.0130
	Bottom	0.3943	0.3958	0.3944	0.3957	0.3951	0.0008
	Combined	1.2190	1.1809	1.2178	1.1826	1.2000	0.0212
15°	Fixed	0.9865	1.0890	1.0720	0.9678	1.0288	0.0606
	Top	-0.0497	-0.2126	-0.2356	-0.2329	-0.1827	0.0893
	Bottom	0.4041	0.3608	0.3656	0.3910	0.3804	0.0206
	Combined	1.3409	1.2372	1.2020	1.1259	1.2265	0.0893
20°	Fixed	1.0865	1.0170	1.0868	1.0170	1.0518	0.0402
	Top	-0.1088	-0.1731	-0.1088	-0.1734	-0.1410	0.0372
	Bottom	0.3672	0.3710	0.3672	0.3714	0.3692	0.0023
	Combined	1.3448	1.2150	1.3452	1.2149	1.2800	0.0751

Table 2. Mean Drag Variation for Case of Out-of-Phase Pitch/Plunge Motion

Pitch Amplitude	Drag (N/m)						
	Wing	Mean				Sample Mean	Standard Deviation
		Cycle 1 940 - 960	Cycle 2 960 - 980	Cycle 3 980 - 1000	Cycle 4 1000 - 1020		
10°	Fixed	0.0101	0.0073	0.0100	0.0074	0.0087	0.0016
	Top	-0.0565	-0.0576	-0.0567	-0.0574	-0.0571	0.0005
	Bottom	-0.0633	-0.0631	-0.0633	-0.0631	-0.0632	0.0001
	Combined	-0.1097	-0.1135	-0.1099	-0.1130	-0.1115	0.0020
15°	Fixed	0.0346	0.0123	0.0094	0.0047	0.0152	0.0133
	Top	-0.0973	-0.0904	-0.0881	-0.0898	-0.0914	0.0040
	Bottom	-0.0950	-0.0954	-0.0953	-0.0945	-0.0950	0.0004
	Combined	-0.1577	-0.1734	-0.1741	-0.1796	-0.1712	0.0094
20°	Fixed	0.0132	0.0032	0.0132	0.0033	0.0082	0.0057
	Top	-0.1330	-0.1355	-0.1328	-0.1358	-0.1343	0.0016
	Bottom	-0.1286	-0.1257	-0.1286	-0.1244	-0.1268	0.0021
	Combined	-0.2484	-0.2580	-0.2482	-0.2569	-0.2529	0.0053

THIS PAGE INTENTIONALLY LEFT BLANK

LIST OF REFERENCES

- [1] Jones, K.D., Castro B. M. Mahmoud, O., and Platzer, “A Numerical and Experimental Investigation of Flapping Wing Propulsion in Ground Effect,” *AIAA Paper No. 2002-0866*, Reno, Nevada, January 2002.
- [2] Papadopoulos, Jason, “An Experimental Investigation of the Geometric Characteristics of Flapping-Wing Propulsion for a Micro-Air Vehicle,” *Master’s Thesis*, Naval Postgraduate School, Monterey, California, June 2003.
- [3] Jones, K.D., T.C. Lund, and M.F. Platzer, “Experimental and Computational Investigation of Flapping Wing Propulsion for Micro Air Vehicles,” *Fixed and Flapping Wing Aerodynamics for Micro Air Vehicle Applications, Progress in Astronautics and Aeronautics*, Vol. 195, Chapter 16.
- [4] Wilmott, P., “Unsteady Lifting-Line Theory by the Method of Matched Asymptotic Expansions,” *Journal of Fluid Mechanics*, Vol. 186, 1988, pp. 303-320.
- [5] Philips, P.J., East, R.A., and Pratt, N.H., “An Unsteady Lifting Line Theory of Flapping Wings with Application to the Forward Flight of Birds,” *Journal of Fluid Mechanics*, Vol. 112, November 1981, pp. 97-125.
- [6] Ahmadi, A.R., and Widnall, S.E., “Unsteady Lifting-Line Theory as a Singular-Perturbation Problem,” *Journal of Fluid Mechanics*, Vol. 153, April 1985, pp. 59-81.
- [7] Lan, C.E., “The Unsteady Quasi-Vortex-Lattice Method with Applications to Animal Propulsion,” *Journal of Fluid Mechanics*, Vol. 93, No. 4, 1979, pp. 747-745.
- [8] Hall, Kenneth C., “A Rational Engineering Analysis of the Efficiency of Flapping Flight,” *Fixed and Flapping Wing Aerodynamics for Micro Air Vehicle Applications, Progress in Astronautics and Aeronautics*, Vol. 195, Chapter 13, pp. 249.
- [9] Jones, K.D., Bradshaw, C.J., Papadopoulos, J. and Platzer, M.F., “Improved Performance and Control of Flapping-Wing Propelled Micro Air Vehicles,” *AIAA Paper No. 2004-0399*, Reno, Nevada, January 2004.
- [10] ESI CFD Inc., “*CFD ACE+ GUI User Manual*,” V2006.
- [11] ESI CFD Inc., “*CFD ACE+ GUI Theory Manual*,” V2006.
- [12] ESI CFD Inc., “*CFD GEOM User Manual*,” V2006.
- [13] ESI CFD Inc., “*CFD VIEW User Manual*,” V2006.

THIS PAGE INTENTIONALLY LEFT BLANK

INITIAL DISTRIBUTION LIST

1. Defense Technical Information Center
Ft. Belvoir, Virginia
2. Dudley Knox Library
Naval Postgraduate School
Monterey, California
3. Professor Max Platzer
Naval Postgraduate School
Monterey, California
4. Professor Kevin D. Jones
Naval Postgraduate School
Monterey, California
5. Professor Christopher Brophy
Naval Postgraduate School
Monterey, California
6. Seng Chuan Lim
Naval Postgraduate School
Monterey, California
7. Professor Yeo Tat Soon
Director, Temasek Defense System Institute (TDSI)
National University of Singapore
Singapore
8. Ms Tan, Lai Poh
Temasek Defense System Institute (TDSI)
National University of Singapore
Singapore
9. Ms Goh Hong Ling
Human Resource Department
DSO National Laboratories
Singapore